

NASA TECHNICAL MEMORANDUM

NASA TM-78298

MATED VERTICAL GROUND VIBRATION TEST

By Edward W. Ivey
Systems Dynamics Laboratory

(NASA-TM-78298) MATED VERTICAL GROUND
VIBRATION TEST (NASA) 96 p HC A05/MF A01
CSCL 22B

N80-32425

Unclas
G3/16 28757

July 1980



NASA

*George C. Marshall Space Flight Center
Marshall Space Flight Center, Alabama*

TABLE OF CONTENTS

| | Page |
|--------------------------------|------|
| I. SUMMARY | 1 |
| II. INTRODUCTION | 1 |
| III. BACKGROUND | 2 |
| IV. TEST REQUIREMENTS | 4 |
| V. INSTRUMENTATION | 5 |
| VI. SHAKERS ^c | 5 |
| VII. TEST EQUIPMENT | 6 |
| VIII. DATA REDUCTION | 6 |
| IX. LAUNCH | 7 |
| X. BOOST | 68 |
| XI. CONCLUSION | 84 |
| BIBLIOGRAPHY | 89 |

PRECEDING PAGE BLANK NOT FILMED

LIST OF TABLES

| Table | Title | Page |
|-------|--|------|
| 1. | Technical Problem Areas and Requirements | 3 |
| 2. | Liftoff Suspension System Modes | 11 |
| 3. | Liftoff FCS Sweeps | 13 |
| 4. | Flight Control Frequency Priorities (Symmetric MVGVT Liftoff Modes)..... | 15 |
| 5. | Flight Control Frequency Priorities (Antisymmetric MVGVT Liftoff Modes) | 16 |
| 6. | Liftoff Pogo Sweeps | 17 |
| 7. | MVGVT Modal Correlation [Configuration - Liftoff (Symmetric)] | 18 |
| 8. | MVGVT Modal Correlation [Configuration - Liftoff (Antisymmetric)]..... | 21 |
| 9. | Payload Bay Sweeps | 45 |
| 10. | MVGVT Liftoff Pitch/Roll Mode, Lox Tank Full | 46 |
| 11. | MVGVT Liftoff Test Pitch/Roll Mode, Lox Tank Empty | 46 |
| 12. | SRB Burnout Suspension System Modes..... | 48 |
| 13. | SRB B/O FSC Sweeps | 49 |
| 14. | Primary FCS Response Frequencies SRB Burnout Transfer Functions | 50 |
| 15. | SRB B/O Pogo Sweeps | 51 |
| 16. | MVGVT Modal Correlation [Configuration - Burnout (Symmetric)] | 52 |
| 17. | MVGVT Modal Correlation [Configuration - Burnout (Antisymmetric)]..... | 54 |
| 18. | SRB RGA Mounting Ring Fix FCS Evaluation | 57 |

LIST OF TABLES (Continued)

| Table | Title | Page |
|-------|--|------|
| 19. | 1307 Bulkhead Computed and Measured Yaw Rates (Deg/Sec) | 59 |
| 20. | Suspension System Modes | 71 |
| 21. | Flight Control Sweeps | 72 |
| 22. | Start Boost Symmetric | 73 |
| 23. | Start Boost Antisymmetric | 74 |
| 24. | Mid Boost Symmetric | 76 |
| 25. | Mid Boost Antisymmetric | 77 |
| 26. | End Boost - Symmetric | 79 |
| 27. | End Boost Antisymmetric | 80 |
| 28. | Lox Tank Low Level Boost | 81 |
| 29. | Samsco Sweeps | 83 |
| 30. | Full Scale Dynamic Testing Experience in Past Programs | 85 |

LIST OF ILLUSTRATIONS

| Figure | Title | Page |
|--------|--|------|
| 1. | Launch configuration..... | 8 |
| 2. | Typical hydraulic dynamic support | 9 |
| 3. | Suspension system for shuttle vehicle | 10 |
| 4. | Space Shuttle MVGVT Orbiter/ET/SRB | 24 |
| 5. | Space Shuttle MVGVT Orbiter/ET/SRB | 25 |
| 6. | Space Shuttle MVGVT Orbiter/ET/SRB | 26 |
| 7. | Space Shuttle MVGVT Orbiter/ET/SRB | 27 |
| 8. | Space Shuttle MVGVT Orbiter/ET/SRB | 28 |
| 9. | Space Shuttle MVGVT Orbiter/ET/SRB External Tank Lift-off Symmetric..... | 29 |
| 10. | Space Shuttle MVGVT Orbiter/ET/SRB External Tank Lift-Off Symmetric | 30 |
| 11. | Space Shuttle MVGVT Dwell Data Orbiter *** External Tank *** Solid Rocket Boosters | 31 |
| 12. | Space Shuttle MVGVT Dwell Data Orbiter *** External Tank *** Solid Rocket Boosters | 36 |
| 13. | Space Shuttle MVGVT Symmetric Orthog Orbiter *** External Tank *** Solid Rocket Boosters | 37 |
| 14. | MVGVT Kinetic Energy Distribution Symmetric Motion Orbiter *** External Tank *** Solid Rocket Boosters | 38 |
| 15. | Space Shuttle MVGVT Symmetric Orthog Orbiter *** External Tank *** Solid Rocket Boosters | 39 |
| 16. | Space Shuttle MVGVT Symmetric X-Orth Orbiter *** External Tank *** Solid Rocket Boosters | 40 |
| 17. | Linear regression analysis | 41 |
| 18. | Linear regression analysis | 42 |
| 19. | Decay trace..... | 43 |

LIST OF ILLUSTRATIONS (Continued)

| Figure | Title | Page |
|--------|--|------|
| 20. | 1307 bulkhead accelerations at 4.7 Hz in g's/lb | 58 |
| 21. | Lox dome acceleration transfer function, pre SRB separation | 60 |
| 22. | Lox dome pressure transfer function, pre SRB separation | 61 |
| 23. | Lox dome acceleration transfer function, 100 second | 62 |
| 24. | Lox dome pressure transfer function, 100 second | 63 |
| 25. | Lox dome acceleration transfer function, 80 second | 64 |
| 26. | Lox dome acceleration transfer function, 80 second | 65 |
| 27. | Bulge mode frequency change with flight time | 66 |
| 28. | Critical damping curve for the lox dome bulge mode | 67 |
| 29. | MVGVT boost configuration | 69 |
| 30. | Suspension system for Orbiter/ET boost configuration ... | 70 |
| 31. | First fuselage symmetric bending linearity check..... | 82 |

TECHNICAL MEMORANDUM

MATED VERTICAL GROUND VIBRATION TEST

I. SUMMARY

The Mated Vertical Ground Vibration Test (MVGVT) was conducted to provide an experimental data base in the form of structural dynamic characteristics for the Shuttle vehicle. This data base was used in developing high confidence analytical models for the prediction and design of loads, pogo controls and flutter criteria for the Space Shuttle under various payloads and operational missions.

The MVGVT program consisted of two basic configurations. The two configurations tested were simulated launch and boost. The launch configuration was composed of two Solid Rocket Boosters (SRB's), an External Tank (ET), and an Orbiter (OV 101).

For the launch configuration, the liftoff and endburn (Pre-SRB Separation) flight conditions were tested. The Liftoff testing began on October 20, 1978, and ended December 2, 1978. The end burn testing started on January 30, 1979, and ended February 28, 1979.

The boost configuration was composed of the ET and the OV-101. For the boost configuration, three flight conditions (start boost, mid boost, and end boost) were tested. The boost test started on May 30, 1978, and ended July 14, 1978.

The Shuttle test program was conducted under Johnson Space Center's (JSC) direction and implemented by Rockwell International Corporation. Marshall Space Flight Center (MSFC) was heavily involved in all phases of the test. They were responsible for the ET, the SRB, and the Space Shuttle Main Engine (SSME) dynamic math models. MSFC was also involved in the LOX modal survey test. For MVGVT, MSFC was responsible for the suspension system design for launch and boost and was also involved in establishing the test plans and requirements. Additional responsibilities included data evaluation and analytical correlation.

II. INTRODUCTION

The purpose of this report is to present the MVGVT boost and launch program evolution, the test configurations, their suspensions, and the test results compared with predicted analytical results.

III. BACKGROUND

71

The dynamic behavior of space vehicles during different mission phases is a key consideration in their design, development, and verification. The complexity of a space vehicle like the Space Shuttle increases the difficulty required to accurately calculate this dynamic behavior especially to the accuracy requirements required by the Shuttle vehicle. The accuracy requirements are shown in Table 1 and were established by the various disciplines of pogo, loads, controls, and flutter. To meet this accuracy a full scale Mated Vertical Ground Vibration Test (MVGVT) program was required. The complexity of the Shuttle vehicle is unique. The Shuttle complexity is created by the coupled interaction of a four body system with many joints and local load paths. In addition, the Shuttle includes the viscoelastic effects of the SRB's with the unsymmetrical stiffness and mass effects of the Orbiter.

In the early phases of the test program there were a number of test configuration options available that would have possibly met configuration requirements. However, the problem was to arrive at a configuration that would be acceptable for the prediction and verification of an analytical structural dynamic model to a prescribed accuracy for use in controls, loads, pogo, and flutter while maintaining a program of low cost and minimum schedule impact. This led to the inevitable evolution of the test, test article, and test requirements.

The following at one time were considerations in the MVGVT program and deleted:

1) Use of water to simulate the LH_2 in the ET — The water would have introduced hydroelastic effects. Also, an 8 psid internal tank pressure would have had to be maintained in the tank during loading and testing or the aft dome would have sustained structural failure.

2) Use of polystyrene granules to simulate the LH_2 in the ET — The granules would have caused friction which could have affected damping and the granules themselves would have been costly.

3) Testing the maximum Q time condition — This time point was eliminated primarily due to cost; however, it was felt that testing of the two end conditions (liftoff and end burn) would be adequate.

4) Reduction of the orbiter payload from 65,000 to 32,000 lb — The payload weight was reduced because 32,000 lb was the heaviest payload flown on the first six flights. It was believed that the rigid 32,000 lb payload would adequately "work" the longerons in the payload bay without unduly influencing orbiter modes. Since it was not feasible to simulate various payload configurations, the scheme of adding ballast to the existing approach and landing test pallets was the least expensive method of providing for a dummy payload.

TABLE 1. TECHNICAL PROBLEM AREAS AND REQUIREMENTS

| Items/Users | Control | Pogo | Flutter | Loads |
|---------------------|---|---|---|--|
| Structure Model | <u>Motion Sensor</u> <u>Gimbal Force</u> | <u>Propellant Pressure</u> <u>Thrust Force</u> | <u>Surface Motion</u> <u>Aero Forces</u> | <u>High Stress Points</u> <u>All Forces</u> |
| Frequency Range | 0 - 10 Hz | 0 - 40 Hz | 0 - 40 Hz | 0 - 40 Hz |
| Frequency Accuracy | 5% < 4 Hz, 10% > 4 Hz | 5% < 3 Hz, 15% > 3 Hz | 5% | 10% |
| Damping Range | > 0.005 | ~ 0.01 | ~ 0.01 | ~ 0.01 |
| Damping Accuracy | 10% < 4 Hz, 20% > 4 Hz | 20% | 20% | 20% |
| Slope Accuracy | 10% < 4 Hz, 20% > 4 Hz | N/A | 15% | 20% |
| Deflection Accuracy | 10% < 4 Hz, 20% > 4 Hz | 20% | 15% | 20% |
| Pressure Accuracy | N/A | 30% | Not Tested | Not Tested |

5) Use of water or drillers mud instead of inert propellant in the SRB for maximum Q - The use of these materials would have introduced adverse hydroelastic effects.

6) Have the SRB motors loaded with inert propellant to maximum Q then ballast the SRB for liftoff with sleeves either internal or external - This would have degraded the viscoelastic effect and in addition the stiffness of the SRBs would have been different from flight.

7) Considered a flexible payload, rather than one that was rigid - This would have overly complicated the analysis and math model correlation and subsequent modification of the math model benefit, although a rigid simulation on flexible supports was advantageous to check out payload/Orbiter interaction.

In the early phase of MGVGT there was a concern in the boost test that the test article would couple dynamically with Building 4550 through the overhead support truss and air bag assembly to the extent that the test data would be invalidated. To resolve this question, structural dynamic math modes of Building 4550, the overhead truss and air bag assembly, and the test article were generated. Modal characteristics of the coupled system were calculated and compared. The results showed that the spring supported test article provided isolation from Building 4550 and that the elastic modes of the test article were not affected by the modes of the building and the overhead truss.

IV. TEST REQUIREMENTS

The test article was subjected to sinusoidal excitation by driving shakers selected and located so as to excite and isolate all significant modes of vibration both symmetrical and antisymmetrical. The frequency range of interest that was surveyed is as follows:

- 1) For transverse excitation 1.5 to 30.0 Hz.
- 2) For longitudinal excitation 1.5 to 50.0 Hz.

The test objectives of the Shuttle vehicle MGVGT were:

1) To verify the coupled dynamic math models of the mated Shuttle configurations through correlation of analytical predictions to measured test data. These data shall consist of mated structural resonant frequencies, mode shapes and damping characteristics for selected simulated flight conditions.

2) To obtain experimentally the modal translation and rotations at the Orbiter and SRB guidance sensor and effector locations for the mated Orbiter/ET and Orbiter/ET/SRB configurations.

3) To obtain experimentally the test transfer functions from the excitation sources to the guidance and control sensor locations for the mated configurations.

4) To measure ET umbilical feedline modal data to verify the feedline math model.

A listing of the accuracy requirements for the Shuttle dynamic modal data as specified by the users, namely controls, pogo, flutter and loads are listed by disciplines in Table 1.

V. INSTRUMENTATION

The accelerometer locations selected were based on the Shuttle System pretest vibration analysis. The interfaces, ET/SRB (launch) and the ET/Orbiter (launch and boost), were of prime importance and were heavily instrumented. Instrumentation on the ET LOX tank, side walls, bulkhead, and sump areas were also emphasized such that the instrumentation correlated as much as possible with the LOX tank modal survey test. The instrumentation used was as follows:

- | | |
|-------------------------|----------------|
| 1) Accelerometers | - 320 Channels |
| 2) Strain Gauges | - 30 Channels |
| 3) Force Transducers | - 40 Channels |
| 4) Pressure Transducers | - 10 Channels |
| 5) Rate Gyros | - 9 Channels |

VI. SHAKERS

The shakers used in the MGVVT were either rigid or suspended 150 lbf and 1000 lbf electrodynamic shakers. The rigid shakers were such that the combined shaker and support had no natural frequencies less than 100 Hz. The suspended shakers were free pendulum with a maximum frequency of 0.5 Hz.

For the launch liftoff and end burn tests, the pendulum frequencies of the cable mounted shaker assemblies prevented adequate shaker force from being transmitted to the test vehicle at low frequencies (Up to 2.5 Hz). This problem was solved by rigid mounting 20 selected 1000 lbf shakers which, once the low frequency data were obtained, were derigidized and cable mounted again.

VII. TEST EQUIPMENT

The data acquisition system used was SMTAS. The system has the capability to monitor, record, and process excitation input parameters up to 24 channels and display selected input parameters to the console operators. It has the capability to monitor, record, and process signals from 320 accelerometers and rate gyros, 45 force, and 50 pressure and strain gauge measurements. SMTAS provided control for a maximum of 24 shaker channels capable of driving a maximum of 38 shakers.

VIII. DATA REDUCTION

The modal frequencies determined to be of interest during the sweeps were individually tuned and purified. This isolation was accomplished by utilizing the following techniques.

- 1) Observation of input force/velocity Lissajous patterns.
- 2) Vector resolutions of force and acceleration in coquad plots.
- 3) Strip chart recordings of selected channels and decay traces.
- 4) Orthogonality charts.

SMTAS provided data printout for test evaluation by furnishing the following data formats:

- 1) Normalized orthogonality matrix showing mode numbers.
- 2) Shaker force distribution and polarity listing.
- 3) Transfer function plots — transducer response (Engineering units) versus frequency.
- 4) Modal vector plots.
- 5) Coincident — quadrature plots versus frequency.
- 6) Kinetic energy distribution tables.
- 7) Modal dwell data.
- 8) Plots of digitized decay traces.
- 9) Calculated force distribution listings.
- 10) Linear regression plots (launch).
- 11) Cross orthogonality plots (launch).

IX LAUNCH

A. Liftoff

1. Configuration. The liftoff (T + 0 sec) configuration tested consisted of the OV-101 Orbiter mated with an ET and two full solid SRB (Fig. 1).

a. External Tank. The ET was a flight weight tank assembly of production design configuration including the nose fairing, LOX tank assembly, intertank assembly, LH₂ tank assembly, orbiter to tank attach fitting, SRB to tank attach fittings, feedline and external tank to orbiter feedline disconnects. There was no simulated LH₂. The LOX tank fuel was simulated with de-ionized sodium-chromate-inhibited water.

b. Orbiter. The Orbiter OV-101 was a flight type production with modifications required for MVGVT. The OMS Pc' were mass simulators with elastic link actuator simulators with gimbal clocks. The payload installed on the orbiter consisted of two 16,000 lb rigid ballasted pallets.

c. SRB. The SRB's were flight type production assemblies. A pressure ring on each of the SRB's for liftoff only was installed at the aft SRB/ET attachment. These rings were installed to simulate the effects of internal pressure of the ignited SRB's by adding stiffness. The pressure rings were removed later during the test to examine the dynamic effects between the "rings on" and "rings off" condition. The SRB nozzles were omitted.

2. Suspension. The liftoff test configuration utilized a soft suspension system that was provided by the four existing Saturn V Hydrodynamic Support (HDS) Units. The HDS's provided the vertical support as shown in Figure 2 and six degrees of freedom for the supported vehicle. Each SRB aft skirt was attached to an adapter truss which rested on the HDS system. The lateral stability and soft spring rate in pitch and yaw were provided by Firestone air bags #323 and #319, respectively. The lower bags were attached to the SRB aft skirt and the upper bags were attached to the SRB frustrum. The suspension system is presented in Figure 3.

3. Test Results and Analysis.

a. Suspension System Modes. Six rigid body suspension system modes were obtained and are summarized in Table 2. The suspension system modes assure that an adequate separation exists between the elastic modes and the rigid body modes. Phasing of the instrumentation was also accomplished at this time. All six modes showed excellent agreement.

1. TEST FACILITY BUILDING 4550
2. EXTERNAL TANK
3. SRB'S (2)
4. FLIGHT ORBITER (OV-101)
5. LATERAL RESTRAINTS
6. ACTUAL TEST BAY AREA
7. SHAKER
8. TYPICAL PLATFORMS
9. HYDRODYNAMIC SUPPORTS (HDS)
10. HDS-SRB ADAPTER

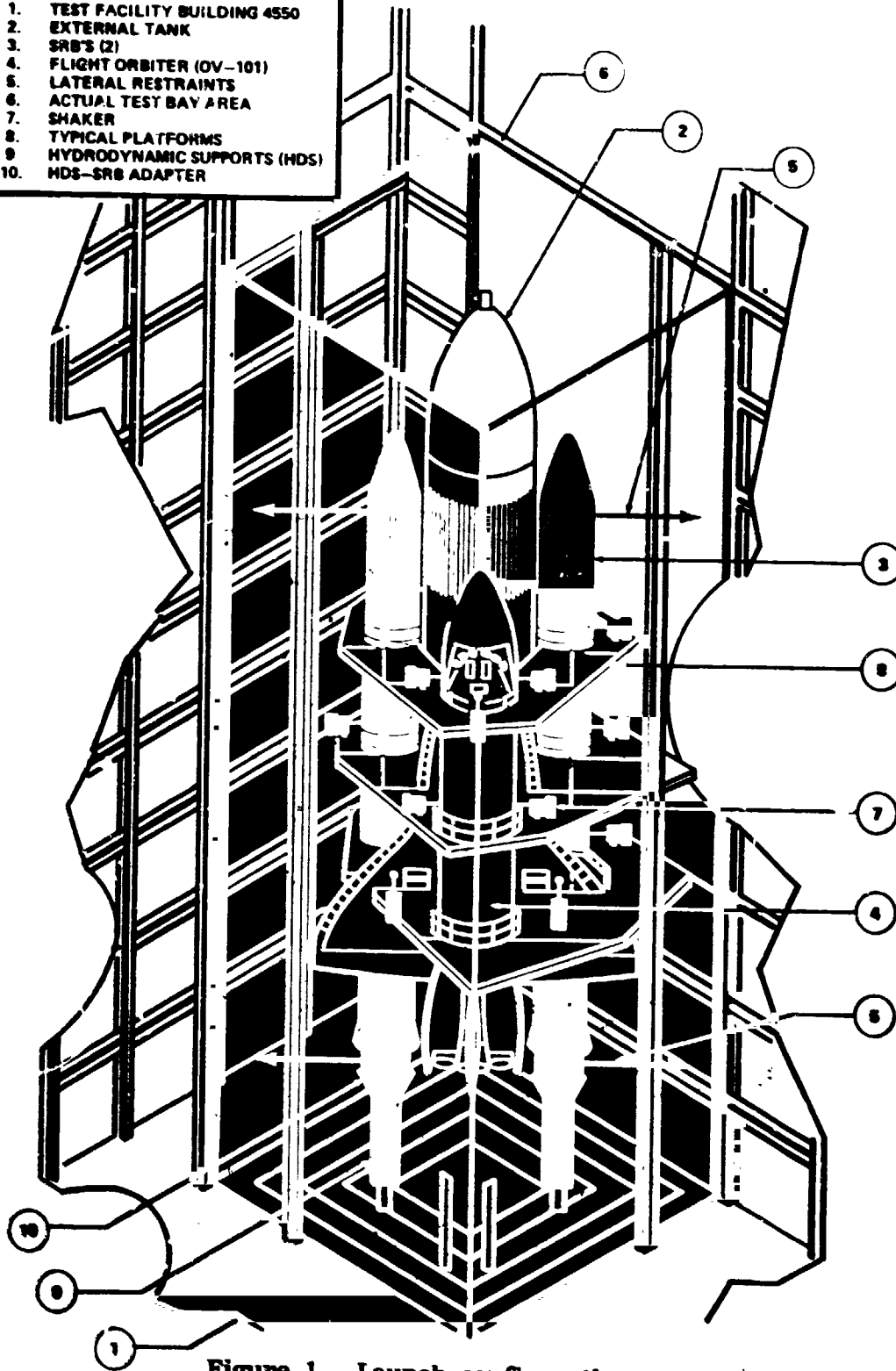


Figure 1. Launch configuration.

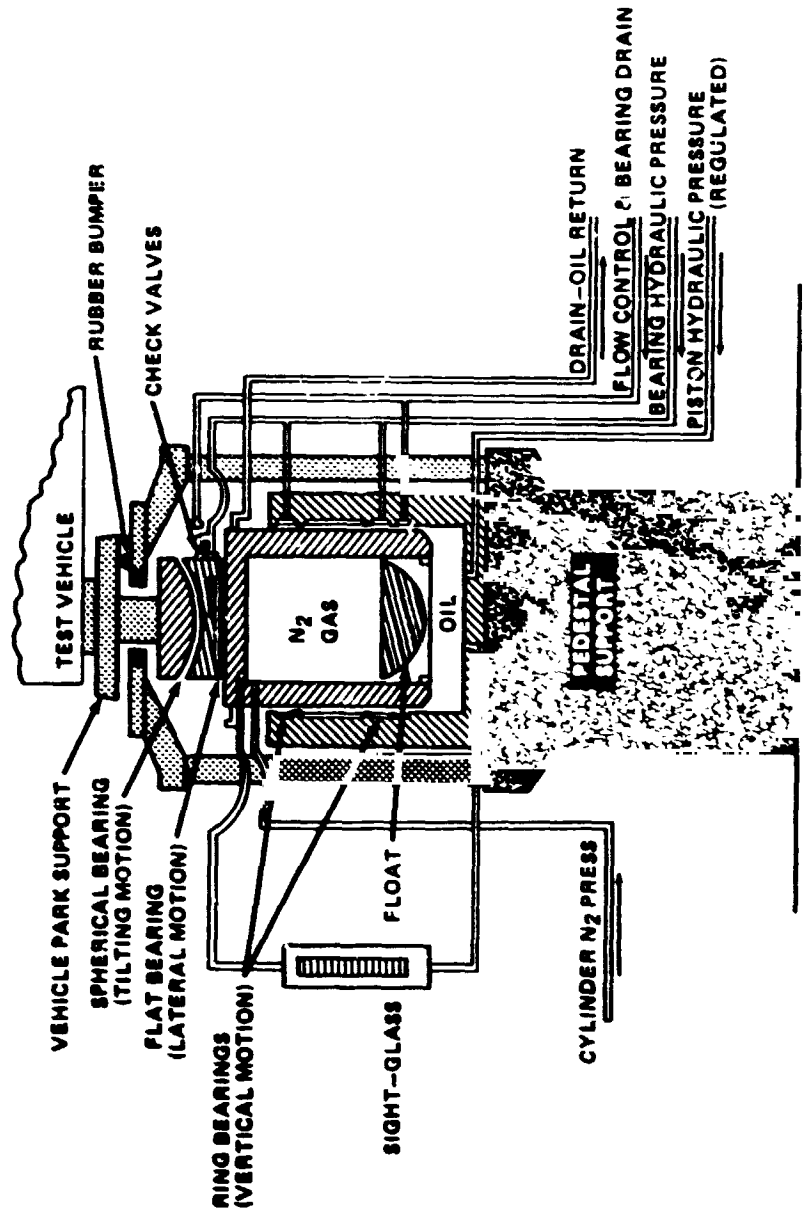


Figure 2. Typical hydraulic dynamic support.

ORIGINAL PAGE IS
OF POOR QUALITY

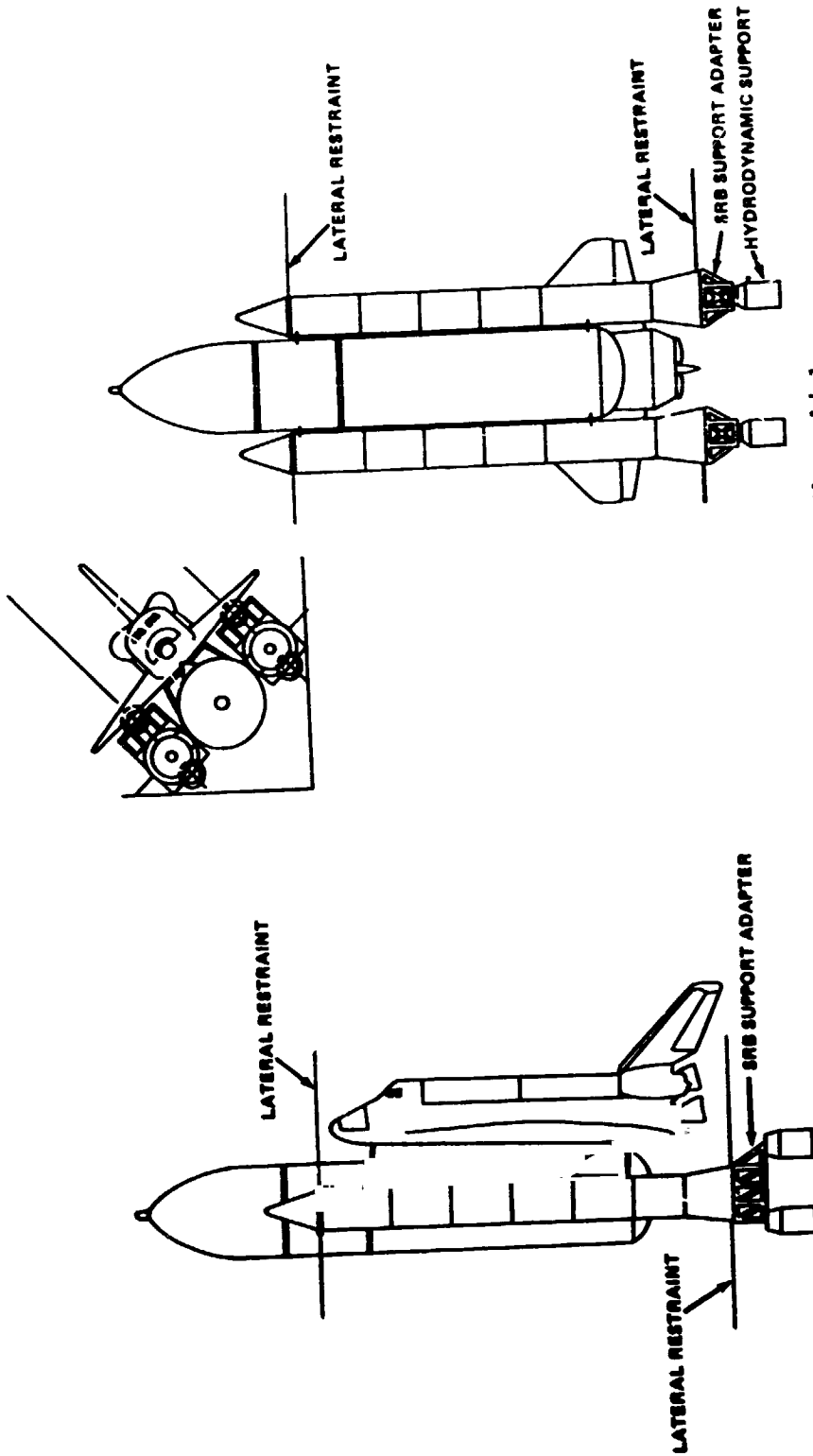


Figure 3. Suspension system for shuttle vehicle.

TABLE 2. LIFTOFF SUSPENSION SYSTEM MODES

| Mode No. | Test Frequency (Hz) | Predicted Frequency (Hz) | Description of Motion |
|----------|---------------------|--------------------------|-----------------------|
| 3 | 0.196 | 0.193 | Z-Translation |
| 6 | 0.24 | 0.23 | Y-Translation |
| 35 | 0.27 | 0.27 | ϕX (Roll) |
| 4 | 0.314 | 0.338 | ϕY (Pitch) |
| 4 | 0.510 | 0.50 | ϕZ (Yaw) |
| 1 | 0.67 | 0.68 | X-Translation |

b. Flight Control Transfer Functions. Flight control transfer functions for seven sweeps are enumerated in Table 3. Three additional sweeps were taken using shakers on the Orbiter and SRB to excite the modes and are shown in Table 3A.

During one of the sweeps an abnormally high transfer function value was observed on both SRB's at the forward SRB mounting rings where the rate gyros are mounted. This was due to a local resonance of the rate gyros caused by a large (Approximately 200 lb) avionic box mounted on the ring frame. The left SRB local resonance occurred at 23 Hz and the right SRB resonance occurred at 25 Hz. These local resonances were subsequently verified in a separate modal survey test of the left and right SRB forward skirt and nose cone assembly. To alleviate this problem, the ring frames of both SRB's were structurally stiffened which increased the local resonant frequency and decreased the amplitude gain.

The flight control group identified a number of significant structural modes that appeared on the transfer function sweeps. These modes were assigned priority numbers based on importance to flight controls and are listed in Tables 4 and 5.

c. Pogo Wide Band Sweeps. Wide band frequency sweeps were run independently on all three orbiter main engines. The excitation force in each case was along the engine longitudinal axis. Table 6 lists the sweep number and frequency range for each engine sweep. The six engine axial modes above 16 Hz were identified and dwells were taken.

d. Modal Test Results versus Pretest Analysis. All acceptable modes tuned during liftoff symmetric tests are shown in Table 7. The antisymmetrical modes are shown in Table 8. The correlating pretest analytical frequency and the computed modal damping from the decay traces are also shown in those tables. The last column gives the percent error between the test and analytical mode.

For each modal dwell, at a resonant frequency, a set of data was generated by SMTAS for that mode. A typical data set is shown in Figures 4 through 19. This particular mode is a symmetric mode that occurs at a frequency of 2.059 Hz and is a coupled pitch/roll mode of the SRB's. Figures 4 through 10 show the overall view of the test article with displacement vectors (quad amplitude) which is an aid in defining the mode.

Figure 11 presents a tabulation of the acceleration broken down into coincident (CO) and quadrature (quad) with phase angle for each accelerometer recorded. Figure 12 shows the force levels used to tune that particular mode to its resonance. There are 32 shakers available; however, only a few selected ones are used in the tuning of a particular mode. The orthogonality between the test modes is shown in a matrix in Figure 13 and Figure 15 lists the modal generalized mass.

TABLE 3. LIFTOFF FCS SWEEPS







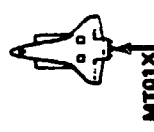
| Sweep No. | Shakers | Phase (deg) | Type Motion | SMTAS Sweep No. | | |
|-----------|----------------------------|----------------|---|-----------------|---------|----------|
| | | | | 1-7 Hz | 7-17 Hz | 17-30 Hz |
| 1 | RT/RB14Y LT/LB14Y | 180/0 0/180 | SRB Yaw  | 1 | 6 | 7 |
| 2 | FL10Y FL11Y | 0 0 | ORB Yaw  | 5 | 8 | 3 |
| 3 | RR06Z/RL07Z LL06Z/LR07Z | 0/180 0/180 | SRB Pitch  | 17 | 19 | 20 |
| 4 | FB10Z/FB11Z | 0/0 | ORB Pitch  | 4 | 10 | 11 |
| 5 | RR06Z/RL07Z LL06Z/LR07Z | 180/0 0/180 | SRB Roll  | 18 | 21 | 22 |
| 6 | FB10Z/FB11Z | 0/180 | ORB Roll  | 3 | 12 | 13 |
| 7 | MT01X | 0 | ENG No. 1 Axial  | 2-30 Hz 14 | | |

TABLE 3A. (Concluded)


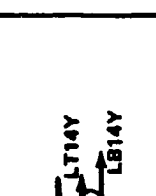

| Sweep No. | Shakers | Phase (deg) | Type Motion | SMTAS Sweep | |
|-----------|--|--------------------------|--|-------------|---------|
| | | | | No. | 2-15 Hz |
| 8 | RR/LL06Z RL/LR07Z FB10Z/FB11Z | 0/180 180/0 0/180 | Pitch  | 24 | |
| 9 | RB/RT14Y LB/LT14Y FL10Y FL11Y | 0/180 180/0 0 0 | Yaw  | 23 | |
| 10 | RR/LL06Z RL/LR07Z FB10Z/FB11Z | 0/180 180/0 0/180 | Roll  | 25 | |

TABLE 4. FLIGHT CONTROL FREQUENCY PRIORITIES
(SYMMETRIC MGVGT LIFTOFF MODES)

| Test | | Approximate Function Resp. Freq. (Hz) | Test Mode Description Dominant Motion (Kinetic Energy) | Response Channel Priority* | | | |
|-------------|-------------------|--|--|----------------------------|-----------------------|---|------------------------------|
| Mode No. | Frequency (Hz) | | | SRB Pitch RGA's | ORB Pitch RGA's | ORB Norm. Fit. Cont. Accel. | Nav. Base Pitch RGA |
| 5 | 2.05 | 2.1 | SRB Pitch (0.25) and Roll (0.34), ORB-ET Z Trans (0.24) | 1 | 1 | 1 | 3 |
| 9 | 3.02 | 3.0 | SRB Pitch (0.38) and Roll (0.27), ET Pitch (0.10), ORB Z Trans (0.10) | 1 | 1 | 1 | 3 |
| 11 | 3.23 | 3.3 | ORB Pitch (0.33), X (0.36), SRB Z Bend (0.25) | 2 | 1 | 1 | 3 |
| 23 | 4.39 | 4.4 | FDLN-X (0.17), ORB Z (0.17), SRB X (0.17), Z (0.22) | | 2 | | 3 |
| 14 | 5.25 | 5.2 | ORB Z Bend (0.17), ET Z Bend (0.27), SRB 1st Z Bend (0.46) | 1 | 2 | 2 | 3 |
| 18 | 5.65 | 5.6 | ORB X (0.18), Z (0.55), SRB Z (0.09) | | 2 | 2 | 3 |
| 13 | 9.0 | 9.0 | ORB Z Bend (0.76), Out of ϕ with SRB Z Bend (0.06) | | | 4 | 4 |
| 2 A/S? | 10.1 A/S? | 10.0 | | 4 | 4 | | 4 |
| 26 | 11.94 | 12.2 | SRB 2nd Y (0.7), I.T. (0.08) | | | | 4 |
| 22 | 12.41 | 12.5 | LWR Ogive (0.19), Dome Bulge, Feedline (0.15) | | | | 4 |
| 19 | 14.52 | 14.5 | F/A Payload X (0.05) Out of ϕ , ORB Z Bend (0.08) LWR ENG P (0.07) | | | | 4 |
| -- | -- | 23 | Local LSRB RGA Ring Resonance/SRB 4th Z Bend | 1 | | | |
| -- | -- | 25 | Local RSRB RGA Ring Resonance/SRB 3rd Y Bend | 1 | | | |

*Code: 1 = Most Significant
4 = Least Significant

TABLE 5. FLIGHT CONTROL FREQUENCY PRIORITIES
(ANTISYMMETRIC MGVGT LIFTOFF MODES)

| Test | | Approximate Transfer Function Response Freq. (Hz) | Test Mode Description Dominant Motion (Kinetic Energy) | Response Channel Priority* | | | | | | |
|-------------|-------------------|---|--|----------------------------|--------------|------|------------------|-----|-----------------------|--|
| Mode No. | Frequency (Hz) | | | SRB Yaw RGA | ORB RGA's | | ORB FC Accel. | | Nav. Base RGA's | |
| | | | | Yaw | Roll | Norm | Lat | Yaw | Roll | |
| 10 | 2.08 | 2.1 | SRB Y Bend (0.63) ET out ; with SRB (0.21). SRB X (0.12) | 1 | | | 1 | 2 | | |
| 8 | 2.23 | 2.2 | SRB Pitch (0.48) and Roll (0.13). ORB Y (0.21) | | 1 | | | | 1 | |
| 11 | 2.47 | 2.5 | SRB Pitch (0.59) and Roll (0.13). ORB Roll and Yaw (0.12). ET Roll | | 1 | | | | 1 | |
| 13 | 3.57 | 3.5 | SRB Pitch (0.12). Roll (0.07) and Yaw (0.08). V.T. Side Bend (0.26) | 2 | | | 2 | | | |
| 27 | 3.53 | 3.5 | Gear Train, ORB Y (0.42). SRB Z (0.28) | 2 | | | 2 | | | |
| 5 | 4.12 | 4.2 | SRB Z Bend (0.62) with Roll (0.08). ORB Yaw (0.18) | 3 | | | 1 | 3 | | |
| 205 | 5.13 | 5.2 | SRB 1st Y Bending | 1 | | | 3 | | | |
| 1 | 5.45 | 5.5 | SRB 1st Z Bend (0.43). Y Bend (0.12). Wing Bend (0.07) | 3 | | | 3 | | | |
| 10 sym? | 6.43 sym? | 6.2 | | 3 | | | | | | |
| 18 | 9.3 | 9.5 | Upper E.T. Torsion | | | | | 4 | | |
| 19 | 10.65 | 10.8 | SRB 2nd Y Bend (0.61). Z Bend (0.29) | 4 | | | | 4 | | |
| 31 | 13.89 | 13.8 | V.T. Torsion (0.68). Elevon Z (0.09) | | | | | 4 | | |
| 7 | 23.84 | 23 | Local 1SRB kGA Ring Resonance/SRB 4th Z Bend (0.65) | 1 | | | | 4 | | |
| 30 | 24.81 | 25 | Local RSRB RGA Ring Resonance/SRB 3rd Y Bend | 1 | | | | | | |

*Code: 1 = Most Significant
4 = Least Significant

TABLE 6. LIFTOFF POGO SWEEPS

| Excitation | Frequency Range Segments, Hz Sweep No. () | | |
|---------------------------|--|--------------|--------------|
| Upper SSME Axial | 2-12 (1) | 12-30 (2) | 30-50 (3) |
| Lower Left SSME Axial | 2-12 (4) | 12-30 (5) | 30-50 (6) |
| Lower Right SSME Axial | 2-12 (7) | 12-30 (8) | 30-50 (9) |

TABLE 7. MGVGT MODAL CORRELATION
[CONFIGURATION - LIFTOFF (SYMMETRIC)]

| Test Mode | | | Analysis Mode | | | Percent Error | |
|-----------|-------|--------|--|----------|-------|---|-------------|
| Mode No. | Freq. | Damp | Description | Mode No. | Freq. | | Description |
| 5 | 2.05 | 0.013 | SRB Roll (0.34), Pitch (0.25), Yaw (0.16), Orbiter Pitch (0.08), ET-Z (0.13) | 4 | 2.11 | SRB Roll (0.38), Pitch (0.45), Yaw (0.04), Orbiter Pitch (0.04), ET-Z (0.07) | 3 |
| 7 | 2.64 | 0.014 | SRB Yaw (0.95), ET Pitch (0.02) | 6 | 2.93 | SRB Yaw (0.84), ET Pitch (0.02) | 11 |
| 8 | 3.02 | 0.017 | SRB Pitch (0.38), Roll (0.27), ET-Z, Bending (0.10), Orbiter-Z (0.07) | 5 | 2.45 | SRB Yaw (0.83), ET X (0.07) | 8 |
| 11 | 3.24 | 0.010 | ORB Bending (0.32), X (0.36), SRB Z-Bending (0.25) | 8 | 3.18 | SRB Pitch (0.38), Roll (0.34), ET-Z, Bending (0.06), Orbiter-Z (0.08) | 5 |
| 12 | 3.88 | 0.015 | SRB-X (0.60), Yaw (0.13), FWD ET Shell (0.24) | 7 | 3.14 | Orbiter Bending (0.44), X (0.43), SRB Z-Bending (0.06) | -3 |
| 23 | 4.39 | 0.0013 | SRB Z-Bending (0.22), Roll (0.08), F/L Fluid (0.17), Orbiter Bend (0.17) | 9 | 3.87 | SRB-X (0.47), Yaw (0.38), FWD ET Shell (0.14) | < 1 |
| 14 | 5.26 | 0.016 | SRB Z-Bending (0.47), ET Bending (0.27), Orbiter Bending (0.17) | 11 | 5.16 | SRB Z-Bending (0.26), Roll (0.06), Orbiter Bending (0.54) | 18 |
| 13 | 5.65 | 0.005 | Orbiter Pitch, Bending, In-Phase Wing Bending (0.55), Orbiter X (0.18) | 12 | 5.39 | SRB Z-Bending (0.15), Y-Bending (0.13), ET Bending, Axial (0.33), ORB Bend (0.15) | 2 |
| 10 | 6.43 | 0.037 | 1st Wing Bending (0.68), Out-of-Phase Upper SSMIE (0.13) | 11 | 5.16 | Orbiter Z, Bending, In-Phase Wing Bending (0.54), Orbiter X (0.03) | -9 |
| 21 | 6.78 | 0.011 | SRB Sym Hdw and Y-Bending (0.85) | 15 | 6.60 | 1st Wing Bending (0.64) | 3 |
| 15 | 7.02 | 0.011 | VERT Tail FWD/AFT Rocking (0.21), Out-of-Phase Wing Bending (0.18) | 18 | 7.62 | SRB Sym Yaw and Y-Bending (0.67), Propellant (0.12) | 12 |
| | | | | 16 | 6.88 | Vert Tail FWD/AFT Rocking (0.07), Out-of-Phase Wing Bending (0.22) | -2 |

*Correlation not reliable
% error error not applicable

TABLE 7. (Continued)

| Test Mode | | | | Analysis Mode | | | Percent Error |
|-----------|-------|-------|---|---------------|-------|---|---------------|
| Mode No. | Freq. | Damp | Description | Mode No. | Freq. | Description | |
| 32 | 7.45 | 0.031 | SSME No. 3 Pitch (0.20), Out-of-Phase V.T. FWD/AFT Rocking (0.11) | 20 | 8.08 | LWR SSME Pitch (0.50), Out-of-Phase V.T. FWD/AFT Rocking (0.41) | 8 |
| 27 | 7.77 | 0.009 | 1st LOX Tank Bulge. UPR LH ₂ (0.34). LOX Ogive (0.14) | 18 | 7.62 | Bulge Mode Overwhelmed by SRB Energy | -2 |
| 16 | 8.42 | 0.016 | SRB 2nd Z-Bending (0.62). Roll (0.05) | 22 | 8.36 | SRB 2nd Z-Bending (0.67), Roll (0.08) | -1 |
| 13 | 9.00 | 0.008 | Orbiter Pitch and Bending (0.76). Out-of-Phase SRB Pitch (0.06) | 26 | 9.40 | Orbiter Pitch and Bending (0.76). Out-of-Phase SRB (0.02) | 4 |
| 26 | 11.94 | 0.025 | SRB 2nd Y-Bending (0.71). Motor Case No. 3 Prop (0.00) | 32 | 10.91 | SRB 2nd Y-Bend (0.37). No. 3 Prop (0.48) | 10 |
| 22 | 12.41 | 0.002 | LOX Dome Bulge (0.0016). F/L (0.15). LOX Tank (0.29) | 50 | 14.20 | SRB 2nd Y-Bend (0.47). ET Y-Bend (0.40) | 19 |
| 19 | 14.52 | 0.010 | FWD/AFT P/L X Out-of-Phase (0.14). LWR SSME Pitch (0.16) | 44 | 12.99 | LOX Dome Bulge (0.0064). F/L (0.0001). LOX Tank (0.55) | 5 |
| 30 | 14.87 | 0.022 | SRB Torsion (0.58). ET (0.14) | 72 | 17.89 | FWD/AFT P/L X Out-of-Phase (0.31) | 23 |
| 31 | 14.87 | 0.030 | Outb'd Elev ROT Out-of-Phase With Inb'd Elev (0.22) | 54 | 14.73 | SRB Torsion (0.31), ET (0.12) | 1 |
| 33 | 15.97 | 0.006 | LOX Dome Bulge (0.0066). LOX Tank (0.30). SRB Axial (0.12) | 53 | 14.61 | Outb'd Elev ROT Out-of-Phase With Inb'd Elev (0.11), SRB Torsion (0.30) | 2 |
| 17 | 15.97 | 0.027 | Payload Pitch (0.12). OMS POD X (0.18). ET (0.25) | 57 | 15.15 | LOX Dome Bulge (0.0025), LOX Tank (0.17), SRB Propellant (0.42) | 5 |

TABLE 7. (Concluded)

| Test Mode | | | Analysis Mode | | | Percent Error |
|-----------|-------|-------|--|----------------|-------|---|
| Mode No. | Freq. | Damp | Description | Mode No. | Freq. | |
| 25 | 16.15 | 0.012 | OMS POS X (0.16), Out-of-Phase P/L X (0.07), Crew Mod X (0.03) and Z (0.05), ET (0.28) | | | |
| 35 | 18.96 | 0.041 | SRB Axial (0.43), LOX Dome (0.0092), ET (0.48) | 6 ² | 15.90 | SRB Axial Out-of-Phase with Propellant (0.12), LOX Dome (0.0054), ET (0.85) |
| 36 | 27.48 | | SSME Axial, UPR Out-of-Phase with LWR (0.22) OMS POD (0.33), ET (0.20) | | | |
| 39 | 30.53 | 0.014 | SSME Axial, LWR Out-of-Phase with UPR (0.28), OMS POD (0.06), ET (0.35) | | | |
| 34 | 31.23 | 0.044 | UPR SSME Axial (0.31), OMS POD (0.19), ET (0.24) | 169 | 32.97 | UPR SSME Axial (0.44), OMS POD (0.07), ET (0.16) |
| 37 | 34.74 | 0.018 | UPR SSME (0.48) Axial In-Phase with LWR (0.01), OMS POD (0.14), ET (0.07) | 184 | 36.69 | UPR SSME Axial (0.56), OMS POD (0.05), ET (0.01) |

**TABLE 8. MGVGT MODAL CORRELATION
[CONFIGURATION - LIFTOFF (ANTISYMMETRIC)]**

| Test Mode | | | | Analysis Mode | | | Percent Error |
|-----------|-------|----------------|--|---------------|-------|--|---------------|
| Mode No. | Freq. | Damp? | Description | Mode No. | Freq. | Description | |
| 10 | 2.08 | 0.010 | SRB Yaw and Y-Bending (0.63), ET YB (0.20) | 4 | 2.20 | SRB Yaw and Y-Bending (0.74) | 6 |
| 8 | 2.24 | 0.010 | SRB Pitch (0.33), Roll (0.18), Orbiter Y-Bend (0.29), Roll (0.03) | 5 | 2.31 | SRB Pitch (0.82), Roll (0.07), Orbiter Y-Bend (0.03) | 3 |
| 11 | 2.47 | 0.014 | SRB Pitch (0.60), Roll (0.12), Orbiter Roll and Yaw (0.12) | 6 | 2.73 | SRB Pitch (0.13), Roll (0.31), Orbiter Roll and Yaw (0.41) | 10 |
| 15 | 3.37 | 0.016 0.022 | SRB X(0.35), Y-Bend (0.16), Vert Tail Y-Bend (0.16) | 7 | 3.61 | SRB X (0.58), Y-Bend (0.13), Vert Tail Y-Bend (0.06) | 7 |
| 27 | 4.53 | 0.005 0.007 | Gear Train, SRB Roll (0.08), ET (0.09), Vert Tail Y-Bend (0.40) | 8 | 3.76 | Gear Train, SRB Roll (0.11), ET (0.01), Vert Tail Y-Bend (0.57) | 7 |
| 5 | 4.12 | 0.014 | SRB Roll (0.20), Z-Bend (0.02), ORB Yaw (0.44), Inclid C/M Y (0.10) | 9 | 3.86 | SRB Roll (0.25), Z-Bend (0.16), ORB Yaw (0.27), Inclid C/M Y (0.07) | 7 |
| 21 | 4.71 | 0.010 | SRB Roll (0.27), Pitch (0.12), ORB Yaw and Roll (0.39) | 11 | 4.88 | SRB Yaw (0.25), Pitch (0.05), Roll (0.02), ORB Yaw and Roll (0.58) | 4 |
| 28 | 4.98 | 0.016 | Wing 1st Bend (0.38), SRB Y (0.14), SRB Z (0.19), FUS Y (0.06) | 15 | 6.0 | Wing 1st Bending (0.27), F P/L Y (0.20), SRB Y (0.09), SRB Z (0.06), Fuse Y (0.05) | |
| 20 | 5.14 | 0.014 0.017 | SRB Y-Bend (0.59), Z (0.13), Roll (0.03), ET Y Bend (0.13) | 12 | 5.42 | SRB Y-Bend (0.41), ET Y-Bend (0.23) | 5 |
| 1 | 5.45 | 0.013 | SRB Z-Bend (0.43), Y-Bend (0.12), OMS POD Y (0.05) | 14 | 5.55 | SRB Z-Bend (0.64), Y-Bend (0.03), Roll (0.03) | 2 |
| 25 | 5.57 | 0.016 | Orbiter Yaw and Y-Bend (0.31), SRB Y-Bend (0.18), Z-Bend (0.15), Roll (0.04) | 15 | 6.01 | Orbiter Yaw and Y-Bend (0.47), SRB Y-Bend (0.09), Z-Bend (0.07) | 8 |

TARIE 8. (Continued)

| Test Mode | | | | Analysis Mode | | | |
|-----------|-------|--------------|--|---------------|-------|---|---------------|
| Mode No. | Freq. | Damp | Description | Mode No. | Freq. | Description | Percent Error |
| 16 | 7.41 | 0.22 0.28 | ET Y-Bend (0.72), SRB Y-Bend (0.11) | 18 | 6.99 | ET Y-Bend (0.46), SRB Y-Bend (0.28) | 8 |
| 24 | 8.30 | 0.010 | Payload Y Out-of-Phase (0.21), FUS Torsion (0.21), Out-of-Phase Wing Bend (0.10) | 23 | 8.90 | AFT Payload (0.03), FUS Torsion (0.20), Out-of-Phase Wing Bend (0.14) | 7 |
| 18 | 9.28 | 0.011 | ET LOX Tank Torsion | 28 | 10.21 | ET LOX Tank Torsion | 10 |
| 2 | 10.10 | 0.028 | SRB 2nd Z-Bend (0.60), Yaw (0.10), Axial (0.04) | 32 | 10.63 | SRB 2nd Z-Bend (0.56), Yaw (0.15), Axial (0.04) | 5 |
| 19 | 10.65 | 0.022 | SRB 2nd Y-Bend (0.61), Z-Bend (0.29) | 35 | 11.24 | SRB 2nd Y-Bend (0.60), Z-Bend (0.19) | 6 |
| 31 | 13.89 | | Vert Tail Torsion (0.68) | 61 | 16.22 | Vert Tail Torsion (0.39), Outb'd Elev. Twist (0.15) | 17 |
| 17 | 14.56 | 0.010 | Gear Train W/SRB Torsion ET Roll (0.53), SRB Torsion (0.36) | 47 | 14.20 | Gear Train W/SRB Torsion, ET Roll (0.53), SRB Torsion (0.15) | 3 |
| 12 | 14.72 | 0.028 | Gear Train W/ET Torsion (0.12), and SRB Torsion (0.59) | 47 | 14.20 | | 4 |
| 3 | 16.85 | 0.037 | SRB 3rd Z-Bend (0.61), ET Shell (0.24) | 64 | 16.69 | SRB 3rd Z-Bend (0.55), ET Shell (0.19) | 1 |
| 29 | 17.61 | | Crew MOD Y (0.06), Out-of-Phase FWD FUS Side Bend (0.29) | 72 | 18.30 | Crew MOD Y (0.06), Out-of-Phase FWD FUS Side Bend (0.21) | 4 |
| 14 | 18.90 | 0.030 | SRB Axial (0.78) | 87 | 20.75 | SRB Axial (0.59), Y-Bend (0.28) | 10 |
| 26 | 21.64 | 0.02 | Fuselage Torsion, Side Bend, Yaw (0.25), OMS POD (0.17) | 72 | 18.30 | Fuselage Torsion, Side Bend, Yaw (19), OMS POD (0.15) | 18 |

TABLE 8. (Concluded)

| Test Mode | | | | Analysis Mode | | | Percent Error |
|-----------|-------|-------|--------------------------|---------------|-------|----------------------|---------------|
| Mode No. | Freq. | Damp | Description | Mode No. | Freq. | Description | |
| 7 | 23.84 | 0.022 | SRB 4th Z-Bend (0.65) | 112 | 24.89 | SRB Z-Bending (0.41) | 4 |
| 30 | 24.81 | 0.012 | SRB 4th Y-Bending (0.63) | 123 | 26.35 | SRB Y-Bending (0.47) | 6 |

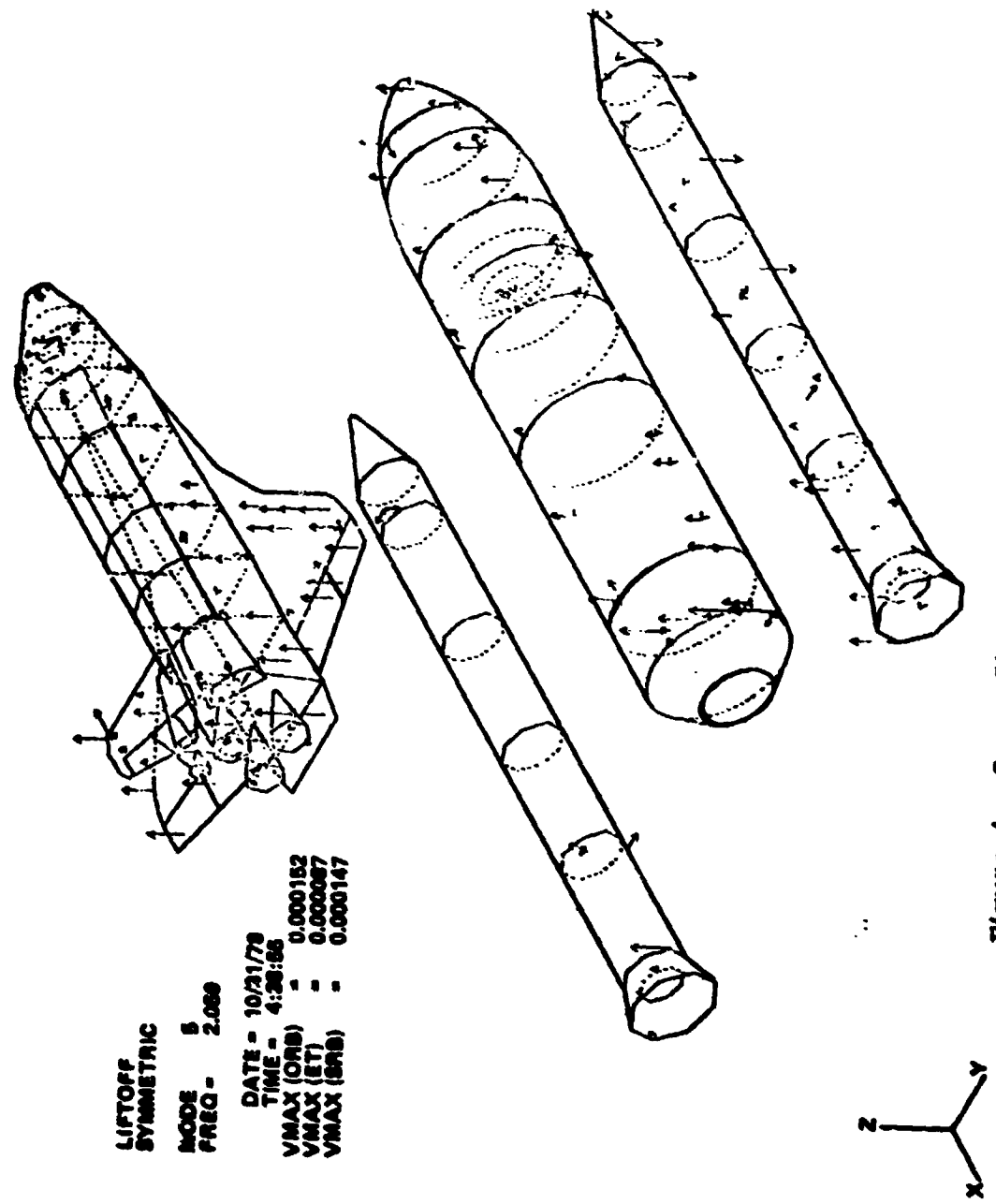


Figure 4. Space Shuttle -MVGVT Orbiter/ET/SRB.

LIFTOFF
SYMMETRIC

MODE 5
FREQ = 2.056

DATE = 10/31/78
TIME = 4:38:56
VMAX (ET) = 0.000067
VMAX (SRB) = 0.000147

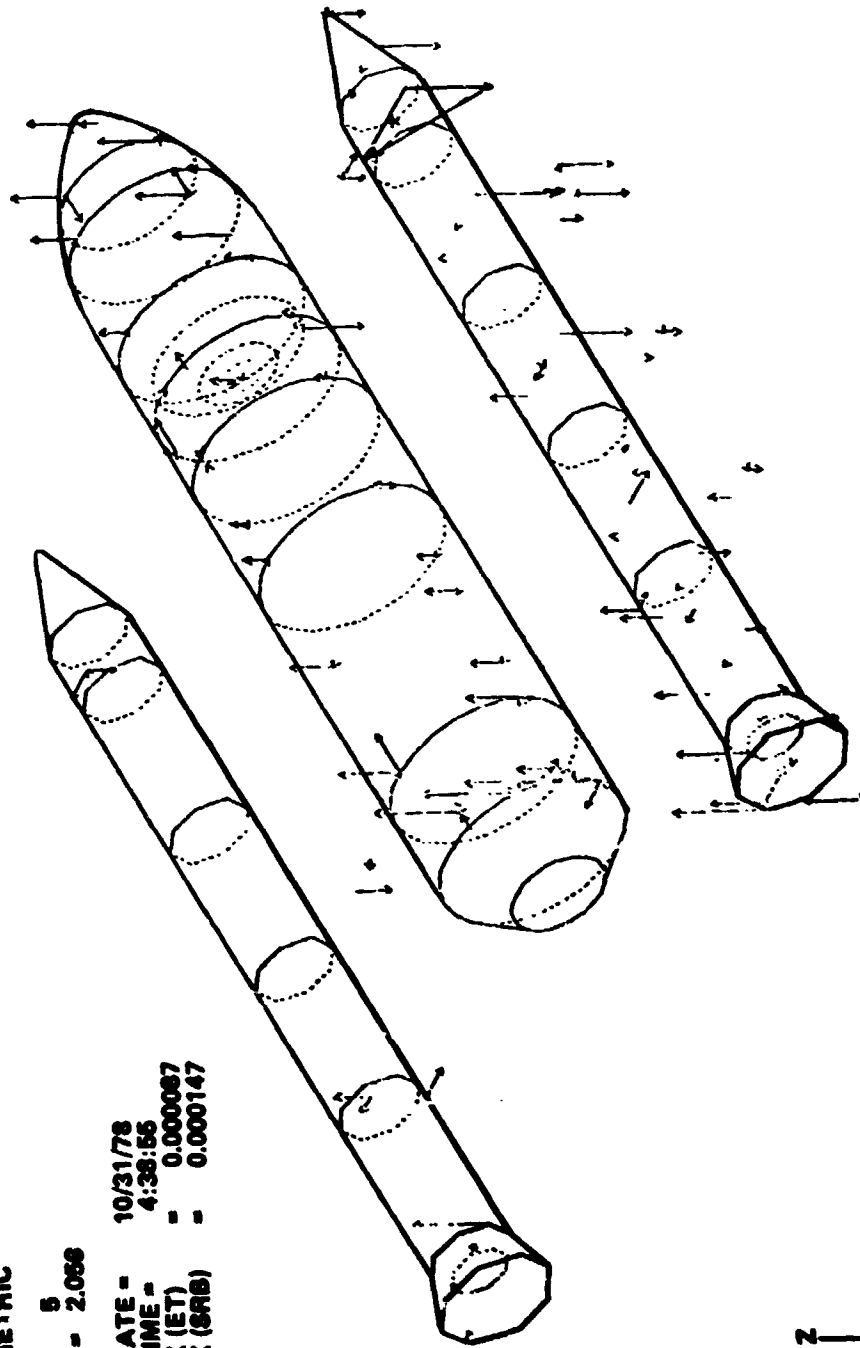


Figure 5. Space Shuttle MGVVT Orbiter/ET/SRB.

LIFTOFF
SYMMETRIC

MODE 5
FREQ = 2.069

DATE = 10/31/78
TIME = 4:38:56
VMAX = 0.000152

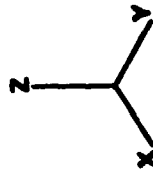
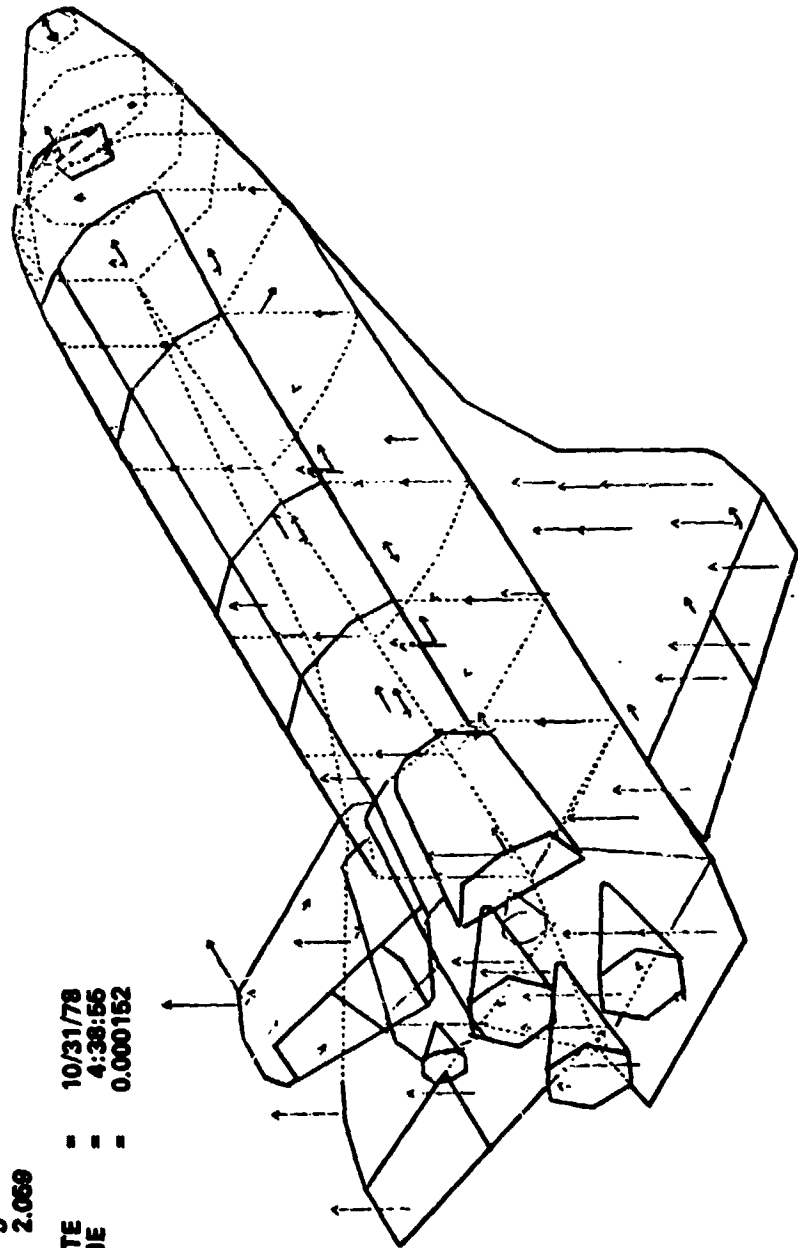
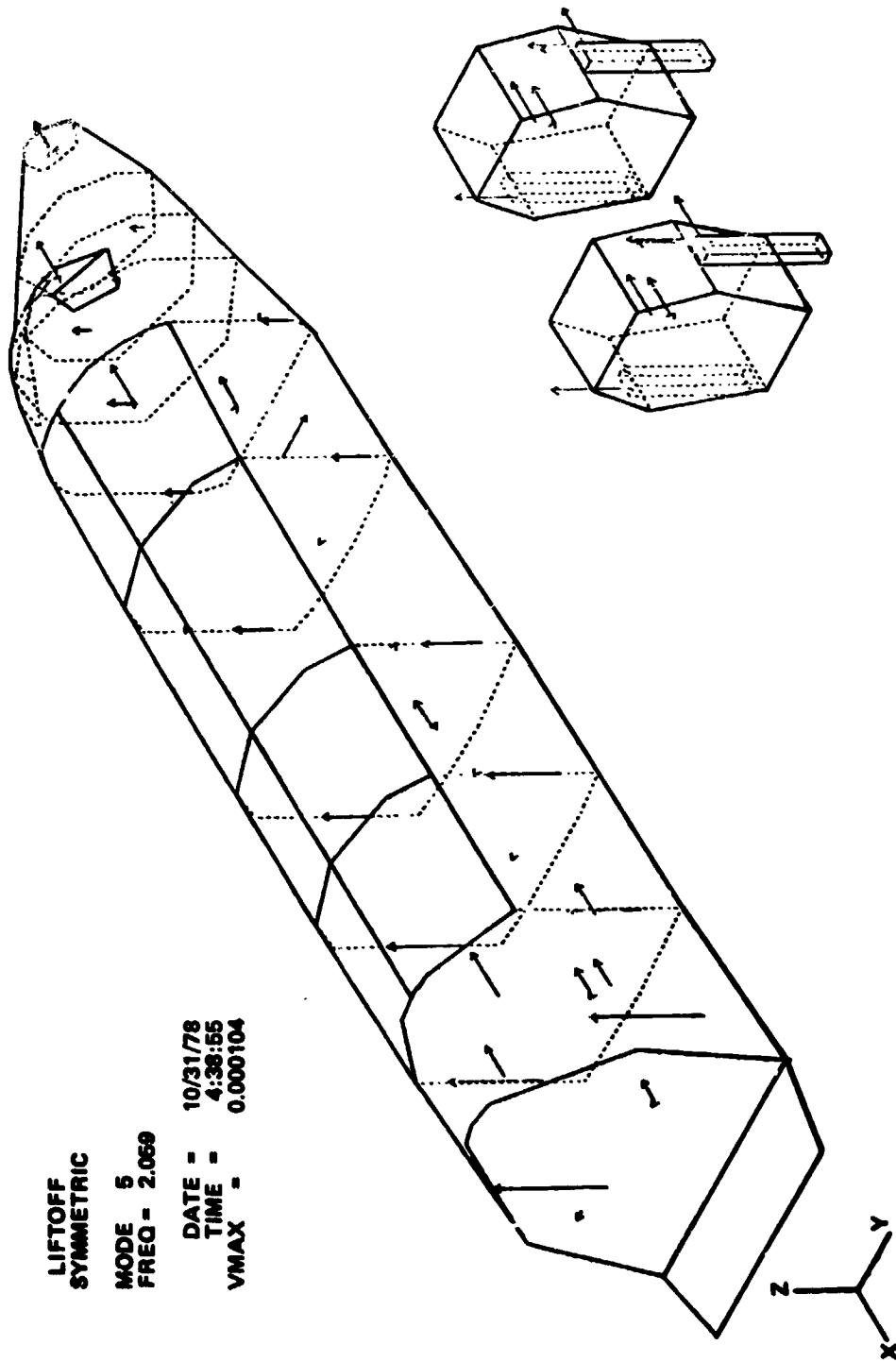


Figure 6. Space Shuttle MGVGT Orbiter/ET/SRB.



LIFTOFF
 SYMMETRIC
 MODE 5
 FREQ = 2.069
 DATE = 10/31/78
 TIME = 4:38:55
 VMAX = 0.000104

Figure 7. Space Shuttle MGVGT Orbiter/ET/SRB.

LIFTOFF
SYMMETRIC

MODE 5
FREQ = 2.069

DATE = 10/31/78
TIME = 4:38:55
VMAX = 0.000152

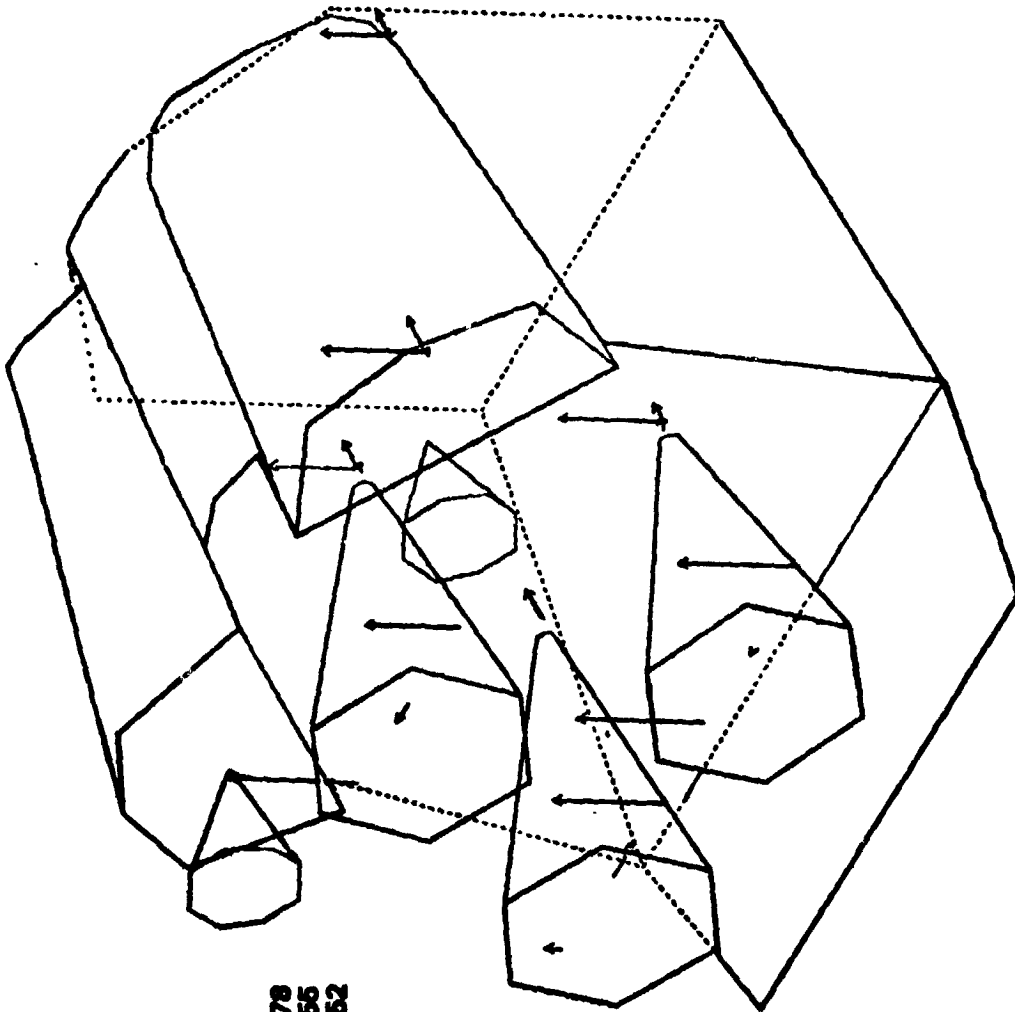
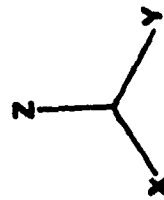


Figure 8. Space Shuttle MVGVT Orbiter/ET/SRB.

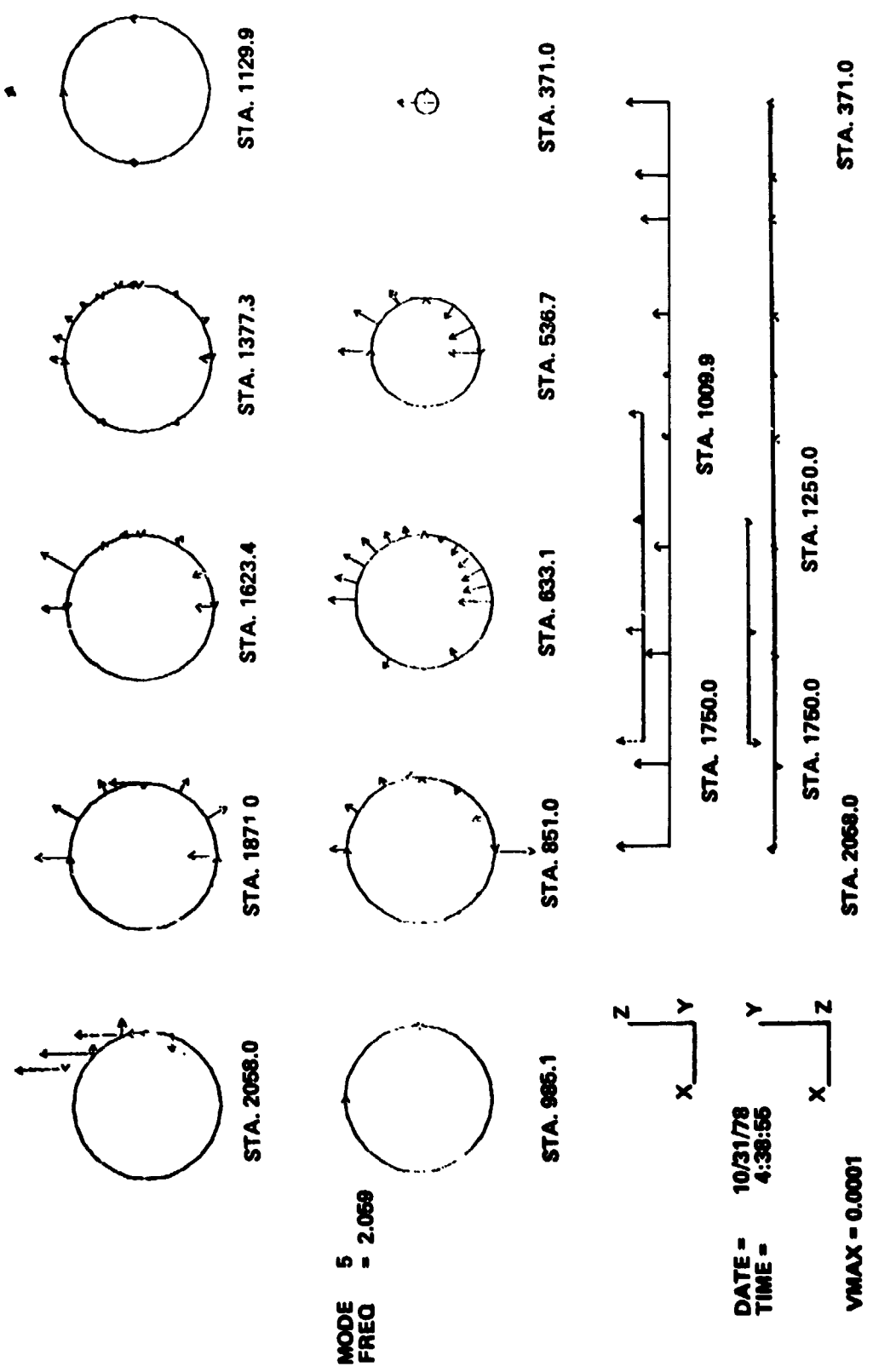
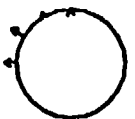


Figure 9. Space Shuttle MGVGT Orbiter/ET/SRB External Tank Lift-Off Symmetric.

LH2 TANK AFT BULKHEAD



STA. 2161.4

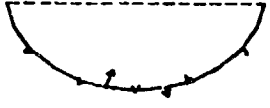
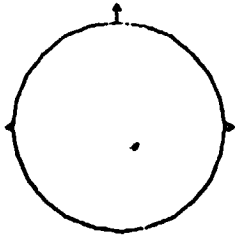


STA. 911.2

LOX TANK AFT BULKHEAD



STA. 951.5



MODE 5
FREQ - 2.088

DATE - 10/31/78
TIME - 4:38:56

VMAX - 0.0001

Figure 10. Space Shuttle MGVVT Orbiter/ET /SRB External Tank Lift-Off Symmetric.

SYNTHETIC
 1985 3
 FROM 2.0008

L I F T O F F

10/31/70
 4:50:55

DATE
 TIME

REF. FORCE FB16Z

| ACC LOC | CO G/LB | QUAD G/LB | ACC LOC | CO G/LB | QUAD G/LB | ACC C | PHASE | ACC C | PHASE |
|-----------|-----------|-----------|------------|-----------|-----------|--------|--------|--------|--------|
| 1 F7C91X | -0.000055 | -0.000053 | 43 F7C95X | -0.000037 | -0.000010 | 0.0012 | -99.3 | 0.0012 | -99.3 |
| 2 F7C91Y | -0.000071 | -0.000059 | 45 F7C95Z | 0.000016 | 0.000000 | 0.0054 | 77.2 | 0.0054 | 77.2 |
| 3 F7C92X | -0.000073 | 0.000009 | 47 F7C97X | -0.000007 | -0.000013 | 0.0026 | -93.8 | 0.0026 | -93.8 |
| 4 F7C92Y | -0.000022 | 0.000022 | 42 F7C96X | -0.000007 | -0.000013 | 0.0052 | -93.0 | 0.0052 | -93.0 |
| 5 F7C92Z | -0.000034 | 0.000014 | 49 F7C97Z | 0.000015 | 0.000032 | 0.0052 | 73.4 | 0.0052 | 73.4 |
| 6 F7C93X | 0.000033 | 0.000015 | 39 F7C96Z | -0.000007 | -0.000013 | 0.0027 | -93.6 | 0.0027 | -93.6 |
| 7 F7C93Y | -0.000027 | -0.000019 | 51 F7C97X | 0.000016 | 0.000007 | 0.0050 | 73.3 | 0.0050 | 73.3 |
| 8 F7C93Z | -0.000042 | 0.000022 | 52 F7C97Y | -0.000007 | -0.000007 | 0.0071 | -101.0 | 0.0071 | -101.0 |
| 9 F7C94X | -0.000026 | -0.000023 | 53 F7C97Z | -0.000001 | -0.000001 | 0.0050 | 107.7 | 0.0050 | 107.7 |
| 10 F7C94Y | -0.000027 | 0.000023 | 54 F7C98X | -0.000008 | -0.000033 | 0.0070 | -99.4 | 0.0070 | -99.4 |
| 11 F7C94Z | -0.000022 | 0.000022 | 55 F7C98Y | 0.000016 | 0.000037 | 0.0053 | 79.4 | 0.0053 | 79.4 |
| 12 F7C95X | -0.000023 | 0.000015 | 56 F7C98Z | -0.000009 | -0.000021 | 0.0054 | 67.6 | 0.0054 | 67.6 |
| 13 F7C95Y | -0.000026 | -0.000023 | 57 F7C99X | -0.000004 | -0.000027 | 0.0049 | -90.5 | 0.0049 | -90.5 |
| 14 F7C95Z | -0.000026 | 0.000023 | 58 F7C99Y | 0.000017 | 0.000018 | 0.0047 | 105.9 | 0.0047 | 105.9 |
| 15 F7C96X | -0.000022 | -0.000021 | 59 F7C99Z | -0.000007 | -0.000007 | 0.0056 | -93.1 | 0.0056 | -93.1 |
| 16 F7C96Y | -0.000022 | 0.000021 | 60 F7C99X | -0.000003 | -0.000017 | 0.0047 | -90.5 | 0.0047 | -90.5 |
| 17 F7C96Z | -0.000023 | 0.000020 | 61 F7C99Y | -0.000004 | -0.000017 | 0.0041 | -91.9 | 0.0041 | -91.9 |
| 18 F7C97X | -0.000023 | -0.000023 | 62 F7C99Z | -0.000004 | -0.000023 | 0.0042 | -91.5 | 0.0042 | -91.5 |
| 19 F7C97Y | 0.000027 | 0.000023 | 63 F7C99X | -0.000003 | -0.000023 | 0.0047 | -101.1 | 0.0047 | -101.1 |
| 20 F7C97Z | 0.000027 | 0.000023 | 64 F7C99Y | 0.000019 | 0.000019 | 0.0049 | -90.7 | 0.0049 | -90.7 |
| 21 F7C98X | -0.000029 | -0.000022 | 65 F7C99Z | -0.000003 | -0.000019 | 0.0052 | 92.1 | 0.0052 | 92.1 |
| 22 F7C98Y | -0.000021 | 0.000022 | 66 F7C99X | -0.000003 | -0.000018 | 0.0051 | -101.0 | 0.0051 | -101.0 |
| 23 F7C98Z | -0.000027 | 0.000022 | 67 F7C99Y | 0.000018 | 0.000019 | 0.0051 | 91.4 | 0.0051 | 91.4 |
| 24 F7C99X | -0.000022 | -0.000021 | 68 F7C99Z | -0.000001 | -0.000000 | 0.0049 | -101.6 | 0.0049 | -101.6 |
| 25 F7C99Y | -0.000027 | 0.000021 | 69 F7C99X | -0.000007 | -0.000003 | 0.0047 | -99.1 | 0.0047 | -99.1 |
| 26 F7C99Z | 0.000027 | 0.000021 | 70 F7C99Y | -0.000003 | -0.000003 | 0.0049 | -113.5 | 0.0049 | -113.5 |
| 27 F7C99X | -0.000027 | -0.000023 | 71 F7C99Z | 0.000008 | 0.000007 | 0.0045 | -101.2 | 0.0045 | -101.2 |
| 28 F7C99Y | -0.000027 | 0.000023 | 72 F7C99X | -0.000000 | 0.000000 | 0.0044 | 91.2 | 0.0044 | 91.2 |
| 29 F7C99Z | -0.000021 | -0.000021 | 73 F7C99Y | 0.000021 | 0.000021 | 0.0044 | -101.6 | 0.0044 | -101.6 |
| 30 F7C99X | -0.000027 | 0.000021 | 74 F7C99Z | -0.000007 | -0.000003 | 0.0049 | -91.5 | 0.0049 | -91.5 |
| 31 F7C99Y | -0.000027 | 0.000021 | 75 F7C99X | -0.000005 | -0.000005 | 0.0045 | 79.4 | 0.0045 | 79.4 |
| 32 F7C99Z | -0.000027 | 0.000021 | 76 F7C99Y | 0.000000 | 0.000000 | 0.0045 | -101.6 | 0.0045 | -101.6 |
| 33 F7C99X | -0.000027 | -0.000021 | 77 F7C99Z | 0.000022 | 0.000022 | 0.0045 | 91.5 | 0.0045 | 91.5 |
| 34 F7C99Y | -0.000027 | 0.000021 | 78 F7C99X | -0.000004 | -0.000004 | 0.0045 | -101.6 | 0.0045 | -101.6 |
| 35 F7C99Z | -0.000027 | 0.000021 | 79 F7C99Y | -0.000004 | -0.000004 | 0.0045 | 77.1 | 0.0045 | 77.1 |
| 36 F7C99X | -0.000027 | -0.000021 | 80 F7C99Z | 0.000027 | 0.000027 | 0.0045 | 154.1 | 0.0045 | 154.1 |
| 37 F7C99Y | -0.000027 | 0.000021 | 81 F7C99X | -0.000003 | -0.000003 | 0.0045 | -101.6 | 0.0045 | -101.6 |
| 38 F7C99Z | -0.000027 | 0.000021 | 82 F7C99Y | -0.000003 | -0.000003 | 0.0045 | 79.4 | 0.0045 | 79.4 |
| 39 F7C99X | -0.000027 | -0.000021 | 83 F7C99Z | 0.000027 | 0.000027 | 0.0045 | -101.6 | 0.0045 | -101.6 |
| 40 F7C99Y | -0.000027 | 0.000021 | 84 F7C99X | -0.000003 | -0.000003 | 0.0045 | 79.4 | 0.0045 | 79.4 |
| 41 F7C99Z | -0.000027 | 0.000021 | 85 F7C99Y | -0.000003 | -0.000003 | 0.0045 | -101.6 | 0.0045 | -101.6 |
| 42 F7C99X | -0.000027 | -0.000021 | 86 F7C99Z | 0.000027 | 0.000027 | 0.0045 | 79.4 | 0.0045 | 79.4 |
| 43 F7C99Y | -0.000027 | 0.000021 | 87 F7C99X | -0.000003 | -0.000003 | 0.0045 | -101.6 | 0.0045 | -101.6 |
| 44 F7C99Z | -0.000027 | 0.000021 | 88 F7C99Y | -0.000003 | -0.000003 | 0.0045 | 79.4 | 0.0045 | 79.4 |
| 45 F7C99X | -0.000027 | -0.000021 | 89 F7C99Z | 0.000027 | 0.000027 | 0.0045 | -101.6 | 0.0045 | -101.6 |
| 46 F7C99Y | -0.000027 | 0.000021 | 90 F7C99X | -0.000003 | -0.000003 | 0.0045 | 79.4 | 0.0045 | 79.4 |
| 47 F7C99Z | -0.000027 | 0.000021 | 91 F7C99Y | -0.000003 | -0.000003 | 0.0045 | -101.6 | 0.0045 | -101.6 |
| 48 F7C99X | -0.000027 | -0.000021 | 92 F7C99Z | 0.000027 | 0.000027 | 0.0045 | 79.4 | 0.0045 | 79.4 |
| 49 F7C99Y | -0.000027 | 0.000021 | 93 F7C99X | -0.000003 | -0.000003 | 0.0045 | -101.6 | 0.0045 | -101.6 |
| 50 F7C99Z | -0.000027 | 0.000021 | 94 F7C99Y | -0.000003 | -0.000003 | 0.0045 | 79.4 | 0.0045 | 79.4 |
| 51 F7C99X | -0.000027 | -0.000021 | 95 F7C99Z | 0.000027 | 0.000027 | 0.0045 | -101.6 | 0.0045 | -101.6 |
| 52 F7C99Y | -0.000027 | 0.000021 | 96 F7C99X | -0.000003 | -0.000003 | 0.0045 | 79.4 | 0.0045 | 79.4 |
| 53 F7C99Z | -0.000027 | 0.000021 | 97 F7C99Y | -0.000003 | -0.000003 | 0.0045 | -101.6 | 0.0045 | -101.6 |
| 54 F7C99X | -0.000027 | -0.000021 | 98 F7C99Z | 0.000027 | 0.000027 | 0.0045 | 79.4 | 0.0045 | 79.4 |
| 55 F7C99Y | -0.000027 | 0.000021 | 99 F7C99X | -0.000003 | -0.000003 | 0.0045 | -101.6 | 0.0045 | -101.6 |
| 56 F7C99Z | -0.000027 | 0.000021 | 100 F7C99Y | -0.000003 | -0.000003 | 0.0045 | 79.4 | 0.0045 | 79.4 |

Figure 11. Space Shuttle MGVGT Dwell Data Orbiter *** External Tank
 *** Solid Rocket Boosters.

ORIGINAL PAGE IS
 OF POOR QUALITY

LITTON

| AGE LOC | CS 6/13 | GRAB CALS | AGE 6 | AGE LOC | CS 6/13 | GRAB CALS | AGE 6 | AGE LOC | CS 6/13 | GRAB CALS | AGE 6 | AGE LOC | CS 6/13 | GRAB CALS | AGE 6 |
|------------|----------|-----------|--------|------------|----------|-----------|--------|------------|----------|-----------|--------|------------|----------|-----------|--------|
| 89 WR309Z | 0.000013 | 0.000070 | 0.0367 | 123 ZF133N | 0.000005 | 0.000020 | 0.0199 | 123 ZF133N | 0.000005 | 0.000020 | 0.0199 | 123 ZF133N | 0.000005 | 0.000020 | 0.0199 |
| 90 WR309Z | 0.000016 | 0.000077 | 0.0367 | 124 ZF133N | 0.000002 | 0.000003 | 0.0011 | 124 ZF133N | 0.000002 | 0.000003 | 0.0011 | 124 ZF133N | 0.000002 | 0.000003 | 0.0011 |
| 91 WR309Z | 0.000019 | 0.000074 | 0.0395 | 125 ZF133N | 0.000002 | 0.000001 | 0.0011 | 125 ZF133N | 0.000002 | 0.000001 | 0.0011 | 125 ZF133N | 0.000002 | 0.000001 | 0.0011 |
| 92 WR309Z | 0.000010 | 0.000073 | 0.0417 | 126 ZF133N | 0.000012 | 0.000009 | 0.0312 | 126 ZF133N | 0.000012 | 0.000009 | 0.0312 | 126 ZF133N | 0.000012 | 0.000009 | 0.0312 |
| 93 WR309Z | 0.000022 | 0.000087 | 0.0464 | 127 ZF133N | 0.000004 | 0.000024 | 0.0137 | 127 ZF133N | 0.000004 | 0.000024 | 0.0137 | 127 ZF133N | 0.000004 | 0.000024 | 0.0137 |
| 94 WR309Z | 0.000003 | 0.000023 | 0.0135 | 128 ZF133N | 0.000005 | 0.000014 | 0.0253 | 128 ZF133N | 0.000005 | 0.000014 | 0.0253 | 128 ZF133N | 0.000005 | 0.000014 | 0.0253 |
| 95 WR309Z | 0.000004 | 0.000023 | 0.0135 | 129 ZF133N | 0.000005 | 0.000036 | 0.0136 | 129 ZF133N | 0.000005 | 0.000036 | 0.0136 | 129 ZF133N | 0.000005 | 0.000036 | 0.0136 |
| 96 WR309Z | 0.000004 | 0.000023 | 0.0146 | 130 ZF133N | 0.000009 | 0.000051 | 0.0255 | 130 ZF133N | 0.000009 | 0.000051 | 0.0255 | 130 ZF133N | 0.000009 | 0.000051 | 0.0255 |
| 97 WR309Z | 0.000004 | 0.000021 | 0.0094 | 131 ZF141Y | 0.000001 | 0.000001 | 0.0018 | 131 ZF141Y | 0.000001 | 0.000001 | 0.0018 | 131 ZF141Y | 0.000001 | 0.000001 | 0.0018 |
| 98 WR309Z | 0.000024 | 0.000100 | 0.0532 | 141 ZF142N | 0.000009 | 0.000044 | 0.0233 | 141 ZF142N | 0.000009 | 0.000044 | 0.0233 | 141 ZF142N | 0.000009 | 0.000044 | 0.0233 |
| 99 WR309Z | 0.000025 | 0.000070 | 0.0322 | 142 ZF142N | 0.000008 | 0.000038 | 0.0202 | 142 ZF142N | 0.000008 | 0.000038 | 0.0202 | 142 ZF142N | 0.000008 | 0.000038 | 0.0202 |
| 100 WR103Z | 0.000022 | 0.000112 | 0.0596 | 143 ZF142N | 0.000008 | 0.000039 | 0.0207 | 143 ZF142N | 0.000008 | 0.000039 | 0.0207 | 143 ZF142N | 0.000008 | 0.000039 | 0.0207 |
| 101 WR103Z | 0.000028 | 0.000108 | 0.0544 | 144 ZF142N | 0.000007 | 0.000032 | 0.0171 | 144 ZF142N | 0.000007 | 0.000032 | 0.0171 | 144 ZF142N | 0.000007 | 0.000032 | 0.0171 |
| 102 WR103Z | 0.000024 | 0.000119 | 0.0603 | 145 ZF145N | 0.000005 | 0.000029 | 0.0108 | 145 ZF145N | 0.000005 | 0.000029 | 0.0108 | 145 ZF145N | 0.000005 | 0.000029 | 0.0108 |
| 103 WR103Z | 0.000023 | 0.000101 | 0.0535 | 146 ZF145N | 0.000004 | 0.000024 | 0.0079 | 146 ZF145N | 0.000004 | 0.000024 | 0.0079 | 146 ZF145N | 0.000004 | 0.000024 | 0.0079 |
| 104 VL104Z | 0.000014 | 0.000036 | 0.0265 | 147 ZF147E | 0.000001 | 0.000001 | 0.0029 | 147 ZF147E | 0.000001 | 0.000001 | 0.0029 | 147 ZF147E | 0.000001 | 0.000001 | 0.0029 |
| 105 VL104Z | 0.000014 | 0.000031 | 0.0227 | 148 ZF148N | 0.000001 | 0.000001 | 0.0011 | 148 ZF148N | 0.000001 | 0.000001 | 0.0011 | 148 ZF148N | 0.000001 | 0.000001 | 0.0011 |
| 106 VL104Z | 0.000016 | 0.000039 | 0.0270 | 149 ZF149N | 0.000005 | 0.000021 | 0.0111 | 149 ZF149N | 0.000005 | 0.000021 | 0.0111 | 149 ZF149N | 0.000005 | 0.000021 | 0.0111 |
| 107 VL107Z | 0.000018 | 0.000094 | 0.0545 | 150 ZF150N | 0.000005 | 0.000031 | 0.0162 | 150 ZF150N | 0.000005 | 0.000031 | 0.0162 | 150 ZF150N | 0.000005 | 0.000031 | 0.0162 |
| 108 VL107Z | 0.000019 | 0.000117 | 0.0613 | 151 ZF151N | 0.000005 | 0.000031 | 0.0162 | 151 ZF151N | 0.000005 | 0.000031 | 0.0162 | 151 ZF151N | 0.000005 | 0.000031 | 0.0162 |
| 109 VL107Z | 0.000021 | 0.000115 | 0.0606 | 152 ZF152N | 0.000006 | 0.000039 | 0.0227 | 152 ZF152N | 0.000006 | 0.000039 | 0.0227 | 152 ZF152N | 0.000006 | 0.000039 | 0.0227 |
| 110 VL110Y | 0.000004 | 0.000004 | 0.0022 | 153 ZF153N | 0.000008 | 0.000043 | 0.0270 | 153 ZF153N | 0.000008 | 0.000043 | 0.0270 | 153 ZF153N | 0.000008 | 0.000043 | 0.0270 |
| 111 VL111Z | 0.000019 | 0.000019 | 0.0025 | 154 ZF154E | 0.000006 | 0.000021 | 0.0114 | 154 ZF154E | 0.000006 | 0.000021 | 0.0114 | 154 ZF154E | 0.000006 | 0.000021 | 0.0114 |
| 112 VL112Y | 0.000009 | 0.000017 | 0.0090 | 155 ZF155N | 0.000006 | 0.000019 | 0.0097 | 155 ZF155N | 0.000006 | 0.000019 | 0.0097 | 155 ZF155N | 0.000006 | 0.000019 | 0.0097 |
| 113 VL113Y | 0.000009 | 0.000023 | 0.0120 | 156 ZF156N | 0.000005 | 0.000028 | 0.0146 | 156 ZF156N | 0.000005 | 0.000028 | 0.0146 | 156 ZF156N | 0.000005 | 0.000028 | 0.0146 |
| 114 VL114X | 0.000016 | 0.000110 | 0.0674 | 157 ZF157N | 0.000009 | 0.000052 | 0.0013 | 157 ZF157N | 0.000009 | 0.000052 | 0.0013 | 157 ZF157N | 0.000009 | 0.000052 | 0.0013 |
| 115 VL115Y | 0.000002 | 0.000004 | 0.0127 | 158 ZF158Y | 0.000005 | 0.000023 | 0.0120 | 158 ZF158Y | 0.000005 | 0.000023 | 0.0120 | 158 ZF158Y | 0.000005 | 0.000023 | 0.0120 |
| 116 VL116Z | 0.000019 | 0.000122 | 0.0633 | 159 ZF159Y | 0.000005 | 0.000023 | 0.0120 | 159 ZF159Y | 0.000005 | 0.000023 | 0.0120 | 159 ZF159Y | 0.000005 | 0.000023 | 0.0120 |
| 117 VL117Y | 0.000002 | 0.000004 | 0.0135 | 160 ZF160E | 0.000005 | 0.000021 | 0.0096 | 160 ZF160E | 0.000005 | 0.000021 | 0.0096 | 160 ZF160E | 0.000005 | 0.000021 | 0.0096 |
| 118 VL118Y | 0.000005 | 0.000009 | 0.0082 | 161 ZF161R | 0.000006 | 0.000026 | 0.0137 | 161 ZF161R | 0.000006 | 0.000026 | 0.0137 | 161 ZF161R | 0.000006 | 0.000026 | 0.0137 |
| 119 VL119Y | 0.000004 | 0.000017 | 0.0090 | 162 ZF162Z | 0.000006 | 0.000026 | 0.0137 | 162 ZF162Z | 0.000006 | 0.000026 | 0.0137 | 162 ZF162Z | 0.000006 | 0.000026 | 0.0137 |
| 120 VL120Y | 0.000002 | 0.000002 | 0.0015 | 163 ZF163R | 0.000002 | 0.000002 | 0.0005 | 163 ZF163R | 0.000002 | 0.000002 | 0.0005 | 163 ZF163R | 0.000002 | 0.000002 | 0.0005 |
| 121 VL121Y | 0.000017 | 0.000002 | 0.0422 | 164 ZF164R | 0.000005 | 0.000023 | 0.0120 | 164 ZF164R | 0.000005 | 0.000023 | 0.0120 | 164 ZF164R | 0.000005 | 0.000023 | 0.0120 |
| 122 VL122Y | 0.000017 | 0.000005 | 0.0643 | 165 ZF165R | 0.000001 | 0.000005 | 0.0011 | 165 ZF165R | 0.000001 | 0.000005 | 0.0011 | 165 ZF165R | 0.000001 | 0.000005 | 0.0011 |
| 123 VL123Y | 0.000019 | 0.000008 | 0.0029 | 166 ZF166R | 0.000001 | 0.000001 | 0.0004 | 166 ZF166R | 0.000001 | 0.000001 | 0.0004 | 166 ZF166R | 0.000001 | 0.000001 | 0.0004 |
| 124 VL124Y | 0.000002 | 0.000004 | 0.0084 | 167 ZF167Y | 0.000005 | 0.000022 | 0.0118 | 167 ZF167Y | 0.000005 | 0.000022 | 0.0118 | 167 ZF167Y | 0.000005 | 0.000022 | 0.0118 |
| 125 VL125X | 0.000004 | 0.000004 | 0.0234 | 168 ZF168Z | 0.000005 | 0.000022 | 0.0118 | 168 ZF168Z | 0.000005 | 0.000022 | 0.0118 | 168 ZF168Z | 0.000005 | 0.000022 | 0.0118 |
| 126 VL126X | 0.000002 | 0.000002 | 0.0014 | 169 ZF169Y | 0.000001 | 0.000001 | 0.0005 | 169 ZF169Y | 0.000001 | 0.000001 | 0.0005 | 169 ZF169Y | 0.000001 | 0.000001 | 0.0005 |
| 127 VL127Y | 0.000002 | 0.000002 | 0.0026 | 170 ZF170Y | 0.000001 | 0.000001 | 0.0005 | 170 ZF170Y | 0.000001 | 0.000001 | 0.0005 | 170 ZF170Y | 0.000001 | 0.000001 | 0.0005 |
| 128 VL128E | 0.000002 | 0.000002 | 0.0041 | 171 ZF171X | 0.000001 | 0.000001 | 0.0007 | 171 ZF171X | 0.000001 | 0.000001 | 0.0007 | 171 ZF171X | 0.000001 | 0.000001 | 0.0007 |
| 129 VL129E | 0.000002 | 0.000002 | 0.0149 | 172 ZF172E | 0.000002 | 0.000002 | 0.0007 | 172 ZF172E | 0.000002 | 0.000002 | 0.0007 | 172 ZF172E | 0.000002 | 0.000002 | 0.0007 |
| 130 VL130E | 0.000002 | 0.000002 | 0.0124 | 173 ZF173E | 0.000001 | 0.000001 | 0.0011 | 173 ZF173E | 0.000001 | 0.000001 | 0.0011 | 173 ZF173E | 0.000001 | 0.000001 | 0.0011 |
| 131 VL131Y | 0.000004 | 0.000004 | 0.0087 | 174 ZF174E | 0.000001 | 0.000001 | 0.0005 | 174 ZF174E | 0.000001 | 0.000001 | 0.0005 | 174 ZF174E | 0.000001 | 0.000001 | 0.0005 |
| 132 VL132Y | 0.000004 | 0.000004 | 0.0087 | 175 ZF175E | 0.000001 | 0.000001 | 0.0005 | 175 ZF175E | 0.000001 | 0.000001 | 0.0005 | 175 ZF175E | 0.000001 | 0.000001 | 0.0005 |
| 133 VL133Y | 0.000004 | 0.000004 | 0.0087 | 176 ZF176E | 0.000001 | 0.000001 | 0.0005 | 176 ZF176E | 0.000001 | 0.000001 | 0.0005 | 176 ZF176E | 0.000001 | 0.000001 | 0.0005 |
| 134 VL134Y | 0.000004 | 0.000004 | 0.0087 | 177 ZF177E | 0.000001 | 0.000001 | 0.0005 | 177 ZF177E | 0.000001 | 0.000001 | 0.0005 | 177 ZF177E | 0.000001 | 0.000001 | 0.0005 |
| 135 VL135Y | 0.000004 | 0.000004 | 0.0087 | 178 ZF178E | 0.000001 | 0.000001 | 0.0005 | 178 ZF178E | 0.000001 | 0.000001 | 0.0005 | 178 ZF178E | 0.000001 | 0.000001 | 0.0005 |
| 136 VL136Y | 0.000004 | 0.000004 | 0.0087 | 179 ZF179E | 0.000001 | 0.000001 | 0.0005 | 179 ZF179E | 0.000001 | 0.000001 | 0.0005 | 179 ZF179E | 0.000001 | 0.000001 | 0.0005 |
| 137 VL137Y | 0.000004 | 0.000004 | 0.0087 | 180 ZF180E | 0.000001 | 0.000001 | 0.0005 | 180 ZF180E | 0.000001 | 0.000001 | 0.0005 | 180 ZF180E | 0.000001 | 0.000001 | 0.0005 |
| 138 VL138Y | 0.000004 | 0.000004 | 0.0087 | 181 ZF181E | 0.000001 | 0.000001 | 0.0005 | 181 ZF181E | 0.000001 | 0.000001 | 0.0005 | 181 ZF181E | 0.000001 | 0.000001 | 0.0005 |
| 139 VL139Y | 0.000004 | 0.000004 | 0.0087 | 182 ZF182E | 0.000001 | 0.000001 | 0.0005 | 182 ZF182E | 0.000001 | 0.000001 | 0.0005 | 182 ZF182E | 0.000001 | 0.000001 | 0.0005 |
| 140 VL140Y | 0.000004 | 0.000004 | 0.0087 | 183 ZF183E | 0.000001 | 0.000001 | 0.0005 | 183 ZF183E | 0.000001 | 0.000001 | 0.0005 | 183 ZF183E | 0.000001 | 0.000001 | 0.0005 |

Figure 11. (Continued).

ORIGINAL PAGE IS
OF POOR QUALITY

STANDARD
FORM 8
FORM 8-6000

LIFT OFF

DATE 10/31/70
TIME 4:38:00

REF. FORCE

DATE TIME

PHASE

| ACC LOC | CG C/LB | QUAD C/LB | ACC LOC | CG C/LB | QUAD C/LB | ACC C | PHASE |
|-----------|----------|-----------|------------|----------|-----------|--------|--------|
| 177 EN177 | 0.00001 | 0.00001 | 221 EA231Y | -0.00000 | -0.00000 | 0.0002 | -127.4 |
| 178 EN178 | -0.00000 | -0.00002 | 222 EA222X | -0.00032 | 0.00009 | 0.0049 | 102.2 |
| 179 EN179 | 0.00001 | 0.00001 | 223 EA223Y | -0.00001 | -0.00002 | 0.0011 | -103.2 |
| 180 EN180 | -0.00000 | -0.00001 | 224 EA224Z | -0.00018 | -0.00003 | 0.0432 | -102.3 |
| 181 EN181 | 0.00005 | 0.00002 | 225 EA225X | 0.00002 | 0.00007 | 0.0038 | 76.2 |
| 182 EN182 | 0.00000 | -0.00005 | 226 EA226Y | 0.00013 | 0.00013 | 0.0059 | 77.3 |
| 183 EN183 | 0.00000 | 0.00000 | 227 EA227Z | -0.00016 | -0.00007 | 0.0460 | -100.6 |
| 184 EN184 | 0.00000 | 0.00000 | 228 EA228X | 0.00011 | 0.00006 | 0.0064 | 28.1 |
| 185 EN185 | -0.00001 | 0.00001 | 229 EA229Y | -0.00017 | -0.00007 | 0.0394 | -102.8 |
| 186 EN186 | 0.00000 | 0.00000 | 230 EA230Z | 0.00000 | 0.00000 | 0.0022 | 170.0 |
| 187 EN187 | 0.00000 | 0.00000 | 231 EA231Y | 0.00005 | 0.00024 | 0.0128 | 79.0 |
| 188 EN188 | 0.00000 | 0.00000 | 232 EA232Z | -0.00017 | -0.00007 | 0.0453 | -102.4 |
| 189 EN189 | 0.00000 | 0.00000 | 233 EA233X | -0.00005 | -0.00000 | 0.0156 | -93.8 |
| 190 EN190 | -0.00000 | -0.00000 | 234 EA234Y | 0.00002 | 0.00010 | 0.0054 | -97.6 |
| 191 EN191 | 0.00000 | 0.00000 | 235 EA235X | 0.00000 | 0.00019 | 0.0101 | 77.2 |
| 192 EN192 | -0.00000 | -0.00000 | 236 EA236Y | 0.00000 | 0.00001 | 0.0110 | 77.4 |
| 193 EN193 | 0.00000 | 0.00000 | 237 EA237Z | 0.00004 | 0.00015 | 0.0073 | 74.3 |
| 194 EN194 | 0.00000 | 0.00000 | 238 EA238X | -0.00004 | -0.00007 | 0.0042 | -118.0 |
| 195 EN195 | -0.00000 | -0.00000 | 239 EA239Y | 0.00006 | 0.00002 | 0.0143 | 76.9 |
| 196 EN196 | 0.00000 | 0.00000 | 240 EA240Z | -0.00003 | -0.00001 | 0.0034 | -104.3 |
| 197 EN197 | 0.00000 | 0.00000 | 241 EA241X | 0.00010 | 0.00043 | 0.0223 | 76.3 |
| 198 EN198 | 0.00000 | 0.00000 | 242 EA242Y | -0.00006 | -0.00018 | 0.0079 | -103.3 |
| 199 EN199 | 0.00000 | 0.00000 | 243 EA243X | 0.00003 | 0.00016 | 0.0083 | 77.5 |
| 200 EN200 | -0.00001 | -0.00001 | 244 EA244Y | 0.00001 | 0.00002 | 0.0012 | 67.4 |
| 201 EN201 | 0.00000 | 0.00000 | 245 EA245Z | -0.00001 | -0.00001 | 0.0008 | -140.3 |
| 202 EN202 | 0.00000 | 0.00000 | 246 EA246X | 0.00002 | 0.00002 | 0.0326 | -101.2 |
| 203 EN203 | -0.00001 | -0.00001 | 247 EA247Y | 0.00009 | 0.00046 | 0.0232 | 79.5 |
| 204 EN204 | 0.00000 | 0.00000 | 248 EA248Z | -0.00021 | -0.00106 | 0.0530 | -101.4 |
| 205 EN205 | 0.00000 | 0.00000 | 249 EA249X | 0.00011 | 0.00049 | 0.0261 | -102.7 |
| 206 EN206 | -0.00000 | -0.00000 | 250 EA250Y | 0.00001 | 0.00002 | 0.0011 | 69.8 |
| 207 EN207 | 0.00000 | 0.00000 | 251 EA251Z | -0.00000 | -0.00000 | 0.0018 | 93.1 |
| 208 EN208 | 0.00000 | 0.00000 | 252 EA252X | 0.00002 | 0.00009 | 0.0039 | 73.8 |
| 209 EN209 | 0.00000 | 0.00000 | 253 EA253Y | 0.00001 | 0.00004 | 0.0017 | 67.9 |
| 210 EN210 | 0.00000 | 0.00000 | 254 EA254Z | 0.00008 | 0.00044 | 0.0238 | 79.3 |
| 211 EN211 | 0.00000 | 0.00000 | 255 EA255X | -0.00007 | -0.00036 | 0.0190 | -101.5 |
| 212 EN212 | 0.00000 | 0.00000 | 256 EA256Y | 0.00007 | 0.00033 | 0.0016 | 54.9 |
| 213 EN213 | 0.00000 | 0.00000 | 257 EA257Z | 0.00012 | 0.00068 | 0.0350 | 79.6 |
| 214 EN214 | 0.00000 | 0.00000 | 258 EA258X | -0.00002 | -0.00007 | 0.0048 | -101.6 |
| 215 EN215 | 0.00000 | 0.00000 | 259 EA259Y | 0.00002 | 0.00014 | 0.0058 | 74.6 |
| 216 EN216 | -0.00000 | -0.00000 | 260 EA260Z | -0.00001 | -0.00001 | 0.0019 | -106.3 |
| 217 EN217 | 0.00000 | 0.00000 | 261 EA261X | 0.00017 | 0.00076 | 0.0435 | -102.4 |
| 218 EN218 | 0.00000 | 0.00000 | 262 EA262Y | -0.00009 | -0.00041 | 0.0230 | 81.5 |
| 219 EN219 | 0.00000 | 0.00000 | 263 EA263Z | 0.00000 | 0.00000 | 0.0000 | 74.6 |
| 220 EN220 | -0.00000 | -0.00000 | 264 EA264X | -0.00000 | -0.00000 | 0.0000 | -103.3 |

Figure 11. (Continued).

ALLOYI
1947-1950
1951-1952

GENERAL
1953-1954
1955-1956

| AGE LOG | CO C/LB | GRAB C/LB | AGE C | FRASE | AGE LOG | CO C/LB | GRAB C/LB | AGE C | FRASE |
|------------|---------|-----------|--------|-------|------------|---------|-----------|--------|-------|
| 268 RT2601 | 0.00001 | 0.00001 | 0.0007 | 126.2 | 299 LR181Y | 0.00005 | 0.00046 | 0.0239 | 94.8 |
| 268 RT2602 | 0.00011 | 0.00009 | 0.0011 | 79.4 | 310 LR181Z | 0.00024 | 0.00126 | 0.0633 | 78.0 |
| 268 RT2603 | 0.00022 | 0.00014 | 0.0024 | 71.2 | 311 LR181A | 0.00000 | 0.00000 | 0.0000 | 59.3 |
| 268 RT2604 | 0.00032 | 0.00022 | 0.0042 | 18.5 | 312 LR181B | 0.00003 | 0.00013 | 0.0157 | 96.4 |
| 270 RT2701 | 0.00020 | 0.00017 | 0.0038 | 73.4 | 313 LR181C | 0.00012 | 0.00058 | 0.0306 | 78.4 |
| 271 RT2711 | 0.00010 | 0.00012 | 0.0022 | 103.2 | 314 LR181D | 0.00003 | 0.00019 | 0.0256 | 83.2 |
| 272 RT2721 | 0.00024 | 0.00022 | 0.0048 | 79.2 | 315 LR181E | 0.00003 | 0.00012 | 0.0048 | 168.4 |
| 273 RT2731 | 0.00034 | 0.00032 | 0.0072 | 89.3 | 316 RL299Z | 0.00003 | 0.00012 | 0.0048 | 77.0 |
| 274 RT2741 | 0.00044 | 0.00042 | 0.0092 | 78.4 | 317 RL299A | 0.00018 | 0.00099 | 0.0471 | 101.4 |
| 275 RT2751 | 0.00054 | 0.00052 | 0.0112 | 73.4 | 318 RL299B | 0.00035 | 0.00207 | 0.0173 | 101.4 |
| 276 RT2761 | 0.00064 | 0.00062 | 0.0132 | 77.7 | 319 RL299C | 0.00062 | 0.00407 | 0.0038 | 78.5 |
| 277 RT2771 | 0.00074 | 0.00072 | 0.0152 | 89.5 | 320 RL299D | 0.00086 | 0.00586 | 0.0433 | 101.4 |
| 278 RT2781 | 0.00084 | 0.00082 | 0.0172 | 79.2 | 321 RL299E | 0.00086 | 0.00586 | 0.0176 | 101.5 |
| 279 RT2791 | 0.00094 | 0.00092 | 0.0192 | 78.8 | 322 RL299F | 0.00086 | 0.00586 | 0.0017 | 73.2 |
| 280 RT2801 | 0.00104 | 0.00102 | 0.0212 | 77.1 | 323 RL299G | 0.00086 | 0.00586 | 0.0139 | 102.1 |
| 281 RT2811 | 0.00114 | 0.00112 | 0.0232 | 99.5 | 324 RL299H | 0.00086 | 0.00586 | 0.0097 | 109.6 |
| 282 RT2821 | 0.00124 | 0.00122 | 0.0252 | 101.2 | 325 RL299I | 0.00086 | 0.00586 | 0.0001 | 72.9 |
| 283 RT2831 | 0.00134 | 0.00132 | 0.0272 | 99.6 | 326 RL299J | 0.00086 | 0.00586 | 0.0117 | 102.3 |
| 284 RT2841 | 0.00144 | 0.00142 | 0.0292 | 76.6 | 327 RL299K | 0.00086 | 0.00586 | 0.0203 | 76.4 |
| 285 RT2851 | 0.00154 | 0.00152 | 0.0312 | 76.1 | 328 RL299L | 0.00086 | 0.00586 | 0.0011 | 103.9 |
| 286 RT2861 | 0.00164 | 0.00162 | 0.0332 | 83.6 | 329 RL299M | 0.00086 | 0.00586 | 0.0042 | 100.9 |
| 287 RT2871 | 0.00174 | 0.00172 | 0.0352 | 54.2 | 330 LL199Z | 0.00011 | 0.00037 | 0.0393 | 101.2 |
| 288 RT2881 | 0.00184 | 0.00182 | 0.0372 | 78.1 | 331 LL199A | 0.00002 | 0.00007 | 0.0038 | 73.4 |
| 289 RT2891 | 0.00194 | 0.00192 | 0.0392 | 16.8 | 332 LL199B | 0.00004 | 0.00020 | 0.0103 | 78.4 |
| 290 RT2901 | 0.00204 | 0.00202 | 0.0412 | 77.3 | 333 LL199C | 0.00002 | 0.00010 | 0.0052 | 77.4 |
| 291 RT2911 | 0.00214 | 0.00212 | 0.0432 | 79.1 | 334 LL199D | 0.00001 | 0.00005 | 0.0028 | 73.9 |
| 292 RT2921 | 0.00224 | 0.00222 | 0.0452 | 79.1 | 335 LL199E | 0.00002 | 0.00007 | 0.0359 | 103.8 |
| 293 RT2931 | 0.00234 | 0.00232 | 0.0472 | 0.6 | 336 LL199F | 0.00002 | 0.00007 | 0.0040 | 194.4 |
| 294 RT2941 | 0.00244 | 0.00242 | 0.0492 | 78.4 | 337 LL199G | 0.00000 | 0.00000 | 0.0034 | 65.1 |
| 295 RT2951 | 0.00254 | 0.00252 | 0.0512 | 79.5 | 338 LL199H | 0.00000 | 0.00000 | 0.0048 | 100.3 |
| 296 RT2961 | 0.00264 | 0.00262 | 0.0532 | 138.0 | 339 LL199I | 0.00001 | 0.00001 | 0.0006 | 58.8 |
| 297 RT2971 | 0.00274 | 0.00272 | 0.0552 | 79.2 | 340 LL199J | 0.00001 | 0.00001 | 0.0041 | 103.4 |
| 298 RT2981 | 0.00284 | 0.00282 | 0.0572 | 160.7 | 341 LL199K | 0.00003 | 0.00021 | 0.0110 | 102.2 |
| 299 RT2991 | 0.00294 | 0.00292 | 0.0592 | 103.0 | 342 LL199L | 0.00001 | 0.00010 | 0.0052 | 81.8 |
| 300 RT3001 | 0.00304 | 0.00302 | 0.0612 | 61.7 | 343 LL199M | 0.00012 | 0.00054 | 0.0239 | 77.1 |
| 301 RT3011 | 0.00314 | 0.00312 | 0.0632 | 38.1 | 344 LL199N | 0.00010 | 0.00048 | 0.0250 | 76.4 |
| 302 RT3021 | 0.00324 | 0.00322 | 0.0652 | 109.7 | 345 LL199O | 0.00004 | 0.00013 | 0.0073 | 63.9 |
| 303 RT3031 | 0.00334 | 0.00332 | 0.0672 | 72.5 | 346 LL199P | 0.00004 | 0.00016 | 0.0053 | 73.9 |
| 304 RT3041 | 0.00344 | 0.00342 | 0.0692 | 72.0 | 347 LL199Q | 0.00002 | 0.00005 | 0.0028 | 70.1 |
| 305 RT3051 | 0.00354 | 0.00352 | 0.0712 | 168.3 | 348 LL199R | 0.00000 | 0.00000 | 0.0047 | 7.0 |
| 306 RT3061 | 0.00364 | 0.00362 | 0.0732 | 134.7 | 349 LL199S | 0.00000 | 0.00000 | 0.0042 | 170.8 |
| 307 RT3071 | 0.00374 | 0.00372 | 0.0752 | 100.1 | 350 LL199T | 0.00000 | 0.00000 | 0.0037 | 94.1 |
| 308 RT3081 | 0.00384 | 0.00382 | 0.0772 | 100.1 | 351 LL199U | 0.00000 | 0.00000 | 0.0071 | 84.9 |
| 309 RT3091 | 0.00394 | 0.00392 | 0.0792 | 100.1 | 352 LL199V | 0.00000 | 0.00000 | 0.0071 | 84.9 |
| 310 RT3101 | 0.00404 | 0.00402 | 0.0812 | 100.1 | 353 LL199W | 0.00000 | 0.00000 | 0.0071 | 84.9 |

Figure 11. (Continued).

L I F T O F F

DATE 10/31/76
TIME 4:09:53

SYNTHETIC
FOCUS 5
FEED 2.0003

REF. FORCE FBI0Z

| ACC LOC | CO G/LB | QUAD G/LB | ACC G | PHASE | ACC LOC | CO G/LB | QUAD G/LB | ACC G | PHASE |
|-----------|----------|-----------|--------|--------|------------|----------|-----------|--------|-------|
| 393 7102P | 0.00013 | 0.00037 | 0.441 | 87.0 | 397 PL403X | 0.00001 | 0.00010 | 0.0030 | 82.4 |
| 394 7102Y | 0.00029 | 0.00059 | 0.337 | 97.8 | 398 AJ603Y | 0.00003 | 0.00021 | 0.0112 | 77.5 |
| 395 7102Z | -0.00016 | -0.00036 | 0.007 | -153.0 | 399 AJ301Y | -0.00002 | 0.00038 | 0.0020 | 121.5 |
| 396 7102A | -0.00027 | -0.00057 | 0.642 | 143.6 | 400 AJ042Z | 0.00009 | 0.00003 | 0.0053 | 32.6 |
| 397 7102B | -0.00038 | -0.00078 | 0.0015 | -174.7 | 401 AJ349Z | 0.00003 | 0.00010 | 0.0056 | 73.3 |
| 398 7102C | 0.00039 | 0.00079 | 0.001 | 21.3 | | | | | |
| 399 7102D | 0.00040 | 0.00080 | 0.001 | 164.9 | | | | | |
| 400 7102E | 0.00041 | 0.00081 | 0.001 | 164.5 | | | | | |
| 401 7102F | 0.00042 | 0.00082 | 0.001 | -161.3 | | | | | |
| 402 7102G | 0.00043 | 0.00083 | 0.001 | 163.7 | | | | | |
| 403 7102H | 0.00044 | 0.00084 | 0.001 | -39.9 | | | | | |
| 404 7102I | 0.00045 | 0.00085 | 0.001 | -177.9 | | | | | |
| 405 7102J | 0.00046 | 0.00086 | 0.001 | -28.7 | | | | | |
| 406 7102K | 0.00047 | 0.00087 | 0.001 | 77.9 | | | | | |
| 407 7102L | 0.00048 | 0.00088 | 0.001 | 170.2 | | | | | |
| 408 7102M | 0.00049 | 0.00089 | 0.001 | -16.0 | | | | | |
| 409 7102N | 0.00050 | 0.00090 | 0.001 | 112.0 | | | | | |
| 410 7102O | 0.00051 | 0.00091 | 0.001 | 22.1 | | | | | |
| 411 7102P | 0.00052 | 0.00092 | 0.001 | 133.7 | | | | | |
| 412 7102Q | 0.00053 | 0.00093 | 0.001 | 160.8 | | | | | |
| 413 7102R | 0.00054 | 0.00094 | 0.001 | 57.5 | | | | | |
| 414 7102S | 0.00055 | 0.00095 | 0.001 | 0.2 | | | | | |
| 415 7102T | 0.00056 | 0.00096 | 0.001 | 50.2 | | | | | |
| 416 7102U | 0.00057 | 0.00097 | 0.001 | -1.0 | | | | | |
| 417 7102V | 0.00058 | 0.00098 | 0.001 | 62.1 | | | | | |
| 418 7102W | 0.00059 | 0.00099 | 0.001 | -2.2 | | | | | |
| 419 7102X | 0.00060 | 0.00100 | 0.001 | -1.4 | | | | | |
| 420 7102Y | 0.00061 | 0.00101 | 0.001 | 6.1 | | | | | |
| 421 7102Z | 0.00062 | 0.00102 | 0.001 | 161.2 | | | | | |
| 422 7102A | 0.00063 | 0.00103 | 0.001 | -22.7 | | | | | |
| 423 7102B | 0.00064 | 0.00104 | 0.001 | -153.0 | | | | | |
| 424 7102C | 0.00065 | 0.00105 | 0.001 | -76.2 | | | | | |
| 425 7102D | 0.00066 | 0.00106 | 0.001 | 152.2 | | | | | |
| 426 7102E | 0.00067 | 0.00107 | 0.001 | -47.1 | | | | | |
| 427 7102F | 0.00068 | 0.00108 | 0.001 | 167.0 | | | | | |
| 428 7102G | 0.00069 | 0.00109 | 0.001 | -30.4 | | | | | |
| 429 7102H | 0.00070 | 0.00110 | 0.001 | 119.4 | | | | | |
| 430 7102I | 0.00071 | 0.00111 | 0.001 | 91.9 | | | | | |
| 431 7102J | 0.00072 | 0.00112 | 0.001 | 99.5 | | | | | |
| 432 7102K | 0.00073 | 0.00113 | 0.001 | 109.7 | | | | | |
| 433 7102L | 0.00074 | 0.00114 | 0.001 | 108.9 | | | | | |
| 434 7102M | 0.00075 | 0.00115 | 0.001 | 123.7 | | | | | |
| 435 7102N | 0.00076 | 0.00116 | 0.001 | 37.2 | | | | | |
| 436 7102O | 0.00077 | 0.00117 | 0.001 | 88.2 | | | | | |
| 437 7102P | 0.00078 | 0.00118 | 0.001 | | | | | | |
| 438 7102Q | 0.00079 | 0.00119 | 0.001 | | | | | | |
| 439 7102R | 0.00080 | 0.00120 | 0.001 | | | | | | |
| 440 7102S | 0.00081 | 0.00121 | 0.001 | | | | | | |
| 441 7102T | 0.00082 | 0.00122 | 0.001 | | | | | | |
| 442 7102U | 0.00083 | 0.00123 | 0.001 | | | | | | |
| 443 7102V | 0.00084 | 0.00124 | 0.001 | | | | | | |
| 444 7102W | 0.00085 | 0.00125 | 0.001 | | | | | | |
| 445 7102X | 0.00086 | 0.00126 | 0.001 | | | | | | |
| 446 7102Y | 0.00087 | 0.00127 | 0.001 | | | | | | |
| 447 7102Z | 0.00088 | 0.00128 | 0.001 | | | | | | |
| 448 7102A | 0.00089 | 0.00129 | 0.001 | | | | | | |
| 449 7102B | 0.00090 | 0.00130 | 0.001 | | | | | | |
| 450 7102C | 0.00091 | 0.00131 | 0.001 | | | | | | |
| 451 7102D | 0.00092 | 0.00132 | 0.001 | | | | | | |
| 452 7102E | 0.00093 | 0.00133 | 0.001 | | | | | | |
| 453 7102F | 0.00094 | 0.00134 | 0.001 | | | | | | |
| 454 7102G | 0.00095 | 0.00135 | 0.001 | | | | | | |
| 455 7102H | 0.00096 | 0.00136 | 0.001 | | | | | | |
| 456 7102I | 0.00097 | 0.00137 | 0.001 | | | | | | |
| 457 7102J | 0.00098 | 0.00138 | 0.001 | | | | | | |
| 458 7102K | 0.00099 | 0.00139 | 0.001 | | | | | | |
| 459 7102L | 0.00100 | 0.00140 | 0.001 | | | | | | |
| 460 7102M | 0.00101 | 0.00141 | 0.001 | | | | | | |
| 461 7102N | 0.00102 | 0.00142 | 0.001 | | | | | | |
| 462 7102O | 0.00103 | 0.00143 | 0.001 | | | | | | |
| 463 7102P | 0.00104 | 0.00144 | 0.001 | | | | | | |
| 464 7102Q | 0.00105 | 0.00145 | 0.001 | | | | | | |
| 465 7102R | 0.00106 | 0.00146 | 0.001 | | | | | | |
| 466 7102S | 0.00107 | 0.00147 | 0.001 | | | | | | |
| 467 7102T | 0.00108 | 0.00148 | 0.001 | | | | | | |
| 468 7102U | 0.00109 | 0.00149 | 0.001 | | | | | | |
| 469 7102V | 0.00110 | 0.00150 | 0.001 | | | | | | |
| 470 7102W | 0.00111 | 0.00151 | 0.001 | | | | | | |
| 471 7102X | 0.00112 | 0.00152 | 0.001 | | | | | | |
| 472 7102Y | 0.00113 | 0.00153 | 0.001 | | | | | | |
| 473 7102Z | 0.00114 | 0.00154 | 0.001 | | | | | | |
| 474 7102A | 0.00115 | 0.00155 | 0.001 | | | | | | |
| 475 7102B | 0.00116 | 0.00156 | 0.001 | | | | | | |
| 476 7102C | 0.00117 | 0.00157 | 0.001 | | | | | | |
| 477 7102D | 0.00118 | 0.00158 | 0.001 | | | | | | |
| 478 7102E | 0.00119 | 0.00159 | 0.001 | | | | | | |
| 479 7102F | 0.00120 | 0.00160 | 0.001 | | | | | | |
| 480 7102G | 0.00121 | 0.00161 | 0.001 | | | | | | |
| 481 7102H | 0.00122 | 0.00162 | 0.001 | | | | | | |
| 482 7102I | 0.00123 | 0.00163 | 0.001 | | | | | | |
| 483 7102J | 0.00124 | 0.00164 | 0.001 | | | | | | |
| 484 7102K | 0.00125 | 0.00165 | 0.001 | | | | | | |
| 485 7102L | 0.00126 | 0.00166 | 0.001 | | | | | | |
| 486 7102M | 0.00127 | 0.00167 | 0.001 | | | | | | |
| 487 7102N | 0.00128 | 0.00168 | 0.001 | | | | | | |
| 488 7102O | 0.00129 | 0.00169 | 0.001 | | | | | | |
| 489 7102P | 0.00130 | 0.00170 | 0.001 | | | | | | |
| 490 7102Q | 0.00131 | 0.00171 | 0.001 | | | | | | |
| 491 7102R | 0.00132 | 0.00172 | 0.001 | | | | | | |
| 492 7102S | 0.00133 | 0.00173 | 0.001 | | | | | | |
| 493 7102T | 0.00134 | 0.00174 | 0.001 | | | | | | |
| 494 7102U | 0.00135 | 0.00175 | 0.001 | | | | | | |
| 495 7102V | 0.00136 | 0.00176 | 0.001 | | | | | | |
| 496 7102W | 0.00137 | 0.00177 | 0.001 | | | | | | |
| 497 7102X | 0.00138 | 0.00178 | 0.001 | | | | | | |
| 498 7102Y | 0.00139 | 0.00179 | 0.001 | | | | | | |
| 499 7102Z | 0.00140 | 0.00180 | 0.001 | | | | | | |
| 500 7102A | 0.00141 | 0.00181 | 0.001 | | | | | | |
| 501 7102B | 0.00142 | 0.00182 | 0.001 | | | | | | |
| 502 7102C | 0.00143 | 0.00183 | 0.001 | | | | | | |
| 503 7102D | 0.00144 | 0.00184 | 0.001 | | | | | | |
| 504 7102E | 0.00145 | 0.00185 | 0.001 | | | | | | |
| 505 7102F | 0.00146 | 0.00186 | 0.001 | | | | | | |
| 506 7102G | 0.00147 | 0.00187 | 0.001 | | | | | | |
| 507 7102H | 0.00148 | 0.00188 | 0.001 | | | | | | |
| 508 7102I | 0.00149 | 0.00189 | 0.001 | | | | | | |
| 509 7102J | 0.00150 | 0.00190 | 0.001 | | | | | | |
| 510 7102K | 0.00151 | 0.00191 | 0.001 | | | | | | |
| 511 7102L | 0.00152 | 0.00192 | 0.001 | | | | | | |
| 512 7102M | 0.00153 | 0.00193 | 0.001 | | | | | | |
| 513 7102N | 0.00154 | 0.00194 | 0.001 | | | | | | |
| 514 7102O | 0.00155 | 0.00195 | 0.001 | | | | | | |
| 515 7102P | 0.00156 | 0.00196 | 0.001 | | | | | | |
| 516 7102Q | 0.00157 | 0.00197 | 0.001 | | | | | | |
| 517 7102R | 0.00158 | 0.00198 | 0.001 | | | | | | |
| 518 7102S | 0.00159 | 0.00199 | 0.001 | | | | | | |
| 519 7102T | 0.00160 | 0.00200 | 0.001 | | | | | | |
| 520 7102U | 0.00161 | 0.00201 | 0.001 | | | | | | |
| 521 7102V | 0.00162 | 0.00202 | 0.001 | | | | | | |
| 522 7102W | 0.00163 | 0.00203 | 0.001 | | | | | | |
| 523 7102X | 0.00164 | 0.00204 | 0.001 | | | | | | |
| 524 7102Y | 0.00165 | 0.00205 | 0.001 | | | | | | |
| 525 7102Z | 0.00166 | 0.00206 | 0.001 | | | | | | |
| 526 7102A | 0.00167 | 0.00207 | 0.001 | | | | | | |
| 527 7102B | 0.00168 | 0.00208 | 0.001 | | | | | | |
| 528 7102C | 0.00169 | 0.00209 | 0.001 | | | | | | |
| 529 7102D | 0.00170 | 0.00210 | 0.001 | | | | | | |
| 530 7102E | 0.00171 | 0.00211 | 0.001 | | | | | | |
| 531 7102F | 0.00172 | 0.00212 | 0.001 | | | | | | |
| 532 7102G | 0.00173 | 0.00213 | 0.001 | | | | | | |
| 533 7102H | 0.00174 | 0.00214 | 0.001 | | | | | | |
| 534 7102I | 0.00175 | 0.00215 | 0.001 | | | | | | |
| 535 7102J | 0.00176 | 0.00216 | 0.001 | | | | | | |
| 536 7102K | 0.00177 | 0.00217 | 0.001 | | | | | | |
| 537 7102L | 0.00178 | 0.00218 | 0.001 | | | | | | |
| 538 7102M | 0.00179 | 0.00219 | 0.001 | | | | | | |
| 539 7102N | 0.00180 | 0.00220 | 0.001 | | | | | | |
| 540 7102O | 0.00181 | 0.00221 | 0.001 | | | | | | |
| 541 7102P | 0.00182 | 0.00222 | 0.001 | | | | | | |
| 542 7102Q | 0.00183 | 0.00223 | 0.001 | | | | | | |
| 543 7102R | 0.00184 | 0.00224 | 0.001 | | | | | | |

REF ID: A66888

REF ID: A66888

FORCE DATA

| ITEM NO | ITEM NAME | COORDINATES | FORCE | ANGLE | PLANE |
|---------|-----------|-------------|---------|---------|-------|
| 1 | W10001 | 0.00000 | 0.00000 | 0.00000 | 78.0 |
| 2 | W10002 | 0.00000 | 0.00000 | 0.00000 | 77.0 |
| 3 | W10003 | 0.00000 | 0.00000 | 0.00000 | 78.0 |
| 4 | W10004 | 0.00000 | 0.00000 | 0.00000 | 78.0 |
| 5 | W10005 | 0.00000 | 0.00000 | 0.00000 | 78.0 |
| 6 | W10006 | 0.00000 | 0.00000 | 0.00000 | 78.0 |
| 7 | W10007 | 0.00000 | 0.00000 | 0.00000 | 78.0 |
| 8 | W10008 | 0.00000 | 0.00000 | 0.00000 | 78.0 |
| 9 | W10009 | 0.00000 | 0.00000 | 0.00000 | 78.0 |
| 10 | W10010 | 0.00000 | 0.00000 | 0.00000 | 78.0 |
| 11 | W10011 | 0.00000 | 0.00000 | 0.00000 | 78.0 |
| 12 | W10012 | 0.00000 | 0.00000 | 0.00000 | 78.0 |
| 13 | W10013 | 0.00000 | 0.00000 | 0.00000 | 78.0 |
| 14 | W10014 | 0.00000 | 0.00000 | 0.00000 | 78.0 |
| 15 | W10015 | 0.00000 | 0.00000 | 0.00000 | 78.0 |
| 16 | W10016 | 0.00000 | 0.00000 | 0.00000 | 78.0 |
| 17 | W10017 | 0.00000 | 0.00000 | 0.00000 | 78.0 |
| 18 | W10018 | 0.00000 | 0.00000 | 0.00000 | 78.0 |
| 19 | W10019 | 0.00000 | 0.00000 | 0.00000 | 78.0 |
| 20 | W10020 | 0.00000 | 0.00000 | 0.00000 | 78.0 |
| 21 | W10021 | 0.00000 | 0.00000 | 0.00000 | 78.0 |
| 22 | W10022 | 0.00000 | 0.00000 | 0.00000 | 78.0 |
| 23 | W10023 | 0.00000 | 0.00000 | 0.00000 | 78.0 |
| 24 | W10024 | 0.00000 | 0.00000 | 0.00000 | 78.0 |
| 25 | W10025 | 0.00000 | 0.00000 | 0.00000 | 78.0 |
| 26 | W10026 | 0.00000 | 0.00000 | 0.00000 | 78.0 |
| 27 | W10027 | 0.00000 | 0.00000 | 0.00000 | 78.0 |
| 28 | W10028 | 0.00000 | 0.00000 | 0.00000 | 78.0 |
| 29 | W10029 | 0.00000 | 0.00000 | 0.00000 | 78.0 |
| 30 | W10030 | 0.00000 | 0.00000 | 0.00000 | 78.0 |
| 31 | W10031 | 0.00000 | 0.00000 | 0.00000 | 78.0 |
| 32 | W10032 | 0.00000 | 0.00000 | 0.00000 | 78.0 |
| 33 | W10033 | 0.00000 | 0.00000 | 0.00000 | 78.0 |
| 34 | W10034 | 0.00000 | 0.00000 | 0.00000 | 78.0 |
| 35 | W10035 | 0.00000 | 0.00000 | 0.00000 | 78.0 |
| 36 | W10036 | 0.00000 | 0.00000 | 0.00000 | 78.0 |
| 37 | W10037 | 0.00000 | 0.00000 | 0.00000 | 78.0 |
| 38 | W10038 | 0.00000 | 0.00000 | 0.00000 | 78.0 |
| 39 | W10039 | 0.00000 | 0.00000 | 0.00000 | 78.0 |
| 40 | W10040 | 0.00000 | 0.00000 | 0.00000 | 78.0 |

Figure 12. Space Shuttle MVGVT Dwell Data Orbiter *** External Tank *** Solid Rocket Boosters.

ORIGINAL PAGE IS OF POOR QUALITY

L I F T O F F

GERL NORMALIZED MASS MATRIX

| NODE | FREQ | 0.6667 | 0.3333 | 0.1961 | 0.3137 | 2.6723 |
|------|--------|---------|---------|--------|---------|--------|
| 1 | 0.0000 | 1.0000 | | | | |
| 2 | 0.0000 | -0.6491 | 1.6600 | | | |
| 3 | 0.1561 | -0.0001 | -0.6600 | 1.0000 | | |
| 4 | 0.0000 | 0.0016 | -0.5019 | 0.0035 | 1.0000 | |
| 5 | 2.6523 | 0.0014 | 0.3670 | 0.1020 | -0.0929 | 1.0000 |

Figure 13. Space Shuttle MVGV Symmetric Orthog Orbiter *** External Tank ** Solid Rocket Boosters.

ORIGINAL PAGE IS
OF POOR QUALITY

L I F T O F F

| HOSE | AREA | CMC |
|------|--------|--------------|
| 1 | 9.6667 | 0.0391170277 |
| 2 | 0.0333 | 0.000913298 |
| 3 | 0.1581 | 0.000000487 |
| 4 | 0.0167 | 0.000000006 |
| 5 | 2.0322 | 0.000000000 |

Figure 15. Space Shuttle MGVGT Symmetric Orthog Orbiter ***
External Tank *** Solid Rocket Boosters.

L I F T O F F

| | | | | | | | | | | | | |
|---------|---------|---------|---------|---------|---------|---------|---------|---------|---------|---------|---------|---------|
| 0.0350 | -0.0014 | 0.0660 | 2.1479 | 2.4788 | 2.9277 | 3.1429 | 3.1833 | 3.0720 | 4.7514 | 3.1353 | 5.3581 | 5.6550 |
| 0.7742 | 6.3953 | 6.4798 | 6.9179 | 7.4520 | 7.9203 | 8.0747 | 8.0988 | 8.1551 | 8.0184 | 7.0763 | 9.2163 | 9.3918 |
| 9.4429 | 9.6094 | 9.6176 | 10.3471 | 10.8318 | 10.9203 | 10.9130 | 11.6583 | 11.1373 | 11.1773 | 11.5131 | 11.9489 | 12.0113 |
| 12.4442 | 12.3427 | 12.7320 | 12.9450 | 12.9627 | 13.1457 | 13.6141 | 13.7189 | 13.7984 | 13.9632 | 14.1940 | 14.6271 | 14.8723 |
| 15.6101 | 14.7232 | 14.7500 | 15.0800 | 15.1807 | 15.1967 | 15.3741 | 15.5072 | 15.5829 | 15.7833 | 15.9940 | 16.4235 | 16.4705 |
| 16.8383 | 16.4832 | 16.9336 | 17.6231 | 17.5918 | 17.8847 | 17.8247 | 18.1931 | 18.2803 | 18.4137 | 18.4741 | 18.8739 | 19.0719 |
| 18.0793 | 19.0527 | 19.0200 | 19.6227 | 19.2342 | 19.2877 | 19.2877 | 19.3259 | 19.3382 | 19.6171 | 19.7473 | 19.7484 | 20.0823 |
| 20.0711 | 20.7233 | 20.6500 | 20.7776 | 21.1829 | 21.3707 | 21.6185 | 22.0627 | 22.3109 | 22.4931 | 22.9479 | 22.8311 | 23.3023 |
| 21.1141 | 22.2421 | 22.3113 | 23.0419 | 23.2317 | 23.3200 | 23.6640 | 24.0248 | 23.8718 | 24.0751 | 24.0820 | 24.0743 | 24.5313 |
| 22.1122 | 23.1122 | 23.1427 | 23.6434 | 23.7809 | 23.8903 | 24.0610 | 24.1913 | 24.1879 | 24.2743 | 24.0820 | 24.0743 | 24.5313 |
| 23.1122 | 24.0122 | 24.0122 | 24.4210 | 24.6210 | 24.6210 | 24.6210 | 24.6210 | 24.6210 | 24.6210 | 24.6210 | 24.6210 | 24.6210 |
| 24.0122 | 24.9122 | 24.9122 | 25.1722 | 25.1722 | 25.1722 | 25.1722 | 25.1722 | 25.1722 | 25.1722 | 25.1722 | 25.1722 | 25.1722 |
| 25.0122 | 25.8122 | 25.8122 | 26.0722 | 26.0722 | 26.0722 | 26.0722 | 26.0722 | 26.0722 | 26.0722 | 26.0722 | 26.0722 | 26.0722 |
| 26.0122 | 26.7122 | 26.7122 | 26.9722 | 26.9722 | 26.9722 | 26.9722 | 26.9722 | 26.9722 | 26.9722 | 26.9722 | 26.9722 | 26.9722 |
| 27.0122 | 27.6122 | 27.6122 | 27.8722 | 27.8722 | 27.8722 | 27.8722 | 27.8722 | 27.8722 | 27.8722 | 27.8722 | 27.8722 | 27.8722 |
| 28.0122 | 28.5122 | 28.5122 | 28.7722 | 28.7722 | 28.7722 | 28.7722 | 28.7722 | 28.7722 | 28.7722 | 28.7722 | 28.7722 | 28.7722 |
| 29.0122 | 29.4122 | 29.4122 | 29.6722 | 29.6722 | 29.6722 | 29.6722 | 29.6722 | 29.6722 | 29.6722 | 29.6722 | 29.6722 | 29.6722 |
| 30.0122 | 30.3122 | 30.3122 | 30.5722 | 30.5722 | 30.5722 | 30.5722 | 30.5722 | 30.5722 | 30.5722 | 30.5722 | 30.5722 | 30.5722 |
| 31.0122 | 31.2122 | 31.2122 | 31.4722 | 31.4722 | 31.4722 | 31.4722 | 31.4722 | 31.4722 | 31.4722 | 31.4722 | 31.4722 | 31.4722 |
| 32.0122 | 32.1122 | 32.1122 | 32.3722 | 32.3722 | 32.3722 | 32.3722 | 32.3722 | 32.3722 | 32.3722 | 32.3722 | 32.3722 | 32.3722 |
| 33.0122 | 33.0122 | 33.0122 | 33.2722 | 33.2722 | 33.2722 | 33.2722 | 33.2722 | 33.2722 | 33.2722 | 33.2722 | 33.2722 | 33.2722 |
| 34.0122 | 34.0122 | 34.0122 | 34.2722 | 34.2722 | 34.2722 | 34.2722 | 34.2722 | 34.2722 | 34.2722 | 34.2722 | 34.2722 | 34.2722 |
| 35.0122 | 35.0122 | 35.0122 | 35.2722 | 35.2722 | 35.2722 | 35.2722 | 35.2722 | 35.2722 | 35.2722 | 35.2722 | 35.2722 | 35.2722 |
| 36.0122 | 36.0122 | 36.0122 | 36.2722 | 36.2722 | 36.2722 | 36.2722 | 36.2722 | 36.2722 | 36.2722 | 36.2722 | 36.2722 | 36.2722 |
| 37.0122 | 37.0122 | 37.0122 | 37.2722 | 37.2722 | 37.2722 | 37.2722 | 37.2722 | 37.2722 | 37.2722 | 37.2722 | 37.2722 | 37.2722 |
| 38.0122 | 38.0122 | 38.0122 | 38.2722 | 38.2722 | 38.2722 | 38.2722 | 38.2722 | 38.2722 | 38.2722 | 38.2722 | 38.2722 | 38.2722 |
| 39.0122 | 39.0122 | 39.0122 | 39.2722 | 39.2722 | 39.2722 | 39.2722 | 39.2722 | 39.2722 | 39.2722 | 39.2722 | 39.2722 | 39.2722 |
| 40.0122 | 40.0122 | 40.0122 | 40.2722 | 40.2722 | 40.2722 | 40.2722 | 40.2722 | 40.2722 | 40.2722 | 40.2722 | 40.2722 | 40.2722 |

3 2.0523

GENL NORMALIZED MASS MATRIX

| | | | | | | | | | | | | |
|--------|---------|---------|---------|---------|---------|---------|---------|---------|---------|---------|---------|---------|
| 0.0350 | -0.1723 | -0.0300 | -0.0820 | 0.0227 | 0.0214 | 0.0227 | -0.1450 | 0.1620 | -0.0316 | -0.0182 | -0.4027 | 0.0010 |
| 0.0351 | -0.0322 | -0.0712 | -0.1544 | -0.1513 | 0.0250 | 0.0234 | -0.0227 | -0.0177 | 0.0116 | -0.0130 | -0.0221 | -0.0011 |
| 0.0352 | -0.0223 | 0.0253 | -0.0174 | -0.0257 | -0.0014 | 0.0111 | -0.0602 | 0.0103 | -0.0118 | -0.0217 | -0.0116 | -0.0024 |
| 0.0353 | 0.0151 | 0.0391 | -0.1824 | 0.1171 | 0.0323 | -0.0334 | 0.0223 | -0.0136 | -0.0349 | -0.0713 | 0.0337 | 0.0031 |
| 0.0354 | -0.0639 | -0.0334 | -0.0323 | -0.0714 | 0.0063 | 0.0413 | -0.0220 | 0.0111 | 0.0130 | -0.0226 | 0.0218 | -0.0019 |
| 0.0355 | -0.1246 | 0.0272 | 0.0227 | 0.0773 | 0.0074 | -0.1820 | 0.0759 | 0.1113 | -0.0272 | 0.1213 | -0.0130 | -0.0026 |
| 0.0356 | -0.0723 | 0.0277 | -0.0250 | -0.1128 | -0.1919 | 0.0300 | -0.0328 | 0.0223 | 0.0218 | 0.0213 | -0.0226 | -0.0032 |
| 0.0357 | -0.0227 | -0.0223 | 0.0223 | -0.0227 | -0.0464 | -0.0227 | -0.0328 | 0.0223 | 0.0218 | 0.0213 | -0.0226 | -0.0032 |
| 0.0358 | -0.0227 | -0.0227 | 0.0223 | 0.0227 | 0.0223 | 0.0223 | -0.0328 | 0.0223 | 0.0218 | 0.0213 | -0.0226 | -0.0032 |
| 0.0359 | -0.0227 | -0.0227 | -0.0227 | -0.0227 | -0.0227 | -0.0227 | -0.0328 | -0.0227 | 0.0218 | 0.0213 | -0.0226 | -0.0032 |
| 0.0360 | -0.0227 | -0.0227 | -0.0227 | -0.0227 | -0.0227 | -0.0227 | -0.0328 | -0.0227 | 0.0218 | 0.0213 | -0.0226 | -0.0032 |
| 0.0361 | -0.0227 | -0.0227 | -0.0227 | -0.0227 | -0.0227 | -0.0227 | -0.0328 | -0.0227 | 0.0218 | 0.0213 | -0.0226 | -0.0032 |
| 0.0362 | -0.0227 | -0.0227 | -0.0227 | -0.0227 | -0.0227 | -0.0227 | -0.0328 | -0.0227 | 0.0218 | 0.0213 | -0.0226 | -0.0032 |
| 0.0363 | -0.0227 | -0.0227 | -0.0227 | -0.0227 | -0.0227 | -0.0227 | -0.0328 | -0.0227 | 0.0218 | 0.0213 | -0.0226 | -0.0032 |
| 0.0364 | -0.0227 | -0.0227 | -0.0227 | -0.0227 | -0.0227 | -0.0227 | -0.0328 | -0.0227 | 0.0218 | 0.0213 | -0.0226 | -0.0032 |
| 0.0365 | -0.0227 | -0.0227 | -0.0227 | -0.0227 | -0.0227 | -0.0227 | -0.0328 | -0.0227 | 0.0218 | 0.0213 | -0.0226 | -0.0032 |
| 0.0366 | -0.0227 | -0.0227 | -0.0227 | -0.0227 | -0.0227 | -0.0227 | -0.0328 | -0.0227 | 0.0218 | 0.0213 | -0.0226 | -0.0032 |
| 0.0367 | -0.0227 | -0.0227 | -0.0227 | -0.0227 | -0.0227 | -0.0227 | -0.0328 | -0.0227 | 0.0218 | 0.0213 | -0.0226 | -0.0032 |
| 0.0368 | -0.0227 | -0.0227 | -0.0227 | -0.0227 | -0.0227 | -0.0227 | -0.0328 | -0.0227 | 0.0218 | 0.0213 | -0.0226 | -0.0032 |
| 0.0369 | -0.0227 | -0.0227 | -0.0227 | -0.0227 | -0.0227 | -0.0227 | -0.0328 | -0.0227 | 0.0218 | 0.0213 | -0.0226 | -0.0032 |
| 0.0370 | -0.0227 | -0.0227 | -0.0227 | -0.0227 | -0.0227 | -0.0227 | -0.0328 | -0.0227 | 0.0218 | 0.0213 | -0.0226 | -0.0032 |
| 0.0371 | -0.0227 | -0.0227 | -0.0227 | -0.0227 | -0.0227 | -0.0227 | -0.0328 | -0.0227 | 0.0218 | 0.0213 | -0.0226 | -0.0032 |
| 0.0372 | -0.0227 | -0.0227 | -0.0227 | -0.0227 | -0.0227 | -0.0227 | -0.0328 | -0.0227 | 0.0218 | 0.0213 | -0.0226 | -0.0032 |
| 0.0373 | -0.0227 | -0.0227 | -0.0227 | -0.0227 | -0.0227 | -0.0227 | -0.0328 | -0.0227 | 0.0218 | 0.0213 | -0.0226 | -0.0032 |
| 0.0374 | -0.0227 | -0.0227 | -0.0227 | -0.0227 | -0.0227 | -0.0227 | -0.0328 | -0.0227 | 0.0218 | 0.0213 | -0.0226 | -0.0032 |
| 0.0375 | -0.0227 | -0.0227 | -0.0227 | -0.0227 | -0.0227 | -0.0227 | -0.0328 | -0.0227 | 0.0218 | 0.0213 | -0.0226 | -0.0032 |
| 0.0376 | -0.0227 | -0.0227 | -0.0227 | -0.0227 | -0.0227 | -0.0227 | -0.0328 | -0.0227 | 0.0218 | 0.0213 | -0.0226 | -0.0032 |
| 0.0377 | -0.0227 | -0.0227 | -0.0227 | -0.0227 | -0.0227 | -0.0227 | -0.0328 | -0.0227 | 0.0218 | 0.0213 | -0.0226 | -0.0032 |
| 0.0378 | -0.0227 | -0.0227 | -0.0227 | -0.0227 | -0.0227 | -0.0227 | -0.0328 | -0.0227 | 0.0218 | 0.0213 | -0.0226 | -0.0032 |
| 0.0379 | -0.0227 | -0.0227 | -0.0227 | -0.0227 | -0.0227 | -0.0227 | -0.0328 | -0.0227 | 0.0218 | 0.0213 | -0.0226 | -0.0032 |
| 0.0380 | -0.0227 | -0.0227 | -0.0227 | -0.0227 | -0.0227 | -0.0227 | -0.0328 | -0.0227 | 0.0218 | 0.0213 | -0.0226 | -0.0032 |
| 0.0381 | -0.0227 | -0.0227 | -0.0227 | -0.0227 | -0.0227 | -0.0227 | -0.0328 | -0.0227 | 0.0218 | 0.0213 | -0.0226 | -0.0032 |
| 0.0382 | -0.0227 | -0.0227 | -0.0227 | -0.0227 | -0.0227 | -0.0227 | -0.0328 | -0.0227 | 0.0218 | 0.0213 | -0.0226 | -0.0032 |
| 0.0383 | -0.0227 | -0.0227 | -0.0227 | -0.0227 | -0.0227 | -0.0227 | -0.0328 | -0.0227 | 0.0218 | 0.0213 | -0.0226 | -0.0032 |
| 0.0384 | -0.0227 | -0.0227 | -0.0227 | -0.0227 | -0.0227 | -0.0227 | -0.0328 | -0.0227 | 0.0218 | 0.0213 | -0.0226 | -0.0032 |
| 0.0385 | -0.0227 | -0.0227 | -0.0227 | -0.0227 | -0.0227 | -0.0227 | -0.0328 | -0.0227 | 0.0218 | 0.0213 | -0.0226 | -0.0032 |
| 0.0386 | -0.0227 | -0.0227 | -0.0227 | -0.0227 | -0.0227 | -0.0227 | -0.0328 | -0.0227 | 0.0218 | 0.0213 | -0.0226 | -0.0032 |
| 0.0387 | -0.0227 | -0.0227 | -0.0227 | -0.0227 | -0.0227 | -0.0227 | -0.0328 | -0.0227 | 0.0218 | 0.0213 | -0.0226 | -0.0032 |
| 0.0388 | -0.0227 | -0.0227 | -0.0227 | -0.0227 | -0.0227 | -0.0227 | -0.0328 | -0.0227 | 0.0218 | 0.0213 | -0.0226 | -0.0032 |
| 0.0389 | -0.0227 | -0.0227 | -0.0227 | -0.0227 | -0.0227 | -0.0227 | -0.0328 | -0.0227 | 0.0218 | 0.0213 | -0.0226 | -0.0032 |
| 0.0390 | -0.0227 | -0.0227 | -0.0227 | -0.0227 | -0.0227 | -0.0227 | -0.0328 | -0.0227 | 0.0218 | 0.0213 | -0.0226 | -0.0032 |
| 0.0391 | -0.0227 | -0.0227 | -0.0227 | -0.0227 | -0.0227 | -0.0227 | -0.0328 | -0.0227 | 0.0218 | 0.0213 | -0.0226 | -0.0032 |
| 0.0392 | -0.0227 | -0.0227 | -0.0227 | -0.0227 | -0.0227 | -0.0227 | -0.0328 | -0.0227 | 0.0218 | 0.0213 | -0.0226 | -0.0032 |
| 0.0393 | -0.0227 | -0.0227 | -0.0227 | -0.0227 | -0.0227 | -0.0227 | -0.0328 | -0.0227 | 0.0218 | 0.0213 | -0.0226 | -0.0032 |
| 0.0394 | -0.0227 | -0.0227 | -0.0227 | -0.0227 | -0.0227 | -0.0227 | -0.0328 | -0.0227 | 0.0218 | 0.0213 | -0.0226 | -0.0032 |
| 0.0395 | -0.0227 | -0.0227 | -0.0227 | -0.0227 | -0.0227 | -0.0227 | -0.0328 | -0.0227 | 0.0218 | 0.0213 | -0.0226 | -0.0032 |
| 0.0396 | -0.0227 | -0.0227 | -0.0227 | -0.0227 | -0.0227 | -0.0227 | -0.0328 | -0.0227 | 0.0218 | 0.0213 | -0.0226 | -0.0032 |
| 0.0397 | -0.0227 | -0.0227 | -0.0227 | -0.0227 | -0.0227 | -0.0227 | -0.0328 | -0.0227 | 0.0218 | 0.0213 | -0.0226 | -0.0032 |
| 0.0398 | -0.0227 | -0.0227 | -0.0227 | -0.0227 | -0.0227 | -0.0227 | -0.0328 | -0.0227 | 0.0218 | 0.0213 | -0.0226 | -0.0032 |
| 0.0399 | -0.0227 | -0.0227 | -0.0227 | -0.0227 | -0.0227 | -0.0227 | -0.0328 | -0.0227 | 0.0218 | 0.0213 | -0.0226 | -0.0032 |
| 0.0400 | -0.0227 | -0.0227 | -0.0227 | -0.0227 | -0.0227 | -0.0227 | -0.0328 | -0.0227 | 0.0218 | 0.0213 | -0.0226 | -0.0032 |

Figure 16. Space Shuttle MVGVT Symmetric X-Orth Orbiter External Tank *** Solid Rocket Boosters.

ANAFRQ= 2.108
TSTFRQ= 2.059

ANAMOD= 4
TSTMOD= 5

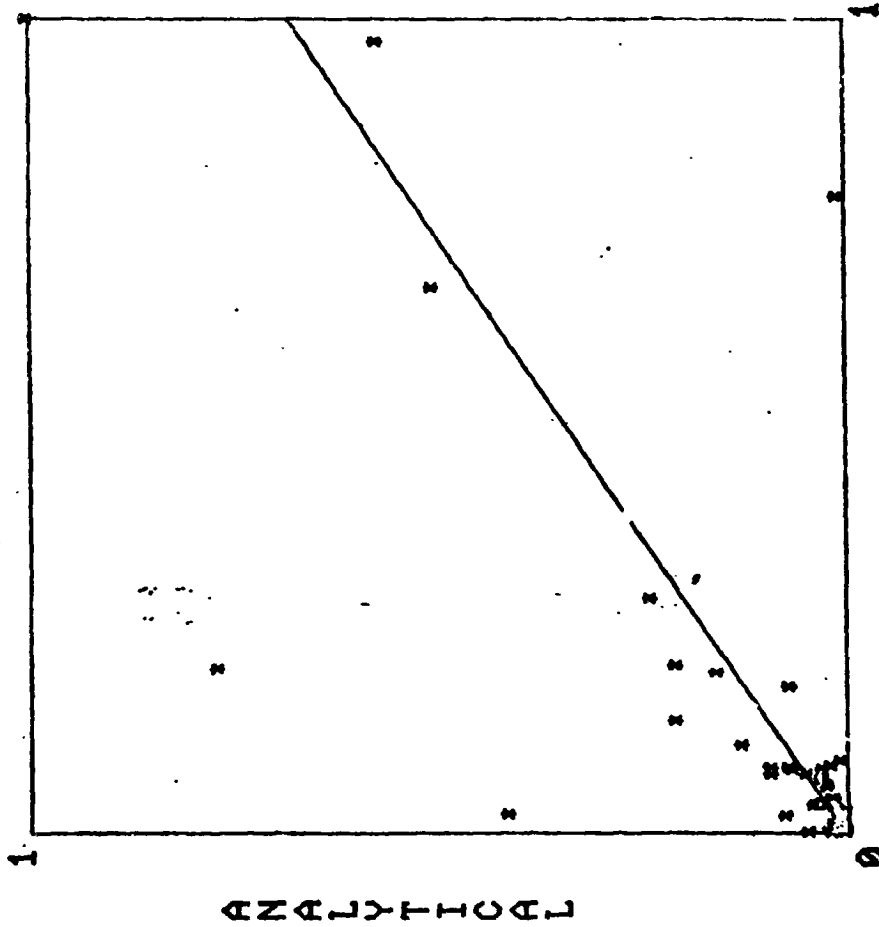
F = A + B * X
A = 0.003
B = 0.679

YINTER= 0.003
XINTER= -0.005
SLOPE = 34.177

STDDEV= 0.398

CO-DET= 0.599
CO-COR= 0.774
STDERR= 0.063

UNORMX= 0.143
UNORMY= 0.180



TEST

Figure 17. Linear regression analysis.

ANAFRQ= 2.454
 TSTFRQ= 2.059

ANAMOD= 5
 TSTMOD= 5

F = A + B * X

A = 0.010
 B = 0.071

YINTER= 0.010
 XINTER= -0.140
 SLOPE = 4.080

STDDEV= 0.210

CO-DET= 0.010
 CO-COR= 0.099
 STDERR= 0.080

UNORMX= 0.143
 UNORMY= 0.329

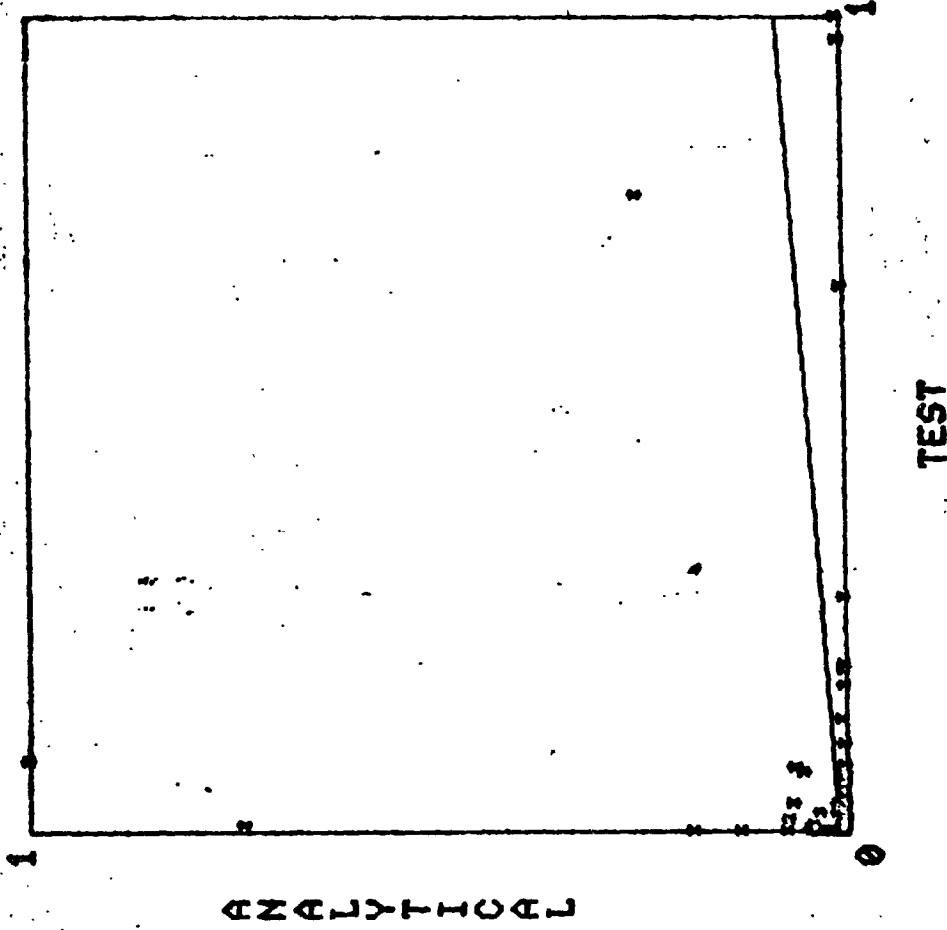


Figure 18. Linear regression analysis.

MODE #5

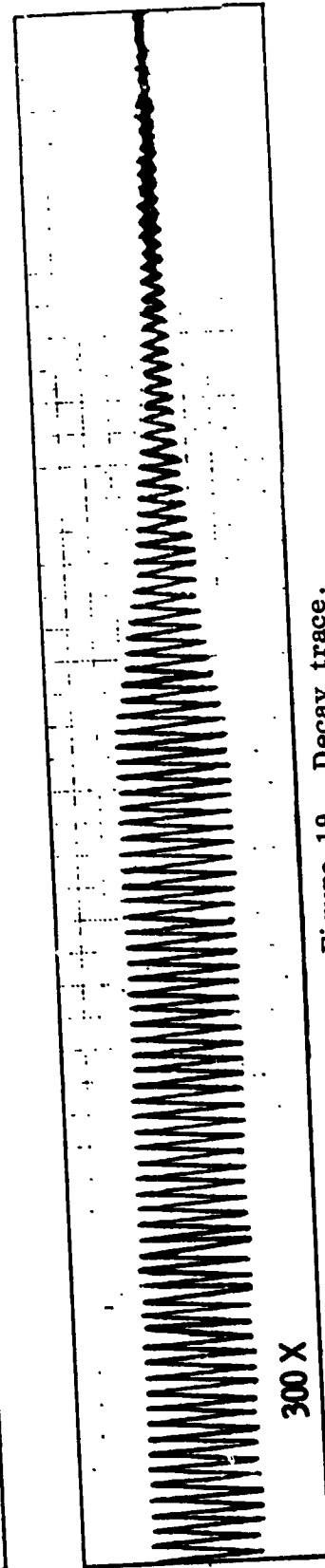
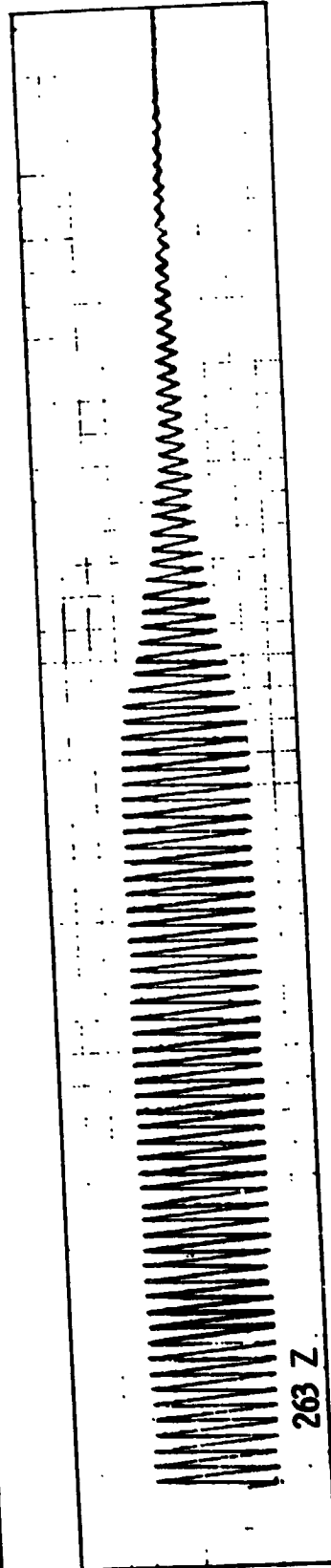
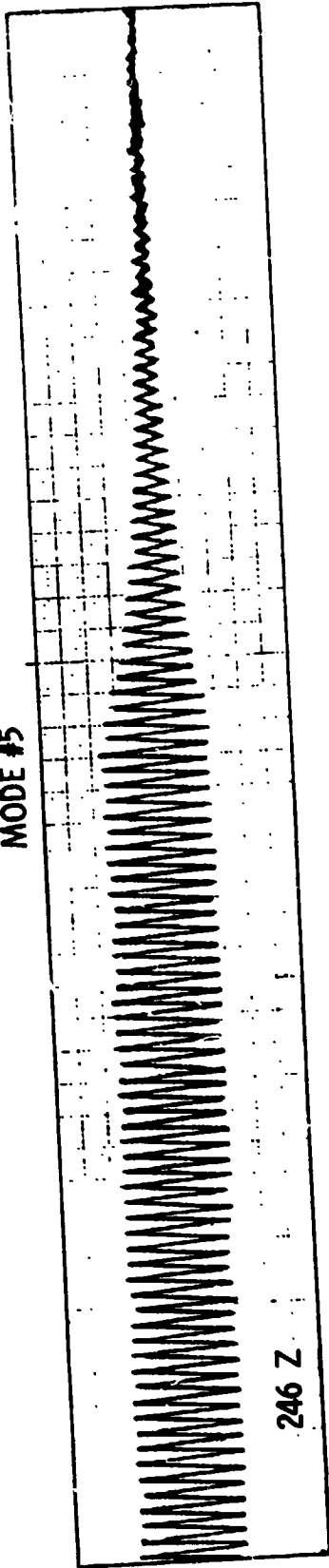


Figure 19. Decay trace.

The kinetic energy distribution for the mode is given in Figure 14. From this listing it can be seen that the principal kinetic energy is in the SRB (76 percent) and that the mode is a roll/pitch mode of the SRB. The cross orthogonality between the analytical mode and the test mode is shown in the lower matrix in Figure 16. The upper matrix in the same figure corresponds to the analytical modal frequency.

The linear regression analysis presented in (Figures 17 and 18) is another aid in matching the analytical mode to the test mode. Ideally the analytical mode matches the test mode when the plotted line is at a 45 degree angle. The decay trace is shown in Figure 19, where selected accelerometers are monitored and the input force is cutoff. Modal damping can be calculated from these decay traces.

e. Payload Bay Response Sweeps. Nine payload bay sweeps were performed during the liftoff testing. Accelerometers were special patched for those sweeps. Accelerometer readings were recorded on the two simulated payloads and on the payload bay. The shakers used, their phasing and frequency ranges for each sweep are shown in Table 9.

f. Pressure Rings Removed. The stiffening rings were attached to the SRB's at the aft ET/SRB interface. These rings were made up of three segments bolted together to simulate the stiffening effect of the SRM chamber pressure during burn. These rings were attached to the SRB's during all of the preceding test phases. These rings were later removed and narrow band sweeps from 1 to 4 Hz were run for symmetric and antisymmetric excitations. The SRB pitch-roll mode which responded more to pressure than other modes was tuned. The symmetric and antisymmetric modes were first tuned with two segments of the ring removed. There was no appreciable change in frequency. The third segment was thought to be stiffening the aft/SRB interface so it was also removed. Again there was no appreciable change in frequency. Table 10 summarizes the result of the above tests.

Altering the aft ET/SRB interface stiffness of the SRB was not effective in changing the pitch/roll modal frequency as the pretest analysis indicated. The analysis assumed that the forward ET/SRB attachment is free to roll. Instrumentation was installed to measure the relative amount of rotation for the last two modes. The test indicated that the interface was locked and was carrying some moment.

g. Special Test of the Forward ET/SRB Interface LOX Tank Empty. It was thought that the LOX tank weight was causing enough friction on the ET/SRB ball joint to prevent free rotation at that interface. To verify this and to determine that the bolt torque was not causing seizing, tests were run with the LOX tank empty and with the bolt torqued and loose (Table 11). The test results, as shown in Table 11, indicated that with the LOX tank empty the SRB/ET ball joint was free to rotate. The bolt torque was not effective.

TABLE 9. PAYLOAD BAY SWEEPS

| Sweep No. | Shaker Used | Shaker Phasing (deg) | Frequency Range (Hz) | Frequency Increment (Hz) | Number of Oscillations Per Increment | | | | | | | | | | | | | | | | | | | | | | | | | | | | | | | | | | | | | | | | | | | | | | | | | | | | | | | | | | | | | | | | | | | | | | | | | | | | | | | | | | | | | | | | | | | | |
|-----------|-------------|----------------------|----------------------|--------------------------|--------------------------------------|---|-------|---|--------|-----|----|-------|-----|---|-------|-----|--------|-----|----|-------|-----|---|-------|-----|--------|-----|----|-------|-----|---|-------|-----|--------|-----|----|-------|-----|-------|-------|-------|--------|-------|-------|-------|--------|-----|-------|-------|--------|-------|-----|-------|-----|-------|-------|-------|--------|-----|----|-------|--------|-------|-------|-------|--------|-----|-------|-------|--------|-------|-------|-------|--------|-------|-------|-------|--------|---|-------|----|--------|-----|----|-------|---|-------|-----|-------|---|---|-------|---|--------|-----|----|-------|---|
| 1 | FL10Y | 0 | 2 - 50 | 0.1 | 10 | | | | | | | | | | | | | | | | | | | | | | | | | | | | | | | | | | | | | | | | | | | | | | | | | | | | | | | | | | | | | | | | | | | | | | | | | | | | | | | | | | | | | | | | | | | | |
| | FL11Y | 0 | | | | 2 | FL10Y | 0 | 2 - 50 | 0.1 | 10 | FL11Y | 180 | 3 | FB10Z | 0 | 2 - 50 | 0.1 | 10 | FB11Z | 180 | 4 | FB10Z | 0 | 2 - 50 | 0.1 | 10 | FB11Z | 0 | 5 | LL06Z | 0 | 2 - 50 | 0.1 | 10 | RR06Z | 180 | LR07Z | 180 | RL07Z | 0 | 6 | LL06Z | 0 | 2 - 50 | 0.1 | 10 | RR06Z | 0 | LR07Z | 180 | RL07Z | 180 | 7 | RB14Y | 0 | 2 - 50 | 0.1 | 10 | RT14Y | 180 | LB14Y | 180 | LT14Y | 0 | 8 | RB14Y | 180 | 2 - 50 | 0.1 | 10 | RT14Y | 0 | LB14Y | 180 | LT14Y | 0 | 9 | LB01X | 0 | 2 - 50 | 0.1 | 10 | LT01X | 0 | RB01X | 0 | RT01X | 0 | | | | | | | | |
| 2 | FL10Y | 0 | 2 - 50 | 0.1 | 10 | | | | | | | | | | | | | | | | | | | | | | | | | | | | | | | | | | | | | | | | | | | | | | | | | | | | | | | | | | | | | | | | | | | | | | | | | | | | | | | | | | | | | | | | | | | | |
| | FL11Y | 180 | | | | 3 | FB10Z | 0 | 2 - 50 | 0.1 | 10 | FB11Z | 180 | 4 | FB10Z | 0 | 2 - 50 | 0.1 | 10 | FB11Z | 0 | 5 | LL06Z | 0 | 2 - 50 | 0.1 | 10 | RR06Z | 180 | | LR07Z | 180 | | | | RL07Z | 0 | 6 | LL06Z | 0 | 2 - 50 | | 0.1 | 10 | | | | RR06Z | 0 | LR07Z | 180 | RL07Z | 180 | | 7 | RB14Y | | | | 0 | 2 - 50 | 0.1 | 10 | RT14Y | 180 | | LB14Y | 180 | | | | LT14Y | 0 | 8 | RB14Y | 180 | 2 - 50 | | 0.1 | 10 | | | | RT14Y | 0 | LB14Y | 180 | LT14Y | 0 | 9 | LB01X | 0 | 2 - 50 | 0.1 | 10 | LT01X | 0 |
| 3 | FB10Z | 0 | 2 - 50 | 0.1 | 10 | | | | | | | | | | | | | | | | | | | | | | | | | | | | | | | | | | | | | | | | | | | | | | | | | | | | | | | | | | | | | | | | | | | | | | | | | | | | | | | | | | | | | | | | | | | | |
| | FB11Z | 180 | | | | 4 | FB10Z | 0 | 2 - 50 | 0.1 | 10 | FB11Z | 0 | 5 | LL06Z | 0 | 2 - 50 | 0.1 | 10 | RR06Z | 180 | | LR07Z | 180 | | | | RL07Z | 0 | 6 | LL06Z | 0 | 2 - 50 | 0.1 | 10 | RR06Z | 0 | | LR07Z | 180 | | RL07Z | | | 180 | 7 | RB14Y | 0 | 2 - 50 | 0.1 | 10 | RT14Y | 180 | LB14Y | | 180 | LT14Y | 0 | 8 | RB14Y | | | | 180 | 2 - 50 | 0.1 | 10 | RT14Y | 0 | LB14Y | 180 | LT14Y | 0 | | 9 | LB01X | | 0 | | | 2 - 50 | 0.1 | 10 | LT01X | 0 | RB01X | 0 | RT01X | 0 | | | | | | | | |
| 4 | FB10Z | 0 | 2 - 50 | 0.1 | 10 | | | | | | | | | | | | | | | | | | | | | | | | | | | | | | | | | | | | | | | | | | | | | | | | | | | | | | | | | | | | | | | | | | | | | | | | | | | | | | | | | | | | | | | | | | | | |
| | FB11Z | 0 | | | | 5 | LL06Z | 0 | 2 - 50 | 0.1 | 10 | RR06Z | 180 | | LR07Z | 180 | | | | RL07Z | 0 | 6 | LL06Z | 0 | 2 - 50 | 0.1 | 10 | RR06Z | 0 | | LR07Z | 180 | | | | RL07Z | 180 | 7 | RB14Y | 0 | 2 - 50 | 0.1 | 10 | RT14Y | 180 | | LB14Y | 180 | | | | LT14Y | 0 | 8 | RB14Y | 180 | 2 - 50 | 0.1 | | 10 | RT14Y | 0 | LB14Y | 180 | | | | LT14Y | 0 | 9 | LB01X | 0 | 2 - 50 | 0.1 | | 10 | LT01X | 0 | RB01X | 0 | | | | RT01X | 0 | | | | | | | | | | | | |
| 5 | LL06Z | 0 | 2 - 50 | 0.1 | 10 | | | | | | | | | | | | | | | | | | | | | | | | | | | | | | | | | | | | | | | | | | | | | | | | | | | | | | | | | | | | | | | | | | | | | | | | | | | | | | | | | | | | | | | | | | | | |
| | RR06Z | 180 | | | | | | | | | | | | | | | | | | | | | | | | | | | | | | | | | | | | | | | | | | | | | | | | | | | | | | | | | | | | | | | | | | | | | | | | | | | | | | | | | | | | | | | | | | | | | | | |
| | LR07Z | 180 | | | | | | | | | | | | | | | | | | | | | | | | | | | | | | | | | | | | | | | | | | | | | | | | | | | | | | | | | | | | | | | | | | | | | | | | | | | | | | | | | | | | | | | | | | | | | | | |
| | RL07Z | 0 | | | | | | | | | | | | | | | | | | | | | | | | | | | | | | | | | | | | | | | | | | | | | | | | | | | | | | | | | | | | | | | | | | | | | | | | | | | | | | | | | | | | | | | | | | | | | | | |
| 6 | LL06Z | 0 | 2 - 50 | 0.1 | 10 | | | | | | | | | | | | | | | | | | | | | | | | | | | | | | | | | | | | | | | | | | | | | | | | | | | | | | | | | | | | | | | | | | | | | | | | | | | | | | | | | | | | | | | | | | | | |
| | RR06Z | 0 | | | | | | | | | | | | | | | | | | | | | | | | | | | | | | | | | | | | | | | | | | | | | | | | | | | | | | | | | | | | | | | | | | | | | | | | | | | | | | | | | | | | | | | | | | | | | | | |
| | LR07Z | 180 | | | | | | | | | | | | | | | | | | | | | | | | | | | | | | | | | | | | | | | | | | | | | | | | | | | | | | | | | | | | | | | | | | | | | | | | | | | | | | | | | | | | | | | | | | | | | | | |
| | RL07Z | 180 | | | | | | | | | | | | | | | | | | | | | | | | | | | | | | | | | | | | | | | | | | | | | | | | | | | | | | | | | | | | | | | | | | | | | | | | | | | | | | | | | | | | | | | | | | | | | | | |
| 7 | RB14Y | 0 | 2 - 50 | 0.1 | 10 | | | | | | | | | | | | | | | | | | | | | | | | | | | | | | | | | | | | | | | | | | | | | | | | | | | | | | | | | | | | | | | | | | | | | | | | | | | | | | | | | | | | | | | | | | | | |
| | RT14Y | 180 | | | | | | | | | | | | | | | | | | | | | | | | | | | | | | | | | | | | | | | | | | | | | | | | | | | | | | | | | | | | | | | | | | | | | | | | | | | | | | | | | | | | | | | | | | | | | | | |
| | LB14Y | 180 | | | | | | | | | | | | | | | | | | | | | | | | | | | | | | | | | | | | | | | | | | | | | | | | | | | | | | | | | | | | | | | | | | | | | | | | | | | | | | | | | | | | | | | | | | | | | | | |
| | LT14Y | 0 | | | | | | | | | | | | | | | | | | | | | | | | | | | | | | | | | | | | | | | | | | | | | | | | | | | | | | | | | | | | | | | | | | | | | | | | | | | | | | | | | | | | | | | | | | | | | | | |
| 8 | RB14Y | 180 | 2 - 50 | 0.1 | 10 | | | | | | | | | | | | | | | | | | | | | | | | | | | | | | | | | | | | | | | | | | | | | | | | | | | | | | | | | | | | | | | | | | | | | | | | | | | | | | | | | | | | | | | | | | | | |
| | RT14Y | 0 | | | | | | | | | | | | | | | | | | | | | | | | | | | | | | | | | | | | | | | | | | | | | | | | | | | | | | | | | | | | | | | | | | | | | | | | | | | | | | | | | | | | | | | | | | | | | | | |
| | LB14Y | 180 | | | | | | | | | | | | | | | | | | | | | | | | | | | | | | | | | | | | | | | | | | | | | | | | | | | | | | | | | | | | | | | | | | | | | | | | | | | | | | | | | | | | | | | | | | | | | | | |
| | LT14Y | 0 | | | | | | | | | | | | | | | | | | | | | | | | | | | | | | | | | | | | | | | | | | | | | | | | | | | | | | | | | | | | | | | | | | | | | | | | | | | | | | | | | | | | | | | | | | | | | | | |
| 9 | LB01X | 0 | 2 - 50 | 0.1 | 10 | | | | | | | | | | | | | | | | | | | | | | | | | | | | | | | | | | | | | | | | | | | | | | | | | | | | | | | | | | | | | | | | | | | | | | | | | | | | | | | | | | | | | | | | | | | | |
| | LT01X | 0 | | | | | | | | | | | | | | | | | | | | | | | | | | | | | | | | | | | | | | | | | | | | | | | | | | | | | | | | | | | | | | | | | | | | | | | | | | | | | | | | | | | | | | | | | | | | | | | |
| | RB01X | 0 | | | | | | | | | | | | | | | | | | | | | | | | | | | | | | | | | | | | | | | | | | | | | | | | | | | | | | | | | | | | | | | | | | | | | | | | | | | | | | | | | | | | | | | | | | | | | | | |
| | RT01X | 0 | | | | | | | | | | | | | | | | | | | | | | | | | | | | | | | | | | | | | | | | | | | | | | | | | | | | | | | | | | | | | | | | | | | | | | | | | | | | | | | | | | | | | | | | | | | | | | | |

WE IS
 RITY

TABLE 10. MGVVT LIFTOFF PITCH/ROLL MODE,
LOX TANK FULL

| Test Condition | Symmetric | | | Antisymmetric | | |
|--------------------|-----------|---------|--------------|---------------|---------|--------------|
| | Mode No. | Freq Hz | Damping C/cc | Mode No. | Freq Hz | Damping C/cc |
| With Rings | 5 | 2.05 | 0.013 | 8 | 2.235 | 0.010 |
| Two Segments Off | 40 | 2.02 | 0.018 | 32 | 2.235 | 0.009 |
| Three Segments Off | 42 | 2.04 | 0.017 | 33 | 2.235 | 0.011 |

TABLE 11. MGVVT LIFTOFF TEST PITCH/ROLL MODE,
LOX TANK EMPTY

| Test Conditions | Symmetric | | | Antisymmetric | | |
|-----------------|-----------|----------|--------------|---------------|----------|--------------|
| | Mode No. | Freq. Hz | Damping C/cc | Mode No. | Freq. Hz | Damping C/cc |
| Bolt Loose | 43 | 2.314 | 0.018 | 44 | 2.196 | 0.012 |
| Bolt Torqued | 45 | 2.314 | 0.017 | -- | ---- | ---- |

h. Special Test of the Forward ET/SRB Interface - LOX Tank Refilled. It was thought that the ball joint had been worn smooth in the previous test (LOX tank empty), so the LOX tank was refilled to simulate the liftoff test condition and the pitch/roll modes were retuned. The test results showed no appreciable change in frequency and damping to the previous test condition with the LOX tank full. It also showed that the LOX tank weight was sufficient to lock the forward interface.

B. End Burn (Pre-SRB Separation)

1. Configuration. The end burn (T+125 sec) configuration tested consisted of the OV-101 Orbiter mated with an ET and two empty SRB. The ET and Orbiter test articles were the same as those used during the liftoff test and have been previously described. The two SRB tanks contained no inert propellant and since the test condition simulated was end burn, the pressure rings used to simulate internal pressure for liftoff were not required. The SRB nozzles were omitted as in liftoff.

2. Suspension. The end burn configuration utilized the same suspension system as was used in liftoff. However, the pressures in the HDS system and the pitch and yaw air bags were reduced to obtain a softer suspension system. This was done to maintain an adequate separation between the rigid body modes and the elastic modes.

3. Test Results and Analysis.

a. Suspension System Modes. The six rigid-body modes were obtained and are summarized in Table 12.

b. Flight Control Transfer Functions. Nine flight control transfer functions were taken for the SRB and Orbiter in roll, pitch, and yaw. These sweeps are presented in Table 13 and show the shakers and phasing used, the type motion produced, and the frequency range covered.

The last three sweeps were taken using shakers on both the Orbiter and the SRB simultaneously to excite the Shuttle pitch, roll, and yaw. Shaker force ratios were specified for these sweeps to simulate actual flight conditions. Significant response frequencies were identified for flight controls and are presented in Table 14.

c. Pogo Wide Band Sweep. Wide band frequency sweeps were run independently on all three orbiter main engines. The excitation force in each case was along the engine longitudinal axis. The three pogo sweeps are listed in Table 15. Four engine axial modes were identified by the pogo group above 16 Hz and dwells were taken for each mode.

d. Modal Test Results versus Pretest Analysis. All acceptable modes tuned during the end burn symmetric tests are shown in Table 16. The antisymmetric modes are listed in Table 17. The correlating pretest analytical frequency and the computed modal damping from the decay traces are also shown in those tables. The last column gives the percent error between the test and the analytical mode.

TABLE 12. SRB BURNOUT SUSPENSION SYSTEM MODES

| Mode No. | Test Frequency Hz | Predicted Frequency Hz | Damping C/cc | Description of Motion |
|----------|-------------------|------------------------|--------------|-----------------------|
| 3 | 0.255 | 0.302 | .077 | Z-Translation |
| 53 | 0.275 | 0.258 | .009 | Y-Translation |
| 51 | 0.549 | 0.528 | .037 | θX (Roll) |
| 54 | 0.549 | 0.603 | .034 | θZ (Yaw) |
| 1 | 0.647 | 0.59 | .022 | X-Translation |
| 2 | 0.657 | 0.671 | .048 | θY (Pitch) |

TABLE 13. SRB B/O FCS SWEEPS

| Sweep No. | Shakers | Phase (deg) | Type Motion | SNTAS Sweep No. | | | Remarks |
|-----------|--|------------------------------|-------------------|-----------------|---------------|----------------|--|
| | | | | 2-7 Hz | 7-17 Hz | 17-30 Hz | |
| 1 | RT14Y/RB14Y LT/LB14Y | 180/0 0/180 | SRB Yaw | 7 | 8 | 9 | |
| 2 | FL10Y FL11Y | 0 0 | ORB Yaw | 5 | 10 | 11 & 11A | |
| 3 | RR06Z/RL07Z LL06Z/LR07Z | 0/180 0/180 | SRB Pitch | 1 | 12 | 13 | |
| 4 | FB10Z/FB11Z | 0/0 | ORB Pitch | 3 | 14 | 15 | |
| 5 | RR06Z/RL07Z LL06Z/LR07Z | 180/0 0/180 | SRB Roll | 2 | 17 | | |
| 6 | FB10Z/FB11Z | 0/180 | ORB Roll | 6 | 16 | | 6-1 (No. 4) Rerun |
| 7 | RR06Z/RL07Z LL06Z/LR07Z FB10Z/FB11Z | 0/180 0/180 180/180 | SRB/ORB Pitch | | 2-15 Hz 18 | 15-30 Hz 19 | Shakers SRM Shakers-1.0* ORB Shakers-3.0 |
| 8 | RB14Y/RT14Y LB14Y/LT14Y FL10Y/FL11Y | 0/180 180/0 0/0 | SRB/ORB Yaw | | 22 | 23 | *= Reference SRM Shakers-1.0* FL10Y -2.0 FL11Y -4.0 |
| 9 | RR06Z/RL07Z LL06Z/LR07Z FB10Z/FB11Z FL10Y | 0/180 180/0 0/180 0 | SRB/ORB Roll | | 20 | 21 | SRM Shakers-1.0* FL10Y -1.15 FB10Z -1.54 FB11Z |

TABLE 14. PRIMARY FCS RESPONSE FREQUENCIES SRB BURNOUT TRANSFER FUNCTIONS

| Sensor/Axis | | Primary Response Frequency (2-7 Hz Freq Range) | |
|---------------|---------|---|-------------------------|
| ORB RGA'S | | SRB Shakers | ORB Shakers |
| 1307 Bulkhead | Roll | 2.5*, 3.9, 5.2 | 2.7*, 4.1, 5.3* |
| | Pitch | 2.6*, 4.8, 6.1 | 2.7, 3.4*, 6.1 |
| | Yaw | 2.5, 4.3 | 4.2 |
| Nav Base | Roll | 2.5*, 4.2 | 2.7*, 4.5, 5.4, 6.8 |
| | Pitch | Low Coherence | 3.4 |
| | Yaw | 2.5 | Low Coherence |
| LSRB | Pitch | 2.6*, 4.8, 6.0 | 2.6*, 6.8 |
| | Yaw | 2.5, 2.6, 4.4 | 2.6, 4.0, 4.4, 5.3, 6.7 |
| | Pitch | 2.6, 4.8, 6.0 | 2.6*, 4.9 |
| RSRB | Yaw | 2.5, 2.6, 4.7 | 2.6, 4.0, 4.4, 5.3, 6.7 |
| | Normal | 2.6, 4.8* | 3.4 |
| | Lateral | 2.5*, 4.2 | 2.6, 4.2 |
| ORB Accel | | | |

* Dominant Modes

** Off Axis Response to 4.8 Hz SRB Pitch Shaker Excitation

TABLE 15. SRB B/O POGO SWEEPS

| Sweep No. | Shakers | SMTAS Sweep No. | | |
|-----------|------------------------------------|-----------------|----------|----------|
| | | 2-12 Hz | 12-30 Hz | 30-50 Hz |
| 1 | MT01X Upper SSME Axial | 1 | 2 | 3 |
| 2 | ML02X Lower Left SSME Axial | 4 | 5 | 6 |
| 3 | MR03X Lower Right SSME Axial | 11 | 10 | 9 |

TABLE 16. MGVGT MODAL CORRELATION
[CONFIGURATION - BURNOUT (SYMMETRIC)]

| Test Mode | | | | Analysis Mode | | | | Percent Error |
|-----------|-------|-------|---|---------------|-------|--|------|---------------|
| Mode No. | Freq. | Damp | Description | Mode No. | Freq. | Description | | |
| 6 | 2.55 | 0.025 | SRB Pitch (0.48), Roll (0.13), Orbiter Pitch (0.19) | 4 | 2.50 | SRB Pitch (0.22), Roll (0.56), Orbiter Pitch (0.08) | 2.0 | |
| 27 | 3.41 | 0.012 | Orbiter Pitch (0.46), Axial (0.38), SRB Pitch (0.01), Roll (0.02) | 5 | 3.11 | Orbiter Pitch (0.37), Axial (0.32), SRB Pitch (0.19), Roll (0.06) | 8.8 | |
| 9 | 3.59 | 0.028 | SRB Y-Bending (0.79), Z-Bending | 7 | 3.57 | SRB Y-Bending (0.51), Z-Bending | 0.6 | |
| 10 | 4.78 | 0.019 | SRB Pitch (0.64), Orbiter Z (0.16) | | | | | |
| 15 | 6.08 | 0.007 | Orbiter Axial (0.32), Z-Bending (0.27), SRB-Z (0.17), ET Feedline (0.03) | 9 | 6.19 | Orbiter Axial (0.41), Z-Bending (0.24), SRB-Z (0.04), ET Feedline (0.14) | 1.8 | |
| 32 | 7.73 | 0.007 | SRB Y (0.35), X (0.19), ET (0.10) | 17 | 8.86 | SRB-Y (0.57), ET (0.27) | 15.0 | |
| 18 | 8.92 | 0.023 | Orbiter Z-Bending (0.38), SRB Pitch (0.13), Roll (0.12) | 19 | 9.04 | Orbiter Z Bending (0.48), and Axial (18), ET (0.21) | 1.3 | |
| 23 | 9.94 | 0.016 | ET (0.51 Intertank and LWR LH ₂ Tank), SRB X (0.14), Y (0.22) | 22 | 10.64 | ET (0.58 Intertank and LWR LH ₂ Tank), SRB X (0.19), Y (-11) | 7.0 | |
| 19 | 11.08 | 0.018 | ORB Z Bending (0.40), Axial (0.14), SRB Z Bending (0.22), Roll (0.09) | 24 | 11.19 | ORB Z Bending (0.29), Axial (0.13), SRB Z Bending (0.15) | 1 | |
| 7 | 12.09 | 0.002 | LOX Dome Bulge (0.18), Feedline (0.14), SRB Axial (0.21), Y Bending (0.12) | | | | | |
| 20 | 13.35 | 0.022 | ORB Z Bending (0.50), Elevons Out-of-Phase (0.16) | 28 | 12.31 | ORB Z Bending (0.06), Elevons Out-of-Phase (0.72) | 8 | |
| 22 | 13.74 | 0.012 | SRB 2nd Y Bending (0.20), SRB Z Bending (0.10), Elevon Rotation (0.14), LWR SSME Z (0.05) | | | | | |
| 26 | 14.56 | 0.012 | ORB 2nd Z Bending (0.40), LH ₂ Tank (0.12) | 36 | 14.3 | ORB 2nd Z Bending (0.26), Wing Bending (0.21), Elevons (0.16) | 2 | |

TABLE 16. (Concluded)

| Test Mode | | | | Analysis Mode | | | | Percent Error |
|-----------|-------|-------|---|---------------|-------|---|----|---------------|
| Mode No. | Freq. | Damp | Description | Mod. No. | Freq. | Description | | |
| 31 | 15.11 | 0.012 | SRB Z Bending with Torsion (0.39), AFT Payload Axial (0.24) | | | | | |
| 24 | 16.05 | 0.011 | LH ₂ Tank Shell Mode (0.20), SRB X (0.1) and Z Bending (0.1), OMS POD Axial (0.09) | | | | | |
| 8 | 16.44 | 0.015 | SRB Axial (0.27) with Y (0.15) and Z (0.09) Bending, LH ₂ Tank (0.16), LOX Tank (0.16) | 41 | 15.26 | SRB Y Bending (0.23), LOX Tank (0.32), LH ₂ (0.08) | 7 | |
| 21 | 17.65 | 0.035 | SSME Z (0.45), LH ₂ Tank (0.10) | | | | | |
| 11 | 16.36 | 0.006 | SRB 2nd Z Bending (0.56) | 53 | 18.12 | SRB Z Bending (0.50), Elevons (0.21) | 1 | |
| 30 | 21.78 | 0.014 | Feedline X (0.20), LH ₂ Tank (0.14), UPR SSME Z (0.07), LWR SSME X (0.06) | 92 | 24.35 | LH ₂ Tank (0.31), LWR SSME X (0.08), UPR SSME Z (0.04) | 12 | |
| 33 | 28.75 | 0.022 | UPR SSME X (0.17), LWR SSME X (0.06), LH ₂ Tank (0.31) | 131 | 32.52 | UPR SSME X (0.11), Z (0.06), LWR SSME Z (0.11), X (0.06), LH ₂ Tank (0.27) | 13 | |
| 29 | 30.45 | 0.026 | UPR SSME X (0.29), LWR SSME X (0.09), Z (0.09), LOX Dome and LH ₂ Tank Axial (0.21) | 135 | 32.96 | UPR SSME X (0.44), LOX Tank (0.08), LH ₂ Tank (0.06) | 8 | |
| 25 | 31.62 | 0.018 | UPR SSME Axial (0.42), LH ₂ Tank (0.19) | 135 | 32.96 | UPR SSME X (0.44), LOX Tank (0.06), LH ₂ Tank (0.06) | 4 | |

TABLE 17. MVGVT MODAL CORRELATION
[CONFIGURATION - BURNOUT (ANTISYMMETRIC)]

| Test Mode | | | Analysis Mode | | | | |
|-----------|-----------|-------|---|----------|------------|--|---------------|
| Mode No. | Freq (Hz) | Damp | Description | Mode No. | Freq. (Hz) | Description | Percent Error |
| 2 | 2.49 | 0.019 | SRB Z Trans (0.45), and Roll (0.08), ORB Yaw (0.14) and Roll (0.11) | 4 | 2.53 | SRB Pitch (0.54), Roll (0.04), ORB Yaw (0.23) and Roll (0.03) | 1.6 |
| 18 | 3.98 | 0.015 | SRB Pitch (0.60), OMS Y (0.05), V.T. and Wing Bend (0.08) | | | None | |
| 20 | 4.19 | 0.015 | SRB Yaw (0.36) ORB Yaw (0.17), Wing Bending (0.13) | 7 | 4.48 | SRB Yaw (0.45), ORB Yaw (0.34) | 7.9 |
| 8 | 6.82 | 0.023 | FWD P/L Y (0.21), FUS Y Bend (0.21), OMS POD Y (0.10) | 10 | 6.10 | FWD P/L Y (0.54), FUS Y Bend (0.14) | 10.6 |
| 10 | 7.529 | 0.016 | SRB X Trans (0.54) and Y Bend (0.30), ET Y Bend (0.14) | 17 | 8.41 | SRB X (0.42), Y Bend (0.23), ET Y Bend (0.21) | 11.7 |
| 11 | 7.92 | 0.037 | SRB Z Bend (0.24), Roll (0.23), ORB Y Bend (0.11), Torsion (0.08) | 12 | 6.721 | SRB Z Bend (0.23), Roll (0.08), Y Bend (0.08), ORB Y Bend (0.28), and Torsion (0.11) | 15.1 |
| 16 | 8.49 | 0.016 | Tuned on AFT Payload Y (0.04), SRB X (0.30), ORB Y (0.19) | | | None | |
| 6 | 9.71 | 0.016 | SRB Y Bend (0.37), ET Y Bend (0.15), AFT P/L Y (0.07), OMS POD Y (0.07) | 22 | 10.01 | SRB 1st Y Bend (0.38), Z Bend (0.20), ET Y Bend (0.24) | 3.1 |
| 22 | 11.86 | 0.013 | SRB Z (0.24) and Y Bend (0.22), and LH ₂ Y Bend (0.32) | | | None | |
| 12 | 12.52 | 0.009 | ET Y Bending (0.90) | 24 | 11.6 | Elev Z (0.35), ET Y Bend (0.16) | 7.4 |
| 17 | 13.35 | | LH ₂ Shell (0.34), SRB Y Bend (0.18), CC Y (0.02) | 36 | 14.83 | LH ₂ Shell (0.24), CC Y (0.08) | 11.1 |

TABLE 17. (Concluded)

| Test Mode | | | | Analysis Mode | | | |
|-----------|------------|-------|---|---------------|------------|---|---------------|
| Mode No. | Freq. (Hz) | Damp | Description | Mode No. | Freq. (Hz) | Description | Percent Error |
| 9 | 14.13 | 0.028 | ORB Y Bend (0.32) and Roll (0.07). CC Yaw (0.12) | 30 | 13.15 | CC Yaw (0.20), C-SSME Y (0.18), ORB Roll (0.08) | 6.9 |
| 19 | 15.73 | 0.015 | ET Y Bend (0.64), SRB Y (0.05) | 41 | 16.25 | ET Y Bend (0.53), SRB Y (0.03) | 3.3 |
| 23 | 17.61 | 0.005 | SRB Torsion (0.58), LH ₂ Shell (0.09) | | | None | |
| 14 | 18.67 | 0.013 | SRB Z Bend (0.52) and Torsion (0.17) | | | None | |

e. Special Tests.

(1) Verification of the SRB RGA Ring. As a result of the liftoff tests, an abnormally high transfer function value was observed on both the left and right forward SRB ring frames where the rate gyros are mounted. These local resonances occurred at 23 and 25 Hz respectively. These rings frames were stiffened subsequent to the liftoff test. An end burn test was used to verify that the "fix" was acceptable for flight control. A comparison of the pre-fix and post-fix test results are shown in Table 18. As can be seen from the table, a response magnitude reduction of 40 on the left SRB rate gyros and 7 on the right SRB rate gyros was obtained as a result of the structural fix.

(2) Investigation of the 1307 Bulkhead Deformation. A special test was conducted to assess the credibility of the yaw rate gyros mounted on the 1307 Orbiter bulkhead. Unexpected yaw rates were read during a symmetric flight control sweep. Twelve additional accelerometers were mounted and read during a special 1307 bulkhead survey sweep. The bulkhead deformation in the symmetric 4.78 Hz mode is shown in Figure 20. The yaw rates computed from accelerometers are compared with rates measured by the yaw rate gyros and are shown in Table 19. This comparison indicated that the readings are credible; however, the readings reflect local deformations only. The flight control transfer functions indicated that the yaw rates were about three times the pitch rate for the 4.78 Hz symmetric mode, which was verified by the accelerometers.

(3) LOX Dome Transfer Functions. LOX dome acceleration and dynamic pressure transfer functions were obtained for the Pre-SRB separation test condition. In addition, the ET liquid level was adjusted to 100 and 80 sec burn times and the transfer functions were repeated. Since the liquid level tests were performed with the SRB's empty (not a flight condition), care must be exercised applying the data directly to the flight vehicle. In all cases the excitation was applied to the SRB bottom.

Acceleration and pressure transfer functions for the pre-SRB separation, 100 and 80 sec tests are shown in Figures 21 through 26. Acceleration and pressure frequency response amplitudes shown are per pound of the reference shaker force used in each sweep. Since two shakers were used on each SRB, the value of the indicated transfer function must be divided by two.

Modal frequencies of the two LOX tank bulge modes in the SRB thrust oscillation frequency regime were plotted as a function of burn time. These data are shown in Figure 27. The damping for each mode is plotted in Figure 28 for the burn times tested. The damping was calculated from the decay traces.

TABLE 18. SRB RGA MOUNTING RING FIX FCS EVALUATION

| | Sensor | Frequency (Hz) | Transfer Function Magnitude (deg/sec) lbf |
|--------------|----------|----------------|---|
| L.O. Data | LSRB RGA | 23 | 80×10^{-5} |
| | RSRB RGA | 25 | 14×10^{-5} |
| B.O. Data | LSRB RGA | 23 | 2×10^{-5} |
| | RSRB RGA | 25 | 2×10^{-5} |
| | LSRB RGA | * 37 | 9.6×10^{-5} |
| | RSRB RGA | * 30-50 | Peak Not Discernable Over 30-50 Hz Range |

* Based on 30-50 Hz Minisweep

Conclusion: Fix is Adequate

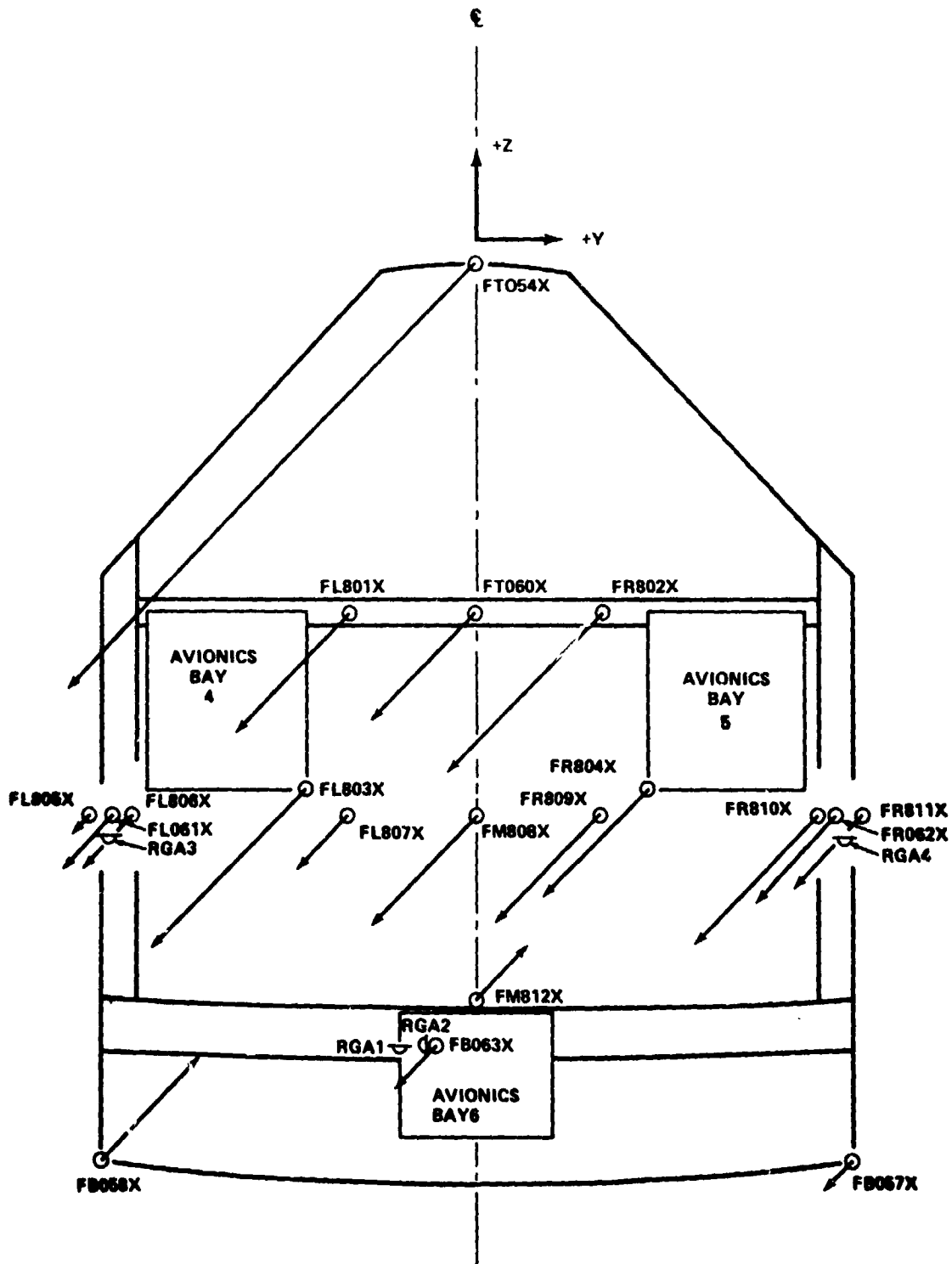


Figure 20. 1307 Bulkhead accelerations at 4.7 Hz in g's/lb.

TABLE 19. 1307 BULKHEAD COMPUTED AND MEASURED YAW RATES (DEG/SEC)

| | Measured from RGA | Computed from Accel. | Ratio |
|-----------------------|-------------------------|----------------------------|-------|
| Left Hand Side | 1.16×10^{-4} | 1.2×10^{-4} | .97 |
| Right Hand Side | 1.05×10^{-4} | 1.8×10^{-4} | .58 |

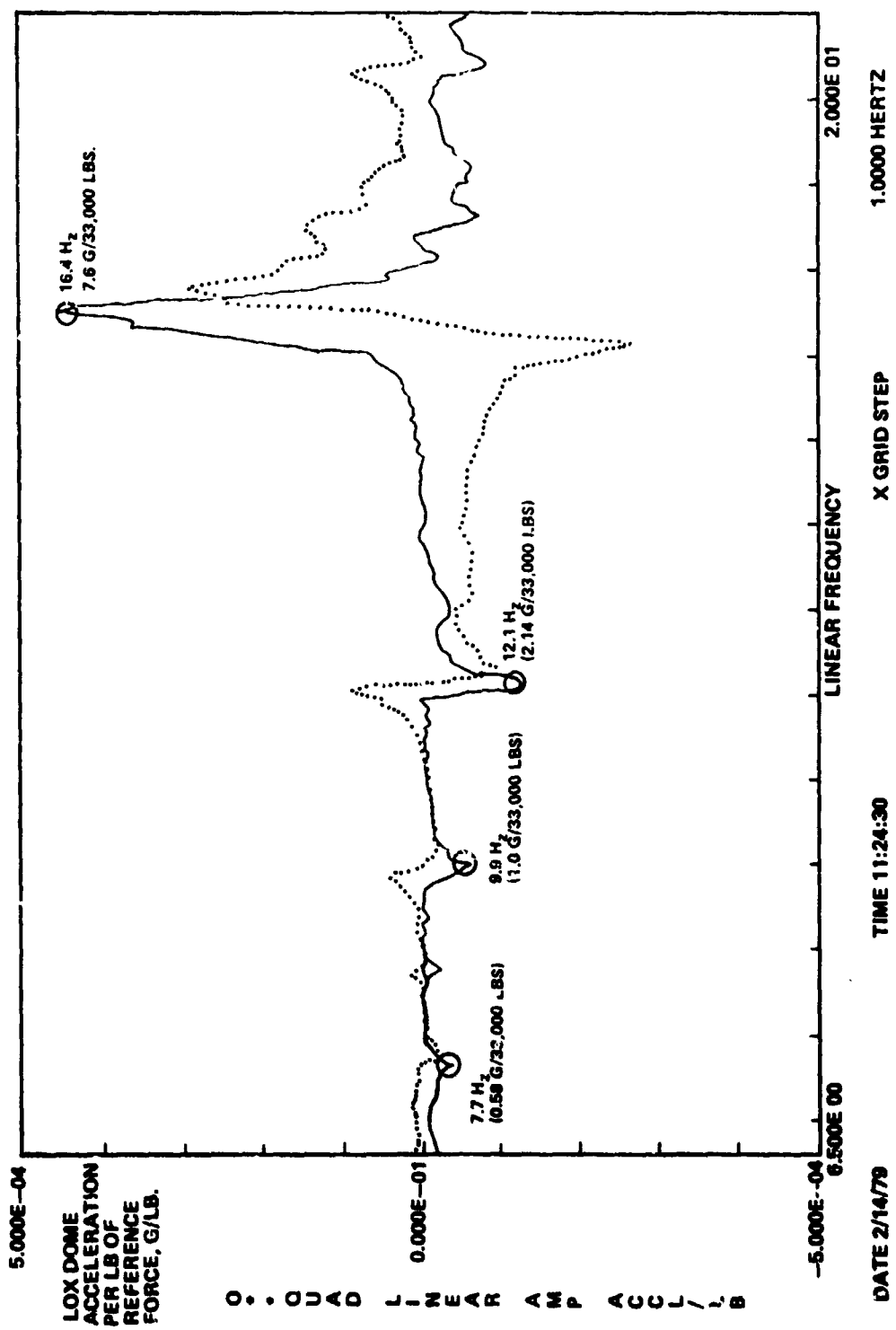
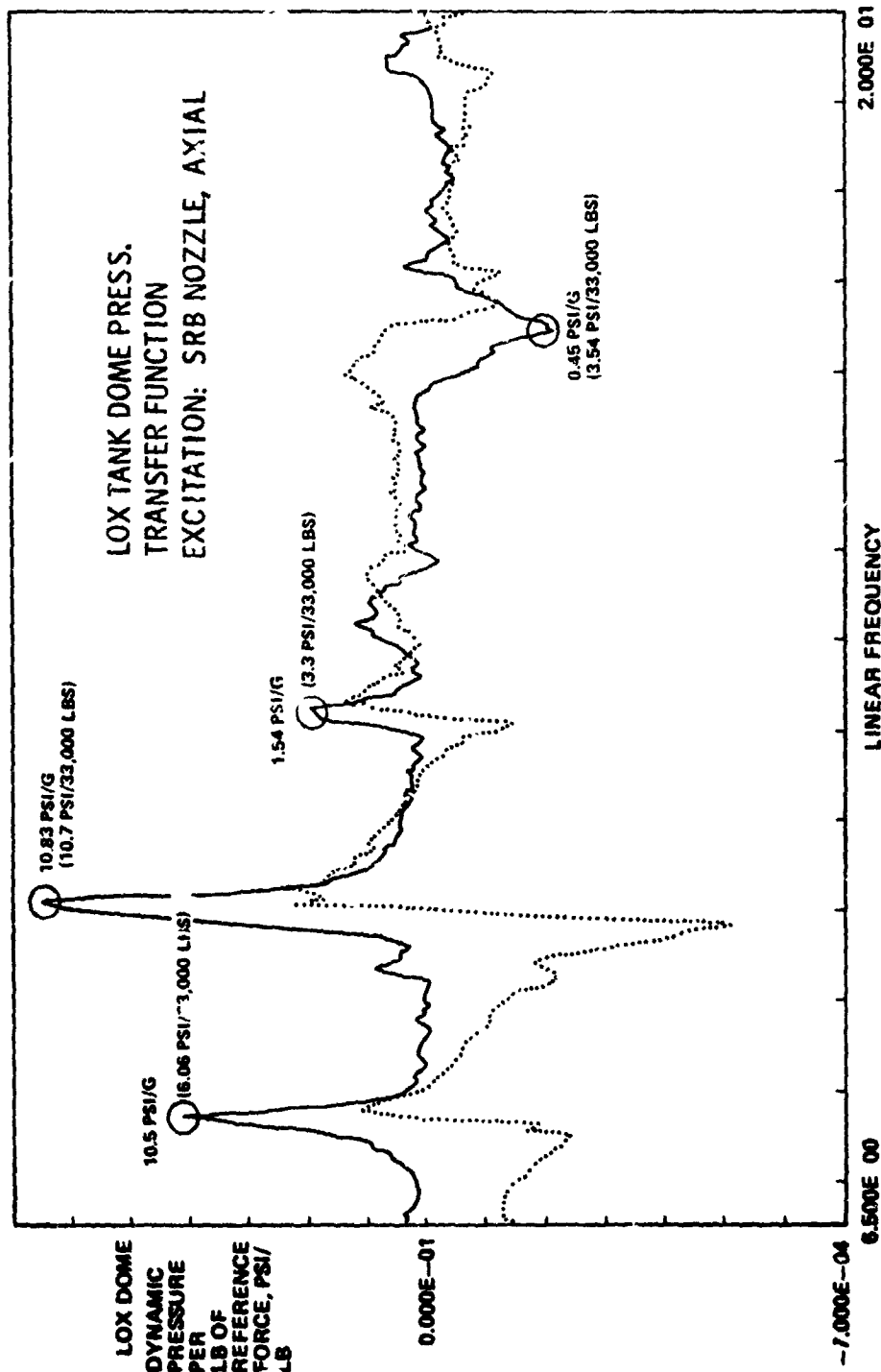


Figure 21. Lox dome acceleration transfer function, pre SRB separation.



FORCE CHANNEL RB01X RESPONSE CHANNEL EM02P
 Figure 22. Lox dome pressure transfer function, pre SRB separation.

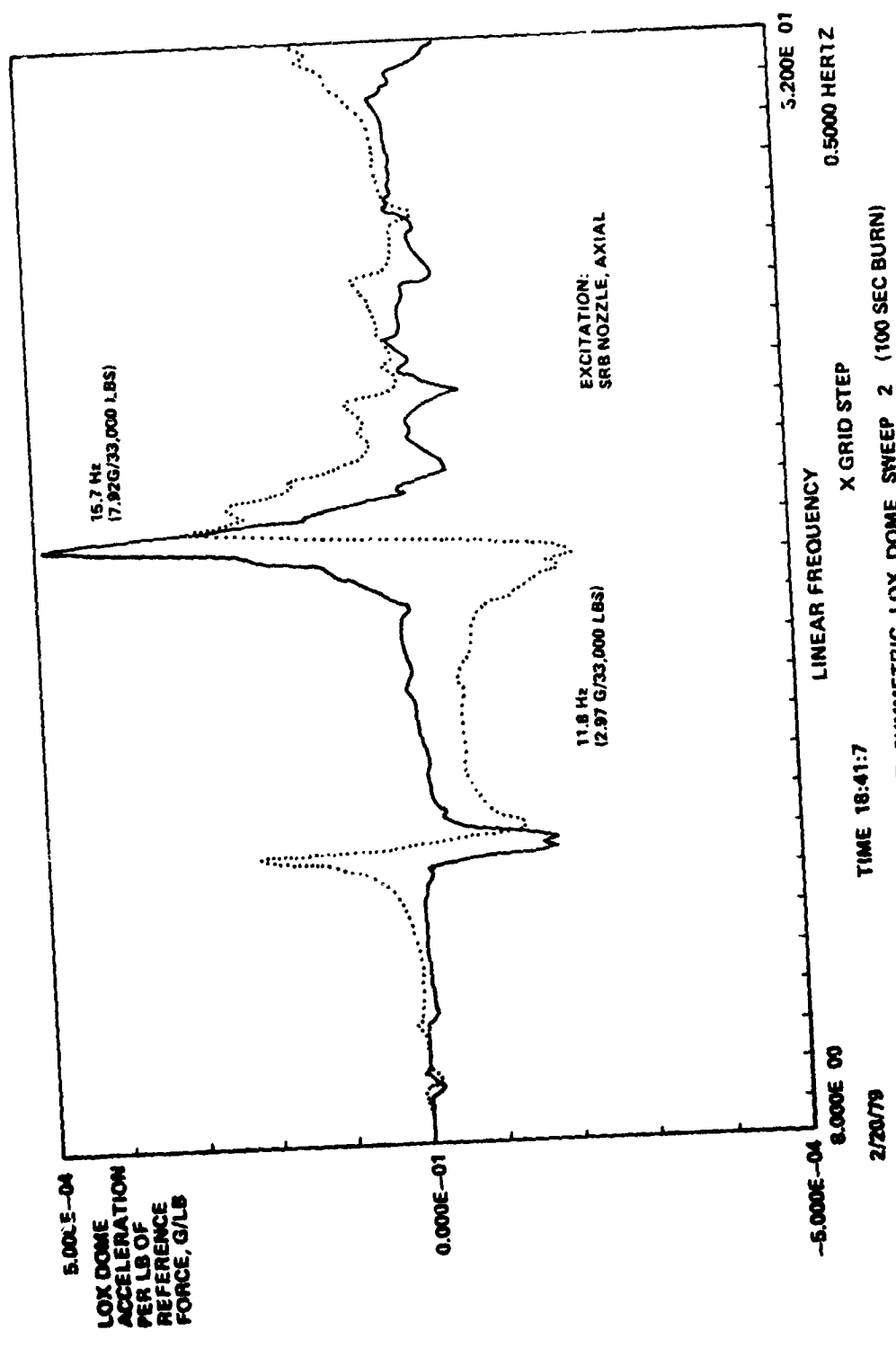
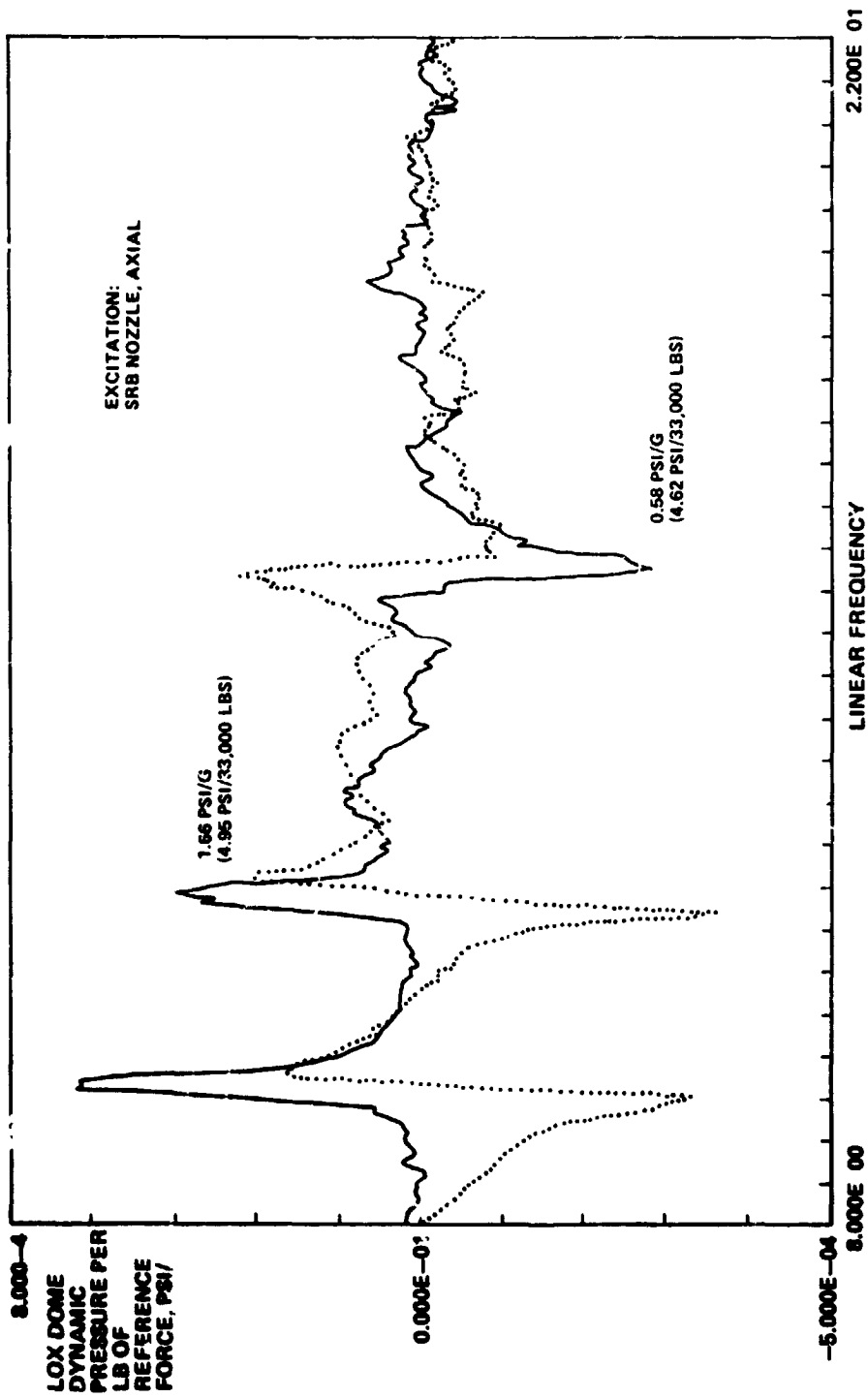


Figure 23. Lox dome acceleration transfer function, 100 second.



DATE 2/20/79 TIME 18:41:7

ORB/ET/SRB BURNOUT SYMMETRIC LOX DOME SWEEP 2 (100 SEC BURN)

FORCE CHANNEL RT01X RESPONSE CHANNEL EMO2P

Figure 24. Lox dome pressure transfer function, 100 second.

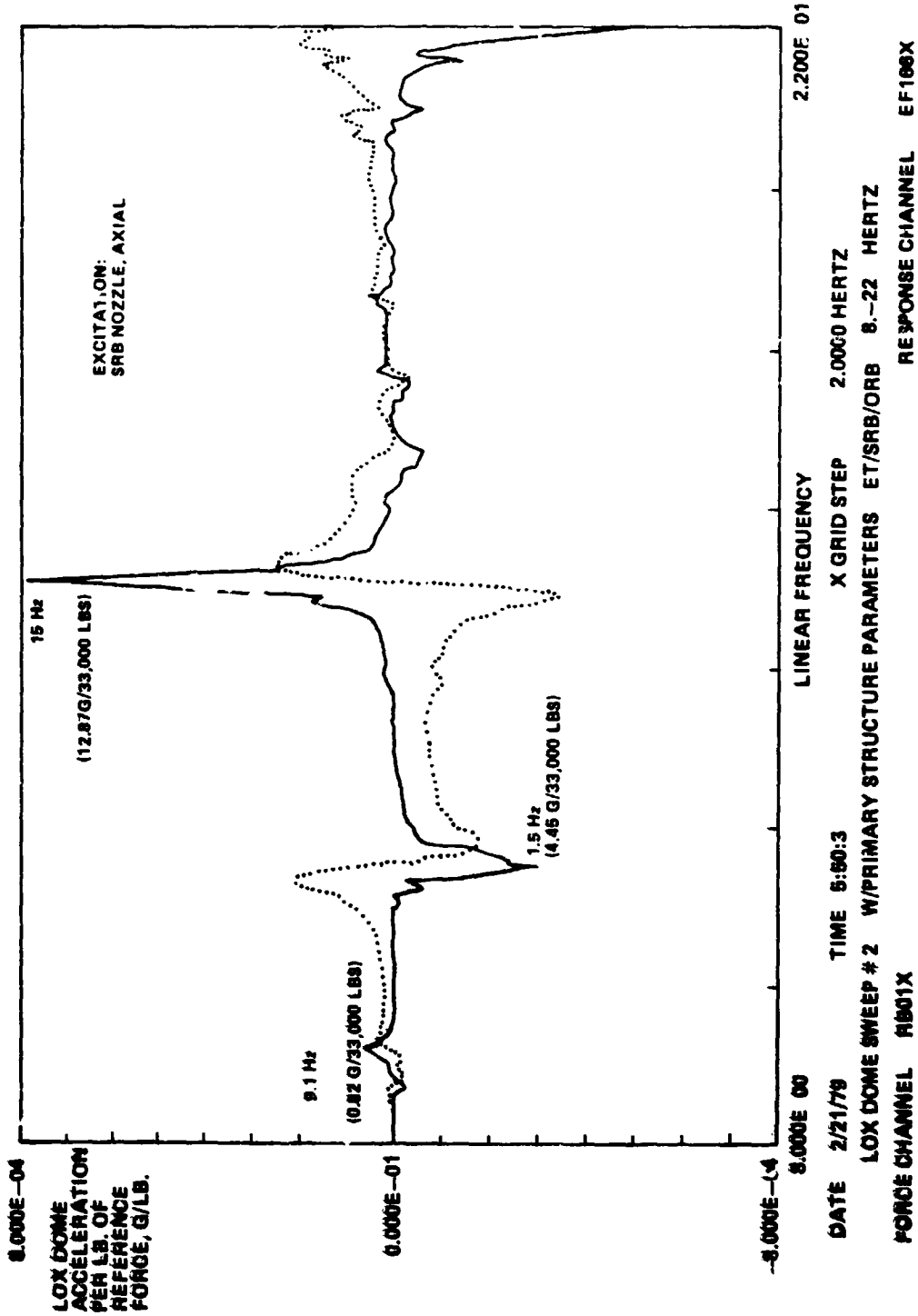
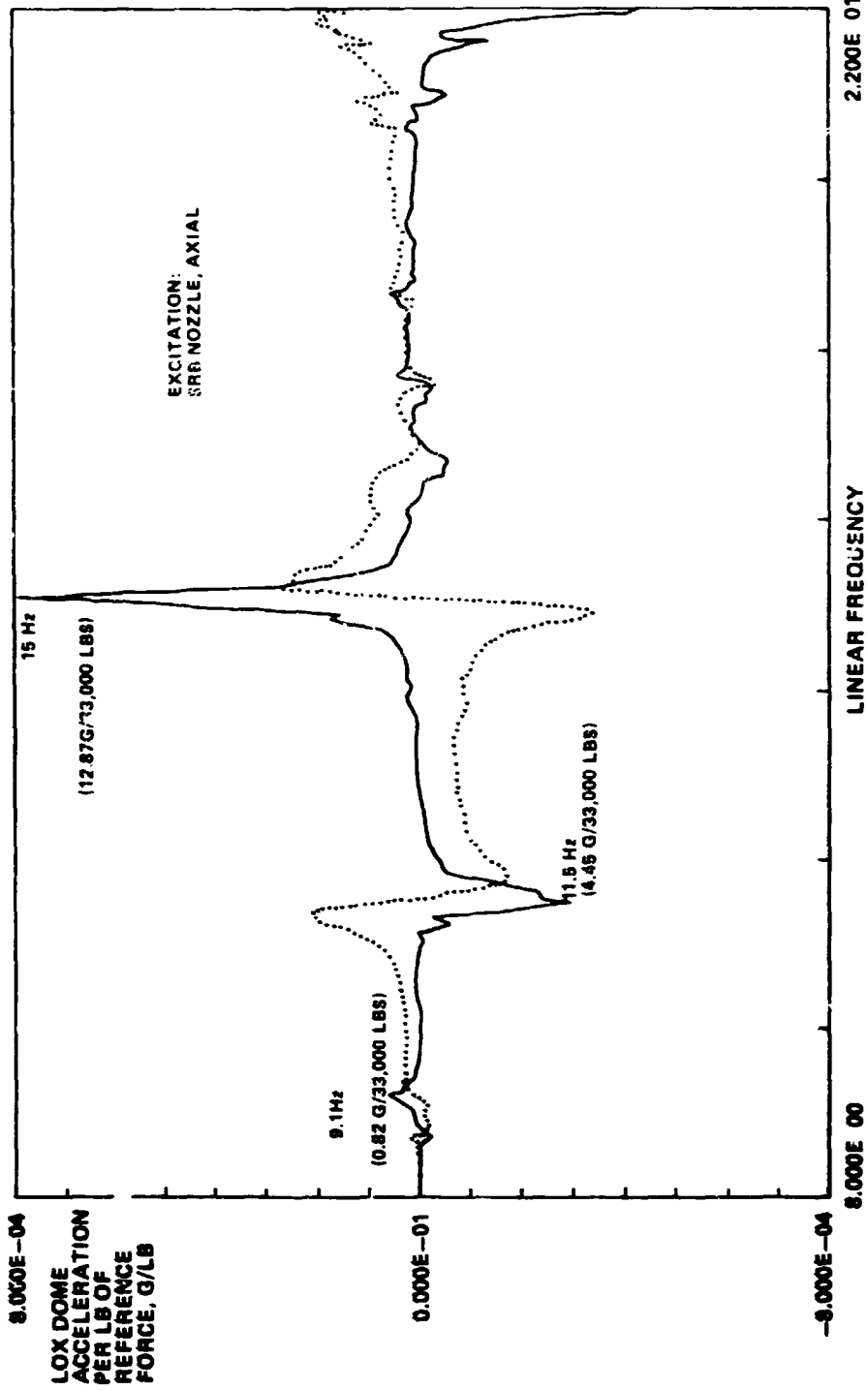
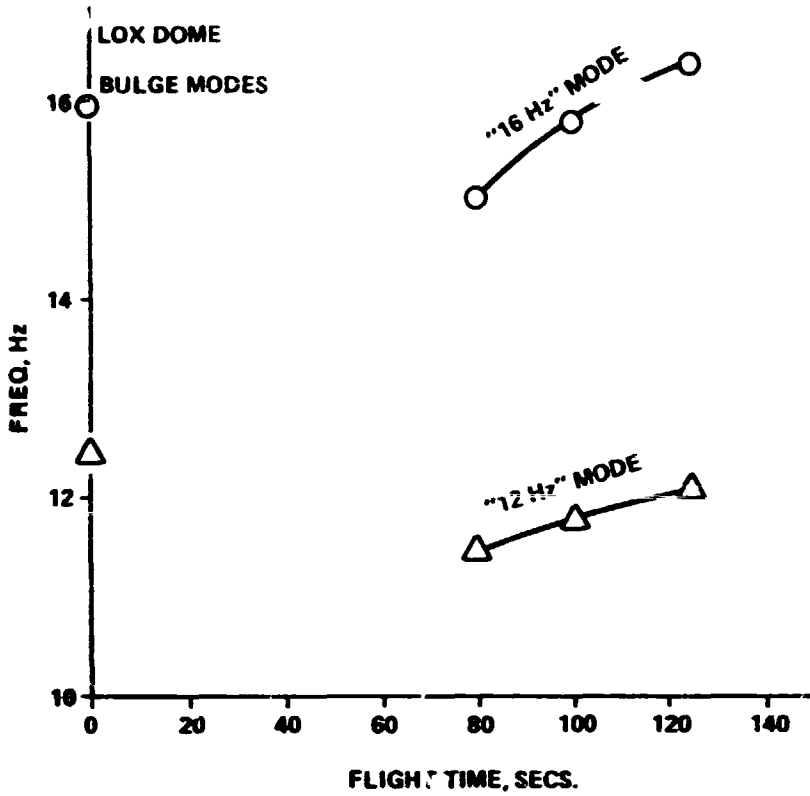


Figure 25. Lox dome acceleration transfer function, 30 second.



DATE 2/21/79 TIME 5:50:3 X GRID STEP 2.0000 HERTZ
 LOX DOME SWEEP # 2 W/PRIMARY STRUCTURE PARAMETERS ET/SRB/ORB 8.-22. HERTZ
 FORCE CHANNEL RB01X RESPONSE CHANNEL EF106X

Figure 26. LOX dome acceleration transfer function, 80 second.



NOTE: EXCITATION APPLIED TO SRB BOTTOM ONLY; SRB'S ARE EMPTY AT 80 AND 100 SECS. LH₂ TANK EMPTY FOR ALL CASES

Figure 27. Bulge mode frequency change with flight time.

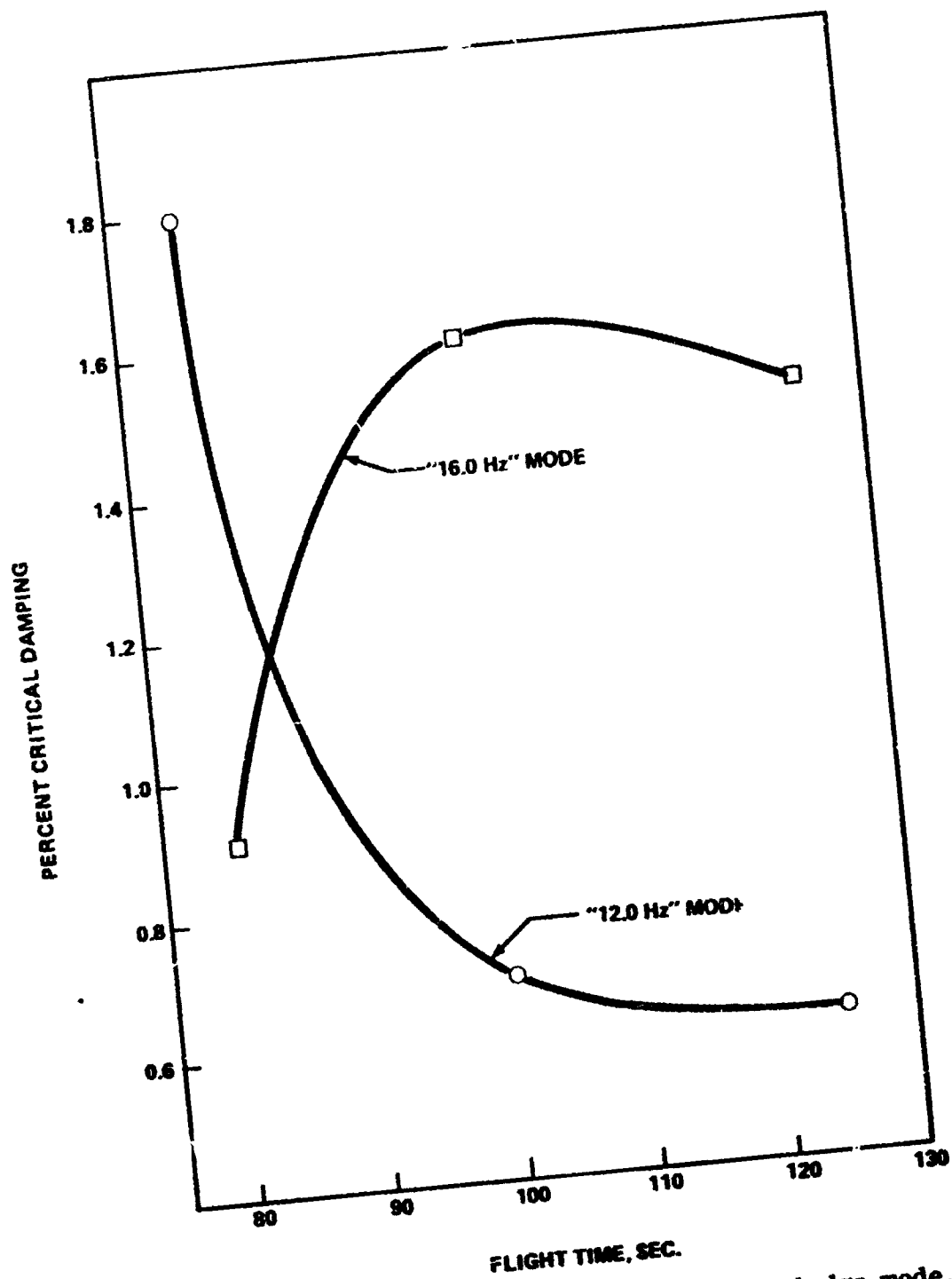


Figure 28. Critical damping curve for the lox dome bulge mode.

X. BOOST

A. Start Boost

1. Configuration. The start boost (T+125 sec) configuration consisted of the OV-101 Orbiter mated to the ET. The Orbiter contained a 32,000 lb simulated payload. The Orbiter and ET are the same as used in the liftoff tests and have been previously described. The start boost configuration tested was canted 9 degrees. The ET LOX tank was filled with 859,800 lb to a level of 320.3 in. ($X_T = 642.3$ in.) of deionized sodium-chromate-inhibited water. The LH₂ tank was empty. The boost configuration was tested in Building 4550 and is depicted in Figure 29.

2. Suspension System. The overhead suspension system for the start boost configuration consisted of two pyramid shaped truss air bag assemblies. Each assembly was composed of 12 #470 Firestone air bags with reservoirs, a rod tension member, spreader beam, cable assembly, and an ET spreader beam, which connected to the test article at the forward ET/SRB attachment. For pitch and yaw stability, upper and lower Firestone air bags #319 and #312, respectively, were used. The upper air bags were attached to the forward ET attach/spreader beam, and the lower air bags were attached in the vicinity of the ET to Orbiter attachment. This suspension system is depicted in Figure 30. Early tests indicated higher lateral restraint damping than anticipated. To reduce friction, steel guides were replaced with roller bearings, and teflon sheets on steel surfaces were installed on each of the lateral restraints. In addition, the yaw or y lateral air bag pressures were reduced to zero and the cables were made slack.

3. Test Results and Analysis.

a. Suspension System Modes. Obtaining rigid body modes for the end burn configuration was found to be very difficult. This was due to the fact that the shakers used were pendulum mounted. The pendulum frequency of the shakers were close to the rigid body frequencies; hence, the excitation force was insufficient to drive the vehicle with sufficient amplitude. This problem was overcome for the start boost and mid boost suspension system test by rigidizing eight shakers. The start boost suspension system frequencies and associated damping are shown in Table 20.

b. Flight Control Transfer Functions. A set of flight control transfer functions were obtained for the start boost condition. The shakers used and the sweep frequency bands are shown in Table 21.

c. Modal Test Results versus Pretest Analysis. All acceptable modes tuned during the start boost symmetric tests are shown in Table 22. The antisymmetric modes are shown in Table 23. The correlating pretest

MATED VERTICAL GROUND VIBRATION TEST (MVGVT)

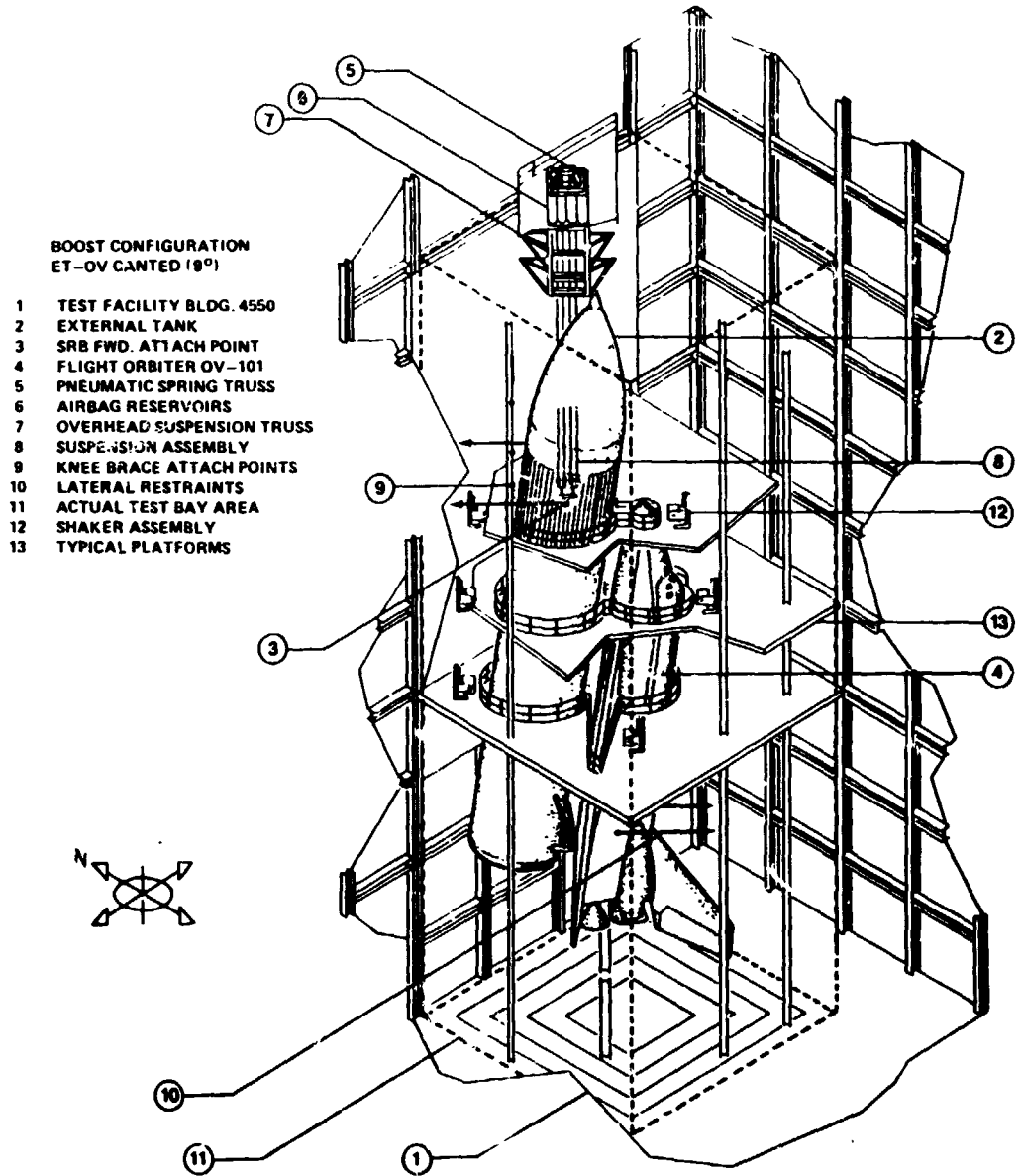


Figure 29. MVGVT boost configuration.

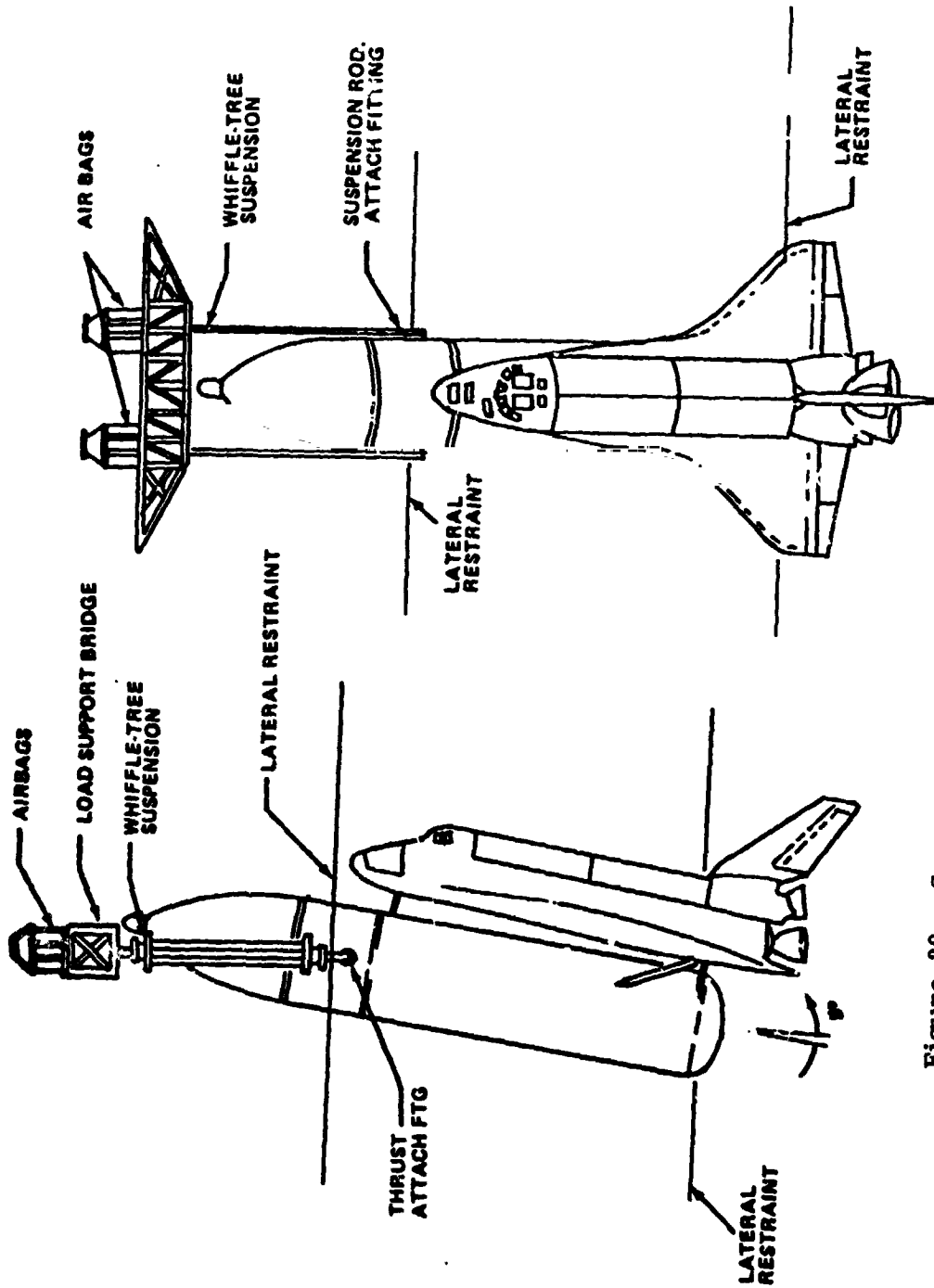


Figure 30. Suspension system for Orbiter/ET boost configuration.

TABLE 20. SUSPENSION SYSTEM MODES

| Modal Description | Start-Boost | | Mid-Boost | | End-Boost | |
|-------------------|----------------|----------------|--------------|--------------|--------------|--------------|
| | Frequency (Hz) | Damping (C/cc) | Frequency Hz | Damping C/cc | Frequency Hz | Damping C/cc |
| X-Translation | .647 | .022 | .647 | .022 | .804 | .040 |
| Y-Translation | .373 | .04-.055 | -- | -- | -- | -- |
| Roll | .804 | >.10 | .647 | .075 | .706 | -- |
| Pitch | .529 | <.10 | .575 | .032 | 1.077 | .08-.12 |
| Yaw | .235 | <.04* | .471 | -- | .431 | .018 |

* With rollers installed on the Z restraints

NOTE: 1. Start and Mid Boost had Y restraints with zero air bag pressure and slack in cable.

2. End Boost had Y restraints with air bag pressure and friction surface coated with teflon.

TABLE 21. FLIGHT CONTROL SWEEPS

| Shaker | Phase (deg) | Force (lb) | Sweep Frequency, Hz | | |
|--------|----------------|---------------|---------------------|-----------|-----------|
| | | | Start Boost | Mid Boost | End Boost |
| FL11Y | - | 500 | 1-26 | 1-26 | 2.5-26 |
| FB10Z | - | 550 | 1-26 | 1-26 | 2.5-26 |
| FB10Z | 0 | 550 | 1-26 | 1-26 | 2.5-26 |
| FB11Z | | 550 | | | |
| FB10Z | 180 | 550 | 1-26 | 1-26 | 2.5-26 |
| FB11Z | | 550 | | | |
| FL10Y | - | 500 | 1-26 | 1-26 | 2.5-26 |
| FB11Z | - | 500 | 1-26 | 1-26 | 2.5-26 |

TABLE 22. START BOOST SYMMETRIC

| Mode No. | Test | | Analytical Mode Freq. Hz | Percent Frequency | Test Mode Description Dominant Motion (Kinetic Energy) |
|----------|------------|-------------|--------------------------|-------------------|--|
| | Freq. (Hz) | Damp (C/CC) | | | |
| 6 | 3.431 | 0.014 | 3.27 | -4.6 | ORB Z Bend (0.47) and OMS X (0.15) |
| 14 | 6.157 | 0.022 | 6.245 | 1.4 | ORB X and Z Bending, Feedline X |
| 7 | 6.471 | 0.03 | 6.70 | 3.5 | 1st Wing Bend (.78) |
| 17 | 7.608 | 0.017 | 7.808 | 2.6 | V.T. Pitch (0.26) O/P W/Fuse Pitch |
| 8 | 8.767 | 0.008 | 8.78 | 0.1 | Feedline X (0.57), FWD Fuse Z (0.14) |
| 12 | 9.08 | 0.010 | 9.174 | 1 | ORB Z Bend (0.47) V.T. X-Z (0.14), UPR LH ₂ Tank (0.19) |
| 10 | 11.43 | 0.031 | - | - | Body Flap Rotation |
| 11 | 12.64 | 0.016 | 8.779 | 30 | Feedline Bend (0.44) and Intertank |
| 15 | 13.386 | 0.012 | 12.459 | -6.9 | LH ₂ Tank Mode (0.68) N = 2 |
| 18 | 16.008 | 0.01 | 19.05 | 19 | Crew CAB X (0.05), P/L (0.08) OMS, LOX Tank |
| 22 | 18.141 | 0.01 | 21.263 | 17.2 | LOX Dome-Feedline Bend Y (0.29), Wing X (0.7) |
| 19 | 19.256 | 0.005 | 19.05 | -1 | Feedline O/P W/LOX Dome (0.13) |
| 16 | 19.55 | 0.03 | 20.29 | 3.7 | Wing 2nd Bend (0.26), Elev (0.10) |
| 23 | 24.814 | - | 24.2 | -2.5 | LOX Tank (0.35), LH ₂ (0.14), Feedline (0.18) |
| 24 | 27.867 | - | - | - | 1307 Bulkhead |
| 21 | 33.366 | 0.014 | 33.24 | -0.4 | Feedline X (Ends O/P (0.29), LH ₂ (0.39) |

TABLE 23. START BOOST ANTISYMMETRIC

| Mode No. | Test | | Analytical Mode | Percent Δ Frequency | Test Mode Description Dominant Motion (Kinetic Energy) |
|----------|------------|-----------------|-----------------|----------------------------|---|
| | Freq. (Hz) | Damp (C/CC) | | | |
| 8 | 3.412 | 0.015/ 0.22 | 3.76 | 10 | FIN 1st Lat (0.80), Bend/FWD FUS LAT (0.11) |
| 4 | 4.47 | 0.018 | 4.58 | 2 | FUS Yaw Out-of-Phase (0.60)/ET Yaw (0.16), Wing Z Bending (0.13) |
| 1 | 5.57 | 0.027 | 5.86 | 6 | 1st Wing Z Bending (0.31), ET Yaw and Roll (0.52) |
| 14 | 6.51 | 0.016/ 0.091 | 6.33 | -3 | ORB/ET (0.44/0.50), F Payload Y (0.30) |
| 21 | 6.902 | 0.004 | 6.60 | -4 | Wing Bending (0.22), In-Phase W.O.B. Elevon O _y (0.20) |
| 15 | 7.608 | 0.022 | 7.91 | 4 | ET Roll (0.32), Out-of-Phase with ORB Roll (0.22) |
| 9 | 12.720 | 0.016 | 13.61 | 7 | Vert Tail 2nd Bend (0.51), ET (0.04) |
| 10 | 13.620 | 0.013 | 16.18 | 19 | Vert Tail Torsion (0.8), ET Shell Mode (0.06) |
| 7 | 14.364 | 0.016 | 14.783 | 3 | FUS Bending (0.14), ET Shell Mode (0.6) |
| 5 | 14.677 | 0.017 | 14.563 | -1 | Elevons (0.38), Out-of-Phase with Wing (0.17) |
| 16 | 15.264 | 0.044 | 16.184 | 6 | Orbiter Roll, LH ₂ Bending |
| 20 | 16.7 | | | | Feedline Mode (0.68), ET Y Bending (0.27) |
| 13 | 19.56 | 0.027 | 22.67 | 16 | LH ₂ Intertank Y Bend (0.73) |
| 12 | 21.19 | 0.027 | 22.31 | 5 | LWR Eng δ_z (0.51), Wing X (0.15) |
| 11 | 23.54 | 0.637 | 27.86 | 17 | ET Torsion (0.25), LWR Fng Y (0.13) |

analytical frequency and the computed modal damping from the decay traces are also shown in those tables. The test mode description and the percent frequency difference between test and analysis are also given.

B. Mid Boost

1. Configuration. The mid boost (T + 301 sec) configuration consisted of the OV-101 Orbiter mated to the ET. The Orbiter contained a 32,000 lb simulated payload. The mid boost configuration tested was canted 9 degrees and is depicted in Figure 29. The ET LOX tank was filled with 385,300 lb to 162 in. ($X_T = 801$ in.) of deionized sodium-chromate-inhibited water. The LH_2 tank was empty.

2. Suspension System. The suspension system for mid boost was the same as that described under the start boost. Again, the lateral yaw air bag pressures were reduced to zero and the cable was made slack.

3. Test Results and Analysis.

a. Suspension System Modes. The suspension system modes for mid boost were obtained with slack in the y restraints with zero air bag pressures. Excitation force was increased for this condition by rigidizing eight of the pendulum shakers. The suspension system frequencies and associated dampings are shown in Table 20.

b. Flight Control Transfer Functions. A set of flight control transfer functions were obtained for the mid boost configuration. The shakers used and the sweep frequency bands are shown in Table 21.

c. Modal Test Results versus Pretest Analysis. All acceptable modes tuned during the mid boost symmetric test are shown in Table 24. The antisymmetric modes are shown in Table 25. The correlating pretest analytical frequencies and the computed damping from the decay traces are also shown in those tables. This test mode description and the percent frequency difference between test and analysis are also given.

C. End Boost

1. Configuration. The end boost (T + 477 sec) configuration consisted of the OV-101 Orbiter mated to the ET. The Orbiter contained a 32,000 lb simulated payload. The end boost configuration tested was canted 9 degrees and is depicted in Figure 29. The ET LOX tank was filled with 88,140 lb to a liquid level of 59.5 in. ($X_T = 603.5$ in.) of deionized sodium-chromate-inhibited water. The LH_2 tank was empty.

2. Suspension System. The suspension system for the end boost was the same as that described under start boost except both the y and z lateral airbags were effective. The suspension system is shown in Figure 30.

TABLE 24. MID BOOST SYMMETRIC

| Mode No. | Test | | Analytical Mode | Percent Δ Frequency | Test Mode Description Dominant Motion (Kinetic Energy) |
|----------|------------|-----------------|-----------------|----------------------------|---|
| | Freq. (Hz) | Damp (C/CC) | | | |
| 6 | 3.70 | 0.012 | 3.37 | -9 | Fuselage 1st Z-Bending |
| 12 | 6.43 | - | 6.50 | 1 | Feedline Axial |
| 11 | 6.47 | 0.037 | 6.56 | 1 | Wing 1st Z-Bending |
| 13 | 7.59 | 0.017 | 7.81 | 3 | V.T. Pitch (0.29), Fuselage Pitch (0.28) |
| 15 | 8.65 | 0.006 | 8.85 | 2 | Feedline 1st Z-Bending (0.73) |
| 16 | 10.53 | 0.058 | 12.30 10.41 | 16 -1 | Elevon Rotation Outboard/ Inboard Out-of-Phase |
| 8 | 11.62 | 0.037 -0.055 | 11.24 | -5 | Body Flip Z (0.24), LH ₂ (0.16), Feedline (0.08), P/L (0.707) |
| 7 | 12.92 | 0.022 | 12.98 | 0 | FUS Z-Bending (0.13), Upper LH ₂ (0.13) |
| 19 | 14.90 | 0.010 | 12.50 | -16 | LH ₂ Tank (N = 2) LOX Dome, PL Axial |
| 5 | 16.01 | 0.030 | | | SSME Pitch (0.50), Fuselage Z (0.11), PL Axial (0.02) |
| 17 | 16.44 | 0.008 | | | Feedline X (0.67), Upper LH ₂ N = 3 (0.24) |
| 14 | 17.28 | 0.028 | 14.24/17.47 | -18/1 | Fuselage Z-Bending (0.40), LH ₂ N = 3 (0.25) |
| 18 | 19.67 | 0.031 | | | Wing 2nd Z-Bending |
| 22 | 20.20 | 0.019 | | | Crew Cabin Axial Out-of-Phase with Orbiter |
| 20 | 20.67 | 0.005 | | | Tank Dome and Feedline |
| 21 | 23.43 | 0.005 | | | Tank Dome and Feedline |
| 23 | 28.92 | 0.008 | | | 1307 Bulkhead Axial |

TABLE 25. MID BOOST ANTISYMMETRIC

| Mode No. | Test | | Damp (C/CC) | Analytical Mode | | Percent Δ Frequency | Test Mode Description Dominant Motion (Kinetic Energy) |
|----------|------------|-------------|-------------|-----------------|-------|---|---|
| | Freq. (Hz) | | | Freq. Hz | | | |
| 1 | 3.471 | 0.022 | 3.78 | | 9 | V.T. 1st Lat Bend (0.84), FUS -Y (0.10), ET-Y and Roll (0.04) | |
| 2 | 4.627 | 0.028 | 4.689 | | 1 | FUS Yaw (0.61), O/P ET Bend and Yaw (0.14), Wing Roll (0.16) | |
| 3 | 5.725 | 0.0157 | 5.812 | | 1.5 | Wing Bend (0.18), W/ET Yaw and Roll (0.23) | |
| 10 | 6.392 | - | 6.358 | | -0.5 | FWD Payload (0.32) + FWD FUS Y (0.26), Wing and Elev Z (0.02) | |
| 6 | 7.609 | 0.15/0.016 | 8.50 | | 11.7 | OR3 Roll (0.62), O/P W/ET Roll (0.35) | |
| 17 | 8.023 | 0.02 | 8.50 | | 6 | FUS Torsion (0.19), Y B (0.25), Wing Z (0.15) | |
| 18 | 11.624 | 0.016 | 11.67 | | 0.4 | IB and OB Elev ROT (0.51), O/P Wing Z (0.11) | |
| 20 | 11.742 | 0.013 | 12.17 | | 3.6 | LWR SSME Y (0.15), I/PW Eng I Y (0.02), Susp Sys (0.23) | |
| 4 | 12.681 | 0.01 | 13.662 | | | V.T. 2nd Bend (0.62) | |
| 5 | 13.62 | 0.02/0.026 | 16.2 | | 18.9 | V.T. Torsion (0.81) | |
| 13 | 14.29 | 0.014/0.02 | 12.17 | | -14.8 | FUS Y Bend (0.16), FT Shell (0.48) | |
| 15 | 14.48 | 0.028 | 12.38 | | -14.8 | Elev (0.37), O/P W Wing (0.16) | |
| 11 | 18.08 | 0.022 | 17.811 | | -1.5 | ET 1st Bend (0.85) | |
| 12 | 23.84 | 0.031/0.037 | 27.387 | | 14.8 | Wing Torsion (0.215), Elev (0.426) | |
| 8 | 24.012 | 0.01 | 27.85 | | 15.9 | Fuse (0.13), ET Torsion (0.22), Feedline (0.21) | |
| 14 | 28.96 | 0.01/0.02 | 22.08 | | -23.8 | ET Bend and Shell (0.90) | |

3. Test Results and Analysis.

a. Suspension System Modes. The suspension system modes for end boost were obtained with air bag pressure in the y and z lateral bags. The restraint lateral friction surfaces were coated with teflon and had not been converted to roller bearings for this test condition. The suspension system frequency and associated damping are also shown in Table 20.

b. Flight Control Transfer Functions. A set of flight control transfer functions were obtained for the mid boost configuration. The shakers used and the sweep frequency bands are shown in Table 21.

c. Modal Test Results versus Pretest Analysis. All acceptable modes tuned during the end boost symmetric test are shown in Table 26. The symmetric modes were obtained with the y and z air bag restraints effective. The antisymmetric test modes are shown in Table 27. For these modes the z air bag restraint was effective; however, the y air bag had zero pressure and the cables were slack. The correlating pretest analytical frequencies and the computed modal damping from the decay traces are also shown in those tables. The test mode description and the percent frequency difference between test and analysis are also given.

D. Contingency Tests

1. LOX Tank Low Level. A LOX tank low level test was conducted to obtain selected payload oriented modes. The LOX tank contained 27,600 lb of water and filled to a level of 25 in. ($X_T = 938.0$ in.) The y restraint air bag pressure was set at zero with slack cables. Seven symmetric modes and two antisymmetric modes were obtained. These test frequencies, corresponding analytical frequency and test mode descriptions are shown in Table 28.

2. Fuselage Symmetric Bending Mode Linearity Check. The results of the horizontal ground vibration test (HGVT) indicated the fuselage first symmetric bending mode is affected by a non-linearity associated with the cargo bay doors. It was felt that the cargo bay doors take axial loads at low force levels and stiffen the fuselage. To assess this non-linearity, plots of the frequency versus excitation force are shown in Figure 31. The frequency curves do indicate that the frequency decreases with increasing excitation force.

3. SAMS0 Sweeps. Four payload bay wide band sweeps were run at the request of The Space and Missile System Office. These sweeps, with the shakers used, are presented in Table 29.

TABLE 26. END ROOST — SYMMETRIC

| Mode No. | Test | | Analytical Mode | | Percent Frequency | Test Mode Description Dominant Motion (Kinetic Energy) |
|----------|------------|--------------|-----------------|--|-------------------|--|
| | Freq. (Hz) | Damp (C/C) | Freq. Hz | | | |
| 8 | 4.16 | 0.016 | 3.70 | | 12 | Fuse 1st Z Bend (0.12), Feedline X (0.12) |
| 17 | 4.24 | 0.01 | 3.70 | | 13 | Fuse Z Bend (0.13), Payload FWD Z (0.11) |
| 18 | 4.51 | 0.009 | 3.70 | | 18 | Fuse 1 ZB (0.34), Feedline (0.17), LOX Tank (0.15), SSME Rocking (0.10), Vert Tail Pitch (0.04) |
| 5 | 6.55 | 0.014, 0.022 | 6.70 | | 6 | 1st Wind Bend (0.87) |
| 9 | 7.25 | 0.006, 0.011 | 7.55 | | 4 | Feedline X (0.21), Out P/W LOX Dome ; (0.16), Vert Tail Pitch 0.14) |
| 20 | 7.26 | 0.006 | 7.55 | | 4 | ET Z Bend (0.35), Feedline X (0.22) and Orb Axial Out P/W ET |
| 17A* | 7.92 | 0.015, 0.009 | | | | V.T. Pitch (Without Water) |
| 10 | 8.53 | 0.007 | 8.97 | | 5 | Feedline X (0.89) |
| 11 | 9.32 | 0.020 | 9.70 | | 4 | 1st Fuse Z Bend (0.50), ET Z Bend |
| 16 | 13.19 | 0.012 | 11.8 | | 1 | Fuse 2nd Z Bend (0.57) |
| 19 | 14.41 | 0.013 | 14.6 | | 1 | Fuse Z Bend (0.30), Feedline (0.12), LH ₂ (0.11) |
| 13 | 14.99 | 0.009 | | | | ET Z Bend, LH ₂ Tank Shell (0.30), ORB ZB (0.27), FWD Pl. X (0.10) Out P/W AFT Pl. X (0.06) |
| 21A* | 15.93 | 0.044 | | | | SSME's Pitching (0.65), OMS POD S X (0.24) |
| 14 | 17.26 | 0.01 | 17.3 | | 0 | LOX Dome Bulge |
| 22 | 18.20 | 0.025 | | | | SSME Pitch (0.23), OMS X (0.15), Feedline (0.22) |
| 15 | 18.26 | 0.01 | | | | Feedline X (0.44), LOX Dome Bend |
| 18A* | 18.85 | | | | | LWR SSME's X |
| 27 | 29.35 | 0.018 | | | | OMS POD X and X Out P/W SSME X |
| 21 | 34.83 | 0.011 | 32.95 | | 5 | UPR SSME X (0.24), LWR SSME Torsion (0.09), OMS POD X (0.11), Fus. X (0.18), Feedline X (0.15) |

TABLE 27. END BOOST ANTISYMMETRIC

| Mode No. | Test | | Analytical Mode | Percent Frequency | Test Mode Description Dominant Motion (Kinetic Energy) |
|----------|------------|-------------|-----------------|-------------------|---|
| | Freq. (Hz) | Damp (C/CC) | | | |
| 1 | 3.47 | 0.016 | 3.83 | 10.4 | V.T. 1st Lat Bend (0.87) |
| 3 | 5.06 | 0.02 | 4.83 | -4.5 | ORB Yaw (0.35), O/P ET Yaw (0.19), Wing Bend O/P V.T. Bend (0.32) |
| 4 | 5.65 | 0.016/0.025 | 5.89 | 4.2 | Wing Bend (0.19), O/P ET Roll, LWR SSME Y (0.08) O/P V.T. |
| 19 | 6.47 | 0.016 | 8.23 | 27.2 | LWR Engine O/P (0.90) |
| 7 | 6.98 | 0.018 | 6.40 | -8.3 | FWD PL Y (0.26), FWD FUS Y (0.26), ET Yaw (0.26) |
| 13 | 7.73 | 0.018 | 6.40 | -17.2 | FUS Roll (0.29), O/P ET Roll (0.29), O.B Elev ROT (0.29) |
| 5 | 8.04 | 0.011 | 8.02 | -0.2 | FWD PL Y (0.24), ET Roll (0.20), FUS Torsion (0.15) |
| 9 | 9.27 | 0.016 | 8.02 | -13.4 | AFT PL Y (0.32), Elev ROT (0.10) |
| 8 | 10.80 | 0.032 | 10.88 | 0.7 | ET Y Bend (0.21), V.T. Y Bend (0.04) |
| 10 | 11.62 | 0.021 | 12.39 | 6.6 | Elev ROT (0.20) I/P Wing Bend (0.05) |
| 2 | 12.72 | 0.018/0.017 | 13.64 | 7.2 | V.T. 2nd Y Bend (0.64) |
| 14 | 13.62 | 0.028 | 14.63 | 7.4 | V.T. Torsion (0.16) |
| 16 | 14.48 | - | - | - | Wing Bend O/P Elev ROT |
| 11 | 20.67 | 0.025 | - | - | ET Y Bending, LH ₂ (0.42) - Ogive (0.31) |
| 15 | 21.31 | 0.037 | 19.47 | -8.6 | Wing Torsion |
| 20 | 22.13 | 0.044/0.027 | 22.31 | -0.8 | LWR Eng. Z O/P (0.43), FUS Roll (0.47) |
| 12 | 24.19 | 0.007 | - | - | Feedline X and Bend (0.47), LWR SSME Z and Y (0.15) |

TABLE 28. LOX TANK LOW LEVEL BOOST

| Mode No. | Test | | Analytical Mode* | Percent Frequency | Test Mode Description Dominant Motion (Kinetic Energy) |
|----------|------------|-------------|------------------|-------------------|---|
| | Freq. (Hz) | Damp (C/CC) | | | |
| 2 | 4.20 | 0.013 | 3.66 | -12.8 | FUS 1st Z Bend (0.45), ET Pitch (0.37), V.T. Pitch (0.05) |
| 1 | 4.55 | 0.018 | 3.66 | -19.6 | FUS 1st Z Bend (0.46), LOX Tank ZB (0.15) |
| 3 | 15.85 | 0.018 | 15.03 | -5.2 | Feedline X (0.32), Susp. System (0.28) |
| 7 | 17.26 | 0.01 | 19.57 | 13.4 | LOX Tank Bulge (Possible) |
| 6 | 18.26 | 0.055 | | | LWR SSME X and Z (0.26), Feedline X (0.19), OMS (0.19) |
| 4 | 20.25 | 0.01 | 19.90 | -1.7 | Feedline X and Z (0.68), LOX Bulge (Possible) |
| 5 | 34.64 | 0.01 | 32.75 | -5.4 | Eng. 1 X (0.23) O/P LWR SSME |
| | | | | | ANTISYMMETRIC MODES |
| 23 | 5.10 | 0.018 | 4.88 | -4.3 | Wing Z B (0.33), FUS (0.13) and ET (0.21) Yaw |
| 24 | 15.19 | - | - | - | Wing Z B (0.39) O/P FUS Roll (0.14), FI, (0.13) |

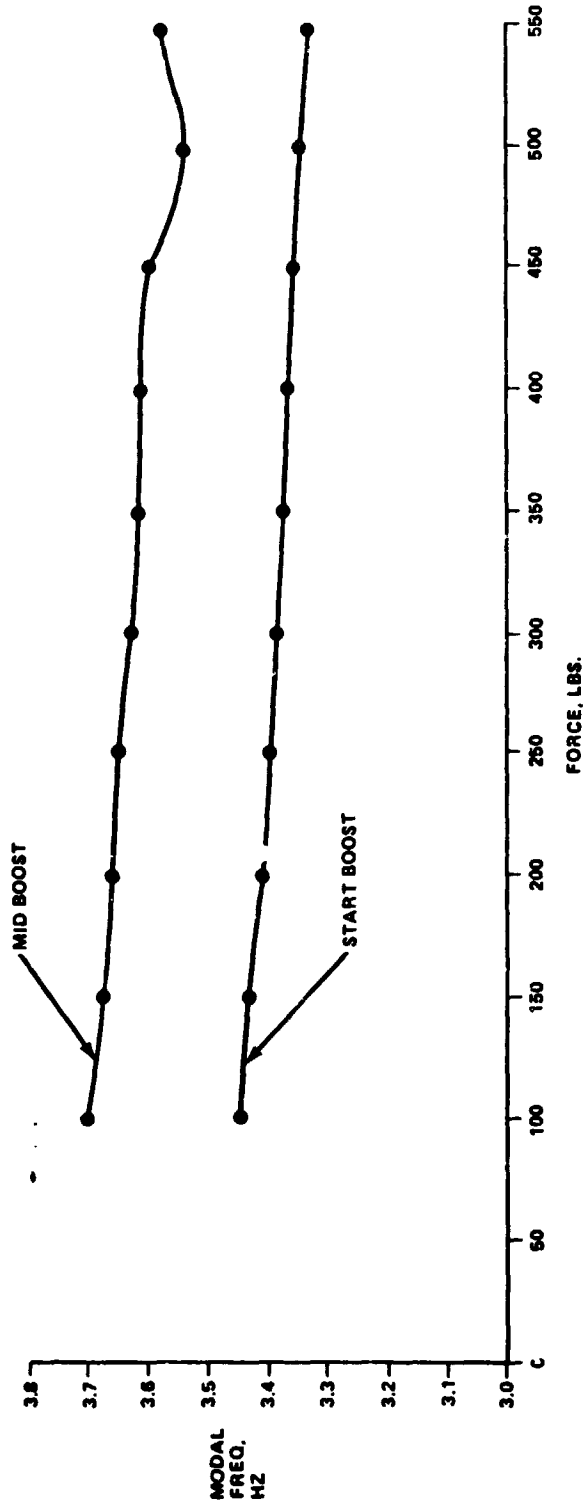


Figure 31. First fuselage symmetric bending linearity check.

TABLE 29. SAMSO SWEEPS

| Shaker | Phase (deg) | Frequency Range (Hz) |
|-------------|-------------|----------------------|
| FL10Y-FL11Y | 0 | 2.5-50 |
| | 180 | 2.5-50 |
| FB10Z-FB11Z | 0 | 2.5-50 |
| | 180 | 2.5-50 |

XI. CONCLUSION

The following is a summary of the most significant results derived from the MGVGT Shuttle Test Program:

- 1) The left and right SRB forward mounted rate gyros exhibited abnormally high transfer functions which required a structural redesign.
- 2) The effect on the frequencies and mode shapes with the SRB stiffening ring on and off was negligible. This lack of difference may have been due to the additional flexibility of the ET at the aft ET/SRB interface.
- 3) The SSME axial modes did not correlate well with pre-test analysis. The pre-test math model used was a symmetric halfshell. A three-dimensional antisymmetric math model of the SSME engine and thrust structure was determined to be required.
- 4) The forward ET/SRB interface, which is a ball and socket design, was found to be fixed in the liftoff test. This interface is intended to transmit only shear forces between the ET and SRB. The ET/SRB interface was fixed due to the frictional forces created by the weight of the loaded ET and Orbiter.
- 5) Pre-test SRB Y bending modes for SRB end burn did not correlate well with test. This required additional shell modeling of the aft SRB/ET interface.
- 6) Unexpected large rate gyro yaw rates were observed on the Orbiter 1307 Orbiter bulkhead during symmetric (pitch) flight control sweeps. This was found to be due to local deformation which the flight controls group assessed as acceptable. The math model of the 1307 bulkhead was remodeled, however.
- 7) Test rate gyro values showed greater response variations than those used in the analytical studies in determining the Redundancy Management (RM) Trip Levels. For STS-1 flight, RM software trip levels and cycle counter levels were increased. The Fault Isolation Routine was modified to inhibit kicking out RGA's and accelerometers after first sensor failure. Changes to the control system for the other flights will be evaluated after STS-1 flight.

With the advent of structural complexity of space vehicles with increasing unsymmetrical jointed structures, the difficulty of dynamist modeling is becoming increasingly greater; therefore, modal survey testing will always be a necessary tool to aid the dynamist in the area of math modeling, and loads, controls, pogo and flutter design. Table 30 lists the various past full scale test programs with the major problems uncovered in each.

TABLE 30. FULL SCALE DYNAMIC TESTING EXPERIENCE IN PAST PROGRAMS

| Test Program | Problems Discovered | Hardware Impacted | Consequences if Not Discovered |
|--------------|--|--|---|
| MVGVT | <p>SRB mounted rate gyros exhibited abnormally high transfer functions. The rate gyros mounted on the forward SRB ring frames resonated at local frequencies and high gains, which were critical to flight controls.</p> | <p>Structural redesign was required to stiffen SRB ring frame which raised the local resonant frequencies and reduced the gain.</p> | <p>Flight control instability and possible loss of vehicle.</p> |
| MVGVT | <p>Axial SSME frequencies and mode shapes did not correlate with pretest analysis. A half shell dynamic math model using symmetry was used in the pretest analysis.</p> | <p>A new three dimensional asymmetric math model of the SSME engines and thrust structure was required. No hardware changes were necessary.</p> | <p>Pogo stability analyses would have been suspect.</p> |
| MVGVT | <p>Test rate gyro values showed greater response variations than analysis. Response variations between RGA's were much larger than those used in the analytical studies in determining the Redundancy Management (RM) trip levels.</p> | <p>*RM software trip levels and cycle counter levels were increased. The fault isolation routine was modified to inhibit kicking out RGA's and ACC's after first sensor failure.</p> | <p>Flight control instability and possible loss of vehicle.</p> |

*Above for STS-1 flight only, other flights will be evaluated.

TABLE 30. (Continued)

| Test Program | Problems Discovered | Hardware Impacted | Consequences if Not Discovered |
|--------------|---|--|---|
| DTV | <p><u>Design deficiency in the SPS tank supports.</u> Unexpectedly high local resonant coupling was detected between SPS tank and bulkhead support.</p> | <p>The upper support bracket for the SPS tanks was redesigned to eliminate a strong tank cantilever mode.</p> | <p>Hardware failure resulting in loss of mission and possible crew loss.</p> |
| DTV | <p><u>High LOX and fuel dynamic tank bottom pressures.</u> These pressures were under predicted by a factor of 2. The significance of these pressures was not understood until after Pogo occurred on AS-502.</p> | <p>The higher tank pressures contributed to the S-IC Pogo accumulator hardware design.</p> | <p>Potential loss of vehicle and crew due to Pogo.</p> |
| DTV | <p><u>High 18 Hz S-IC Crossbeam mode gains.</u> DTV data showed that an accumulator should not be used on the inboard engine.</p> | <p>Elimination of a planned inboard engine accumulator.</p> | <p>Potential loss of vehicle and crew due to Pogo between an 18 Hz accumulator mode and the 18 Hz crossbeam mode.</p> |
| DTV | <p><u>Local rotation of the flight gyro support plate.</u> Vehicle dynamic shears and moments deformed support plate. The math model under predicted this deformation by 135%.</p> | <p>The gyros were relocated to the bottom of the support plate where the local rotation was much less. This required wire harnesses of new length. The flight control filter network was redesigned.</p> | <p>Flight control instability resulting in loss of vehicle.</p> |

TABLE 30. (Continued)

| Test Program | Problems Discovered | Hardware Impacted | Consequences if Not Discovered |
|-----------------|---|--|---|
| MARL | <p>Design deficiency in the IU stable platform. Coupling between the stable platform and the ring modes of the IU provided a mechanism for acoustically driving the platform accelerometer against the stops.</p> | <p>Short channel stiffeners were added to AS-501 on the pad. Damping material and a software "reasonableness" test were added later in the program.</p> | <p>Large guidance errors that could cause loss of lunar mission.</p> |
| DTV | <p>Design deficiency in the CSM interface. The single torsional sway brace produced unpredicted high coupling between command module torsional motion and S-1C engine deflection.</p> | <p>Additional torsional sway braces were installed on AS-501 on the pad. Subsequently, the F-1 engines were reorificed to reduce loads at engine cutoff. An engine precant program was implemented to maintain structural integrity in case of engine out.</p> | <p>structural failure of the CSM interface with loss of vehicle and possible crew loss.</p> |
| Skylab ATM Test | <p>Strong cross coupling between longitudinal and lateral motions indicated a possible structural failure at S-1C cutoff.</p> | <p>A 1-2-2 engine cutoff hardware and software mod was developed to reduce the longitudinal input to the ATM. Hardware redesigns were laid out in case they were proven necessary by further study.</p> | <p>Hardware failure with potential loss of mission.</p> |

TABLE 30. (Concluded)

| Test Program | Problems Discovered | Hardware Impacted | Consequences if Not Discovered |
|--------------------------|---|---|---|
| Skylab Modal Survey Test | <p>The strong cross coupling in the ATM proved to be attenuated rather than amplified by the way ATM cross coupling reacted through vehicle interface.</p> | <p>Test of the total Skylab launch configuration proved the 1-2-2 fix was adequate and that no hardware changes were required.</p> | <p>This test saved a possible redesign of the ATM by verifying structural integrity under the 1-2-2 cutoff.</p> |
| Short-stack | <p>Strong pitch/longitudinal coupling caused by the lunar module increased the S-IC Pogo gain factor by 30%. This effect coupled with the tank pressure underprediction was the reason AS-502 Pogo was not predicted.</p> | <p>Development and installation of the outboard LOX accumulators.</p> | <p>Pogo instability with potential loss of vehicle and crew.</p> |
| Mini A/C | <p>The mechanism triggering S-II Pogo was defined. Coupling between the first four LOX tank hydroelastic modes when they coalesced with the 16 Hz center engine crossbeam mode produced the Pogo instabilities.</p> | <p>An accumulator was developed for the center engine. A backup cutoff system was also developed. The accurate math model developed during this test supported extensive thrust structure design mods on subsequent vehicles without further testing.</p> | <p>Pogo instability with potential loss of vehicle and crew.</p> |

BIBLIOGRAPHY

- STS 79-0006, Mated Vertical Ground Vibration Test Liftoff Configuration on-site Data Evaluation Report, Space Division, Rockwell International, January 1979.
- STS 79-0032, Mated Vertical Ground Vibration Test Pre-SRB Separation Configuration on-site Data Evaluation Report, Space Division, Rockwell International, March 1979.
- SD-78-SH-0170, Mated Vertical Ground Vibration Test Boost Configuration on-site Data Evaluation Report, Space Division, Rockwell International, July 28, 1978.
- ED23-77-205, Finite Element Model of the MGVGT Overhead Suspension System for Boost, MSFC, October 7, 1977.
- ED23-78-30, MGVGT Suspension System Rigid Body Modes, MSFC, March 8, 1978.
- Technical Letter ASD-ED23-21632, Vibration Analysis of the Coupled Building-Vehicle System for the Mated Vertical Ground Vibration Test, Teledyne Brown Engineering, May 21, 1975.
- JSC 08201, Mated Vertical Ground Vibration Test, Test Requirements and Specifications Document, JSC, February 6, 1978.
- MVGVT-FTOR-002 Volume 1, Mated Vertical Ground Vibration Test Liftoff Configuration Test Operations Report, MSFC, February 1979.
- MVGVT-FTOR-003 Volume 1, Mated Vertical Ground Vibration Test Burnout Configuration Test Operations Report, MSFC, February 1979.
- MVGVT-FTOR-001 Volume 1, Mated Vertical Ground Vibration Test Boost Configuration Test Operations Report, MSFC, October 1978.

APPROVAL

MATED VERTICAL GROUND VIBRATION TEST

By W. Ivey

The information in this report has been reviewed for security classification. Review of any information concerning Department of Defense or nuclear energy activities or program has been made by the MSFC Security Classification Officer. This report, in its entirety, has been determined to be unclassified.



ROBERT S. RYAN
Chief, Structural Dynamics Division



GEORGE D. HOPSON
Director, Systems Dynamics Division